Government of **Western Australia**
Department of **Mines and Petroleum**

RECORD 2011/22

NEW INSIGHTS INTO THE REGOLITH OF PARTS OF THE GASCOYNE REGION

by
CBE Krapf


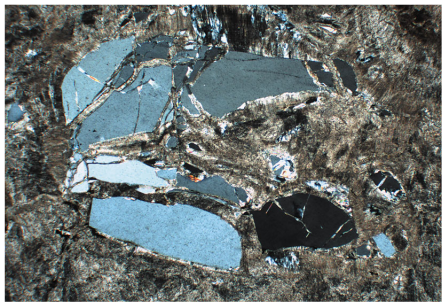


Geological Survey of Western Australia

Government of **Western Australia**
Department of **Mines and Petroleum**

Record 2011/22

NEW INSIGHTS INTO THE REGOLITH OF PARTS OF THE GASCOYNE REGION

by
CBE Krapf

Perth 2011

Geological Survey of Western Australia

MINISTER FOR MINES AND PETROLEUM
Hon. Norman Moore MLC

DIRECTOR GENERAL, DEPARTMENT OF MINES AND PETROLEUM
Richard Sellers

EXECUTIVE DIRECTOR, GEOLOGICAL SURVEY OF WESTERN AUSTRALIA
Rick Rogerson

REFERENCE
The recommended reference for this publication is:
Krapf, CBE 2011, New insights into the regolith of parts of the Gascoyne region:
Geological Survey of Western Australia, Record 2011/22, 54p.

National Library of Australia Card Number and ISBN 978-1-74168-421-6

Grid references in this publication refer to the Geocentric Datum of Australia 1994 (GDA94).
Locations mentioned in the text are referenced using Map Grid Australia (MGA) coordinates, Zone 50.
All locations are quoted to at least the nearest 100 m.

Published 2011 by Geological Survey of Western Australia
This Record is published in digital format (PDF) and is available online at
<http://www.dmp.wa.gov.au/GSWApublications>.

Further details of geological products and maps produced by the Geological Survey of Western Australia are available from:
Information Centre
Department of Mines and Petroleum
100 Plain Street
EAST PERTH WESTERN AUSTRALIA 6004
Telephone: +61 8 9222 3459 Facsimile: +61 8 9222 3444
www.dmp.wa.gov.au/GSWApublications

Contents

Figures

Tables

New insights into the regolith of parts of the Gascoyne region

by

CBE Krapf

Abstract

The Gascoyne region has an extensive regolith cover where some regolith units are genetically related to the underlying bedrock, but others have been transported. There are few age determinations of the regolith, so the relative ages of regolith units are based on their position in the landscape, degree of induration, extent to which they have been dissected by more recent processes, or their relationships with overlying younger material. This study is the first attempt to gain a more detailed insight into the regolith and therefore the landscape evolution of parts of the Gascoyne region, with a focus on the Mount Phillips 1:250 000 Geological Series map sheet area. There is a strong emphasis on identifying residual (i.e. in situ) regolith units, as opposed to relict units that represent remnants of previous landforms. The genetic relationship between both regolith types and the underlying bedrock and their spatial distribution in today's landscape is also documented. Numerous outcrops have been investigated and several stratigraphic sections have been measured and logged, providing detailed descriptions of the outcropping regolith successions and types.

A wide variety of regolith types is present, some of which are genetically related to the underlying bedrock. Most of the transported relict regolith units and some of the older alluvial and colluvial regolith units have been impregnated, cemented and/or lithified during alternating episodes of wet and dry conditions. These units are now preserved either as elevated erosional remnants within the old paleovalleys, or as inverted paleochannels. Differential rates of erosion and weathering during the Cenozoic formed a variety of different regolith profiles on Archean to Phanerozoic rocks. Ferruginization and silicification of this regolith led to the formation of resistant rises, hills, and mesas. Relief inversion is found in many places over partly silicified paleochannel deposits. In situ regolith profiles are retained where the rate of weathering is greater than the rate of erosion, especially along old drainage systems, resulting in the preservation of the old drainage network outline.

KEYWORDS: Gascoyne, regolith, regolith mapping, landscape evolution, weathering, Cenozoic, stratigraphy, regolith profile, paleochannel, duricrust, calcrete

Introduction

A major challenge facing mineral exploration in many parts of Western Australia is exploring effectively and efficiently through a thick and extensive regolith cover in order to discover deeper mineral targets. Mapping and understanding the genesis of regolith is crucial, not only in terms of understanding landscape evolution, but also in terms of providing a framework for regolith sampling programs, and as a basis for interpreting regolith geochemistry. Derivative maps, such as those that distinguish between in situ and transported regolith and identify different types of sample media, are particularly useful for mineral exploration.

Previous regolith studies in Western Australia have mainly focused on regolith materials and geochemistry (Sanders et al., 1999; Sanders, 2000; Cornelius et al., 2007), the relationship between regolith type and landform (Marnham and Hall, 2002), paleochannels and ore systems (Anand and de Broekert, 2005; Butt et al., 2005), and the utilization of multispectral and hyperspectral data to identify different regolith types (Skwarnecki, 2005; Gozzard, 2006; Langford, 2007). Only limited studies have been undertaken in relation to the depositional processes and the stratigraphy of regolith (Skwarnecki, 2005; Gozzard, 2007).

Recent geological mapping and radiometric dating in the Gascoyne region have resulted in a significantly better understanding of the bedrock geology and structural evolution of the Gascoyne Province basement and the overlying Edmund and Collier basins (Martin et al., 2007; Sheppard et al., 2008; Johnson et al., 2009; Sheppard et al., 2010; Johnson et al., 2010b). However, no detailed work has been undertaken on the regolith. The Gascoyne region has an extensive regolith cover of inferred Cenozoic or Quaternary age. Some regolith units are genetically related to the underlying bedrock, whereas others have been transported. Age determinations of regolith units are poor, and are based on criteria such as position in the landscape, degree of induration, the extent to which it has been dissected by more recent processes, and the presence of overlying younger material.

This Record is the first attempt at a systematic study of the regolith of part of the Gascoyne region, with the focus on the Mount Phillips* 1:250 000 Geological Series map sheet area. Individual outcrops of various regolith types have been visited, mapped and described in detail, and representative regolith samples have been collected for geochemical analysis and petrographic examination.

Study area

The study area comprises most of the Mount Phillips map sheet, which is bounded by latitudes 24°00' and 25°00'S and longitudes 115°30' and 117°00'E (Fig. 1). The sheet encompasses rocks of the Paleoproterozoic Gascoyne Province, the mostly Mesoproterozoic Edmund Basin (Bangemall Supergroup), and the Phanerozoic Southern Carnarvon Basin. Previously compiled regolith layers are available for the Mount Phillips, Eudamullah, Mount Augustus, and Yinnetharra 1:100 000 Geological Series map sheets (Fig. 2).

New interpretative regolith layers have been compiled for the Lockier and Pink Hills 1:100 000 Geological Series map sheets as part of this study. These layers were constructed primarily using Landsat TM5 and Landsat ETM7 imagery (Table 1), the pre-existing 1:250 000 Geological Series map of Mount Phillips, and the newly mapped 1:100 000 bedrock geological layer for Lockier and Pink Hills (Johnson et al., 2010a; Johnson et al., 2011). Detailed regolith interpretation was accomplished using high-resolution hill-shaded orthophotographs, Google Earth TM imagery, radiometric data, digital elevation models (DEM), WAROX legacy data, and open-file company reports, where available (Table 1). The interpreted regolith layers have been ground-checked during a 10-day fieldtrip in October 2009, during which 80 field locations were visited, focusing on locations on the Eudamullah, Lockier, Yinnetharra, and Pink Hills 1:100 000 Geological Series map sheets (Fig. 2).

Sixty-five samples were taken from a variety of regolith units and regolith profiles. Thirty samples were geochemically analysed (Appendix 1), and 13 thin sections were prepared from samples of various duricrust types.

Climate

The central Gascoyne region has a semi-arid to arid climate with hot dry summers. The mean daily maximum temperature in January is 40.8°C at Gascoyne Junction and 40.3°C at Mount Phillip (Commonwealth Bureau of Meteorology, 2010). Winters are mild, with a mean daily maximum temperature of 23.8°C at Gascoyne Junction and 22.9°C at Mount Phillip (Commonwealth Bureau of Meteorology, 2010; see Tables 2, 3). Rainfall is low and highly variable with an annual average of 211.9 mm for Gascoyne Junction and 223.1 mm for Mount Phillip

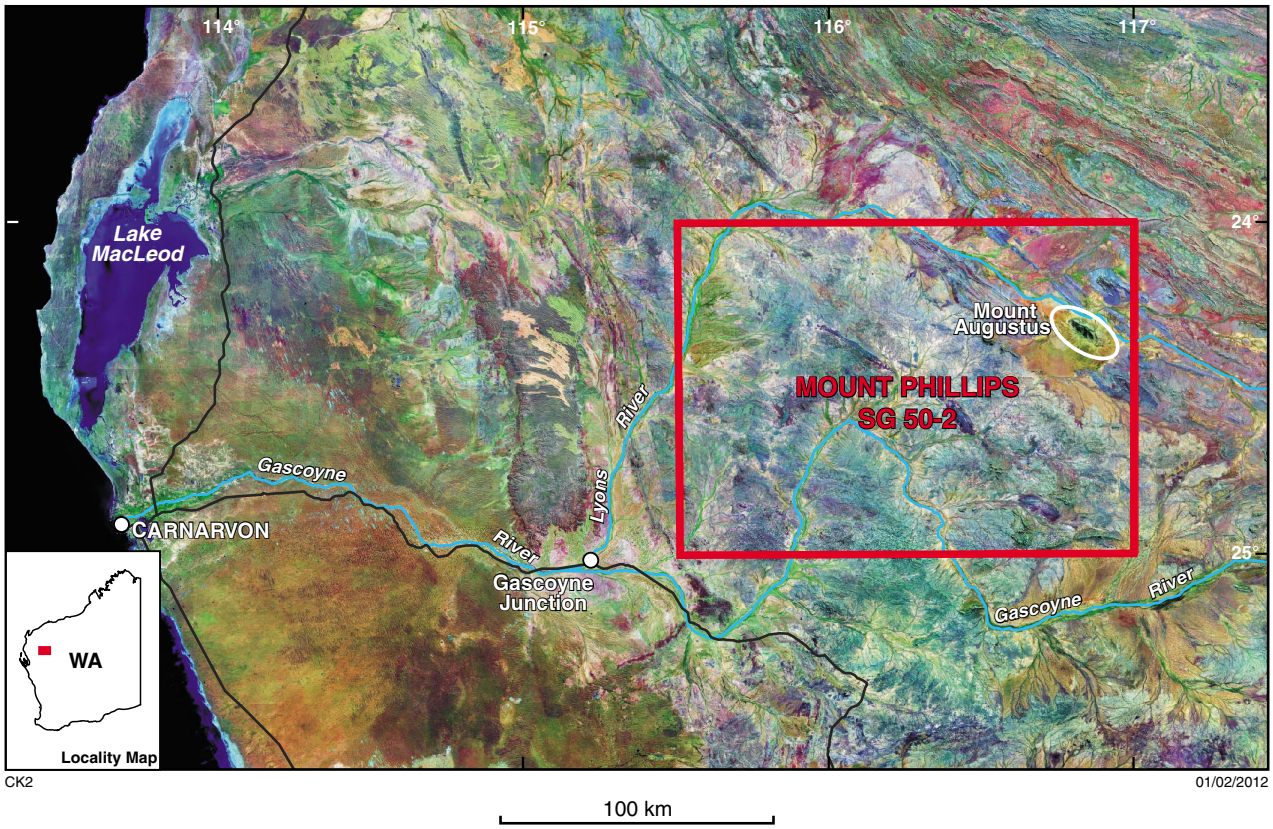

Figure 1. Location of the study area shown on a Landsat ETM7 image. Red box indicates outline of Mount Phillips 1:250 000 Geological Series map sheet (SG 50-2)

* Mount Phillips refers to the Mount Phillips 1:250 000 Geological Series map sheet unless otherwise indicated.

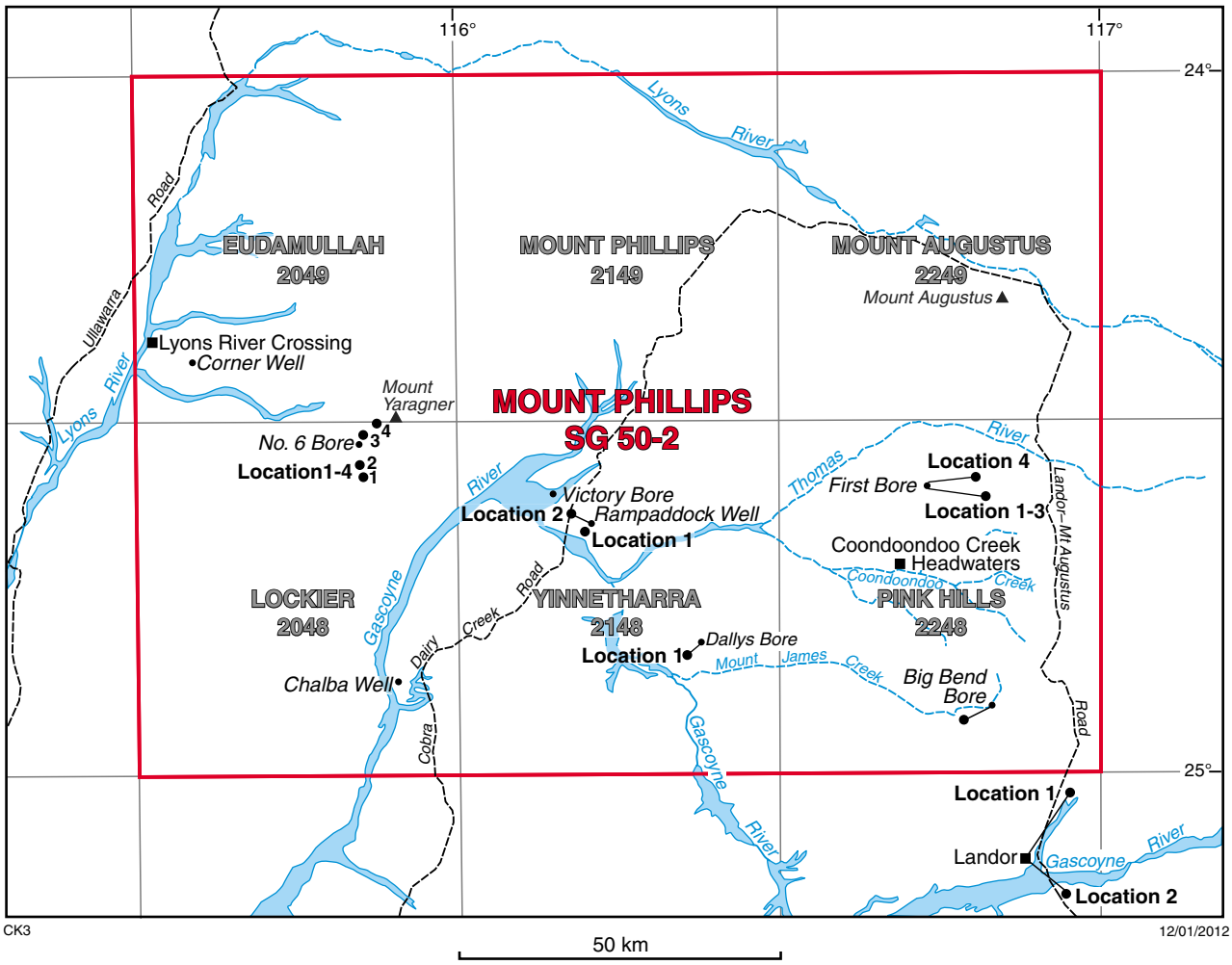

Figure 2. Field localities described in the text. Red box outlines Mount Phillips Geological Series map sheet (SG 50-2), black boxes are 1:100 000 map sheet outlines

(Commonwealth Bureau of Meteorology, 2010; see Tables 2, 3). Rainfall in the summer months (November to April) results from rain-bearing depressions from the northwest as a result of cyclonic activity. In winter, rain is produced by the interaction of tropical cloud bands from the north-northwest with strong cold fronts approaching from the southwest.

Physiography and drainage systems

The physiography of the Mount Phillips Geological Series map sheet area reflects the weathering characteristics of the three underlying geological provinces: the Gascoyne Province, the Edmund Basin, and the Southern Carnarvon Basin. Overall, the area is characterized by a well-dissected plateau capped by relict Cenozoic duricrust with isolated prominent topographic highs, such as Mount Augustus (1106 m AHD), Mount Gascoyne (789 m AHD) and Mount Phillips (780 m AHD) (Williams et al., 1983a; Sanders et al., 1997a).

Minor upland areas are found on igneous and metamorphic rocks of the Gascoyne Province in the central part of Mount Phillips. Here, the topography is generally subdued, averaging around 400 m AHD and sloping gently to the west, to an elevation of about 280 m AHD, although locally rising to 700 m AHD. Outcrops of metamorphic rocks generally give rise to a rugged hilly and dissected terrain, while large granitic areas form undulating plains with scattered low hills.

Northwest–southeast striking anticlines and synclines, developed in sedimentary rocks of the Edmund Group, form prominent ridges in the northeastern corner of the study area, whereas sedimentary rocks of the Southern Carnarvon Basin form a subdued topography with low rolling plains and isolated strike ridges and mesas.

The study area is drained by the Gascoyne, Lyons, and Thomas rivers and their tributaries (Fig. 2), which are part of the Gascoyne River drainage system, covering a catchment area of almost 76 000 km^2 (Fig. 1). The catchment trends westerly across the Gascoyne Province, Edmund Basin, and Southern Carnarvon Basin, including

Table 1. Remote sensing data used in interpreting regolith coverage for MOUNT PHILLIPS 1:250 000 Geological Series map sheet (numbers give image resolution in metres)

Dataset	*MOUNT PHILLIPS SG 50-2*
Orthophotographs (colour)	1.5
Landsat TM 5 (1991–2005)	
RGB741*	30
RGB754†	30
RGB754 DCS^	30
AGSO Ratio#	30
Gozzard Ratio°	30
PC123 of 754+	30
Landsat ETM7	
MrSid image S-51-15 RGB 742	14.25
MrSid image S-51-20 RGB 742	14.25
DEM / Derivatives	
Shaded relief	20
Contour (5 m)	Y
Geological map or digital layer 1:100 000	Y
Geological map 1:250 000	Y
Ternary radiometric image (TRI)	
KTU as RGB	100

*RGB741	RED layer = band 7 (responds to iron rich minerals)
	GREEN layer = band 4 (responds to vegetation)
	BLUE layer = band 1 (responds to water)
†RGB754	RED layer = band 7 (responds to iron rich minerals)
	GREEN layer = band 5 (responds to hydrothermally altered rocks)
	BLUE layer = band 4 (responds to vegetation)
^RGB754 DCS	RED layer = band 7
	GREEN layer = band 5
	BLUE layer = band 4
	Used to differentiate rock types. Sharper colour definition by applying a Decorrelation Stretch (DCS)
#AGSO Ratio	RED layer = Principle Component 2 of band ratios 4/3 and 5/7
	GREEN layer = ratio of bands 5/4
	BLUE layer = composite of bands 1+7
°Gozzard Ratio	RED layer = ratio of bands 5/7
	GREEN layer = ratio of bands 4/7
	BLUE layer = ratio of bands 4/2
+PC 123 of 754	Principal Component 123 of bands 754

Table 2. Climate statistics for Gascoyne Junction (Source: http://www.bom.gov.au/climate/averages/tables/cw_006022.shtml)

STATISTICS	*Jan*	*Feb*	*Mar*	*Apr*	*May*	*Jun*	*Jul*	*Aug*	*Sep*	*Oct*	*Nov*	*Dec*	*Annual*	*Years*	
Temperature															
Mean maximum temperature (°C)	40.8	39.7	37.5	32.8	27.7	23.8	23.0	24.8	28.3	32.1	35.2	38.7	32.0	47	1940 2010
Mean minimum temperature (°C)	23.7	24.3	22.5	18.6	13.8	10.4	9.3	9.9	12.0	15.2	18.1	21.3	16.6	46	1940 2010
Rainfall															
Mean rainfall (mm)	23.6	29.6	29.3	14.9	27.4	31.9	27.7	12.1	3.0	4.4	3.4	4.1	211.9	101	1907 2010
Decile 5 (median) rainfall (mm)	7.0	16.0	7.8	6.9	15.6	23.9	16.0	8.0	0.9	0.2	0.0	0.0	198.5	100	1907 2010
Mean number of days of rain ≥1 mm	2.2	2.7	2.1	1.7	2.8	3.7	3.4	2.1	0.7	0.7	0.6	0.6	23.3	100	1907 2010

Table 3. Climate statistics for Mount Phillips (1940–2010) (Source: http://www.bom.gov.au/climate/averages/tables/cw_007058.shtml)

STATISTICS	*Jan*	*Feb*	*Mar*	*Apr*	*May*	*Jun*	*Jul*	*Aug*	*Sep*	*Oct*	*Nov*	*Dec*	*Annual*	*Years*	
Temperature															
Mean maximum temperature (°C)	40.3	38.8	37.0	32.6	27.4	22.9	22.5	24.8	28.4	32.4	35.2	38.5	31.7	13	1986 2000
Mean minimum temperature (°C)	24.8	25.1	22.8	19.7	14.7	11.2	8.9	10.3	11.8	15.6	18.9	22.4	17.2	13	1986 2000
Rainfall															
Mean rainfall (mm)	29.7	47.6	28.9	16.4	24.9	27.6	18.7	10.4	2.4	2.8	3.9	8.9	223.1	101	1902 2010
Decile 5 (median) rainfall (mm)	14.8	22.9	14.2	7.9	12.6	16.3	9.2	4.2	0.0	0.0	0.0	2.0	203.6	86	1902 2010
Mean number of days of rain ≥1 mm	2.4	2.9	1.9	1.2	1.6	1.9	1.5	0.9	0.3	0.2	0.4	0.9	16.1	86	1902 2010

the Kennedy Ranges, to the coastal plain. Fluvial channels are generally broad and weakly defined by wide floodplains within even wider valleys. Streams only flow after heavy rainfall, although waterholes fed by permanent springs or soaks are present for most of the year (Dodson, 2009).

The Gascoyne River is the longest river in Western Australia extending from the Robinson Ranges at the western extent of the Gibson Desert to the coast at Carnarvon and Shark Bay with a length of about 760 km. It follows a northern sweeping bend, presumably along a paleovalley (Magee, 2009) through the southern central part of the study area. The valley floor is characteristically dominated by a well-defined, flat-bottomed sand and gravel-filled channel that is up to 500 m wide and is accompanied by extensive floodplains.

The Lyons River flows northwestward in a broad valley that drains most of the southwestern margin of the Edmund Basin on northern Mount Phillips. Here it occupies a series of incised channels, braided streams, and local waterholes (Muhling et al., 1978). The river changes course near Minnie Creek Homestead, and heads south-southwest to join the Gascoyne River near Gascoyne Junction.

The physiography of the contemporary landscape in the study area is in an overall state of degradation and erosion, with medium to very high rates of sheetwash and rill erosion (Department of Sustainability, Environment, Water, Population and Communities, 2007). This is reflected in the high density drainage pattern, especially over weathered basement rocks of the Gascoyne Province; relief inversion of relict landforms (see calcretes and paleochannels discussed below); and the high sediment load carried by the major rivers.

Regional geology

The study area encompasses Precambrian rocks of the Capricorn Orogen and the Phanerozoic Carnarvon Basin (Fig. 3). The geology of the Gascoyne Province has recently been reviewed by Sheppard et al. (2010) and Johnson et al. (2010b). It is an assemblage of granitic and medium- to high-grade metamorphic rocks in the western part of the Capricorn Orogen (Fig. 3). Archean to Proterozoic rocks of the Gascoyne Province record the progressive amalgamation of the West Australian Craton, firstly through the collision of the Pilbara Craton with the Glenburgh Terrane during the Ophthalmian Orogeny, then the subsequent collision of a combined Pilbara – Glenburgh Craton with the Yilgarn Craton during the Glenburgh Orogeny (Johnson et al., 2010a; Johnson et al., 2011). The province was structurally and metamorphically reworked on several occasions during the Meso- and Neoproterozoic (Sheppard et al., 2010).

Mesoproterozoic sedimentary rocks of the Edmund Basin (Edmund Group of the Bangemall Supergroup) unconformably overlie rocks of the Gascoyne Province in the northeastern corner of Mount Phillips. They represent a sequence of continental and marine sedimentary rocks, which have been extensively folded and faulted but only weakly metamorphosed (Williams et al., 1983a; Martin et al., 2007).

Phanerozoic sedimentary rocks of the Bidgemia Sub-basin of the Southern Carnarvon Basin crop out in the southwestern corner of the study area. These dominantly comprise Lower Permian glacigene sedimentary rocks that unconformably overlie rocks of the Gascoyne Province (Williams et al., 1983a; Hocking et al., 1987).

Cenozoic geology of Mount Phillips: previous work

In recent years there have been considerable advancements in the understanding of the geology of the Capricorn Orogen (Sheppard et al., 2008; Rasmussen et al., 2010; Sheppard et al., 2010; Thorne, 2010; Johnson et al., 2010b, 2011) but little work has been carried out on the Cenozoic geology and regolith, despite extensive exploration activity for uranium in regolith-hosted calcrete and older calcareous colluvium deposits since the 1970s (Cooper et al., 1998).

Previous descriptions of the Cenozoic geology, including the regolith of the Mount Phillips Geological Series map sheet area involved subdivision into undivided Quaternary alluvial, colluvial, and eolian units, and older semi-consolidated colluvium, lacustrine deposits, calcrete, and remnants of lateritic and siliceous duricrust surfaces of probable Neogene age (Williams et al., 1983a). The only stratigraphic formation encountered in the area is the Nadarra Formation (Fig. 4), a carbonate-rich lacustrine deposit preserved as a distinct but intensively dissected valley-fill deposit (Williams et al., 1983a; Hocking et al., 1987). As the Nadarra Formation is partly overlain by ferruginous duricrust, Hocking et al. (1987) inferred a Miocene to Pleistocene age (Hocking et al., 1987).

Geochemical sampling and regolith-materials mapping was carried out for the Mount Phillips Geological Series map sheet as part of the GSWA regolith geochemistry program (Sanders et al., 1997a). A total of 1038 regolith sites was sampled at a density of one sample per 16 km^2, comprising 933 stream sediments, 57 sheetwash deposits, and 48 soil samples. A map showing the distribution of the different regolith materials was compiled (Sanders et al., 1997b). No samples were taken from relict or residual regolith units such as calcrete or silcrete. The resulting regolith-materials map (Sanders et al., 1997b) is based on the regolith-landform approach to mapping (Anand et al., 1998) where regolith is classified according to its nature and position in an idealized landform profile into one of three regimes: relict, erosional, and depositional. The regolith codes and descriptions used for the Mount Phillips regolith-materials map precede those of the current regolith classification scheme currently employed in GSWA (Hocking et al., 2007). Results of the geochemical sampling showed that granitic rocks of different age and composition could be clearly distinguished by their regolith geochemistry. The Edmund Group rocks differ from other geological units in terms of their dominantly mafic regolith signature due to the

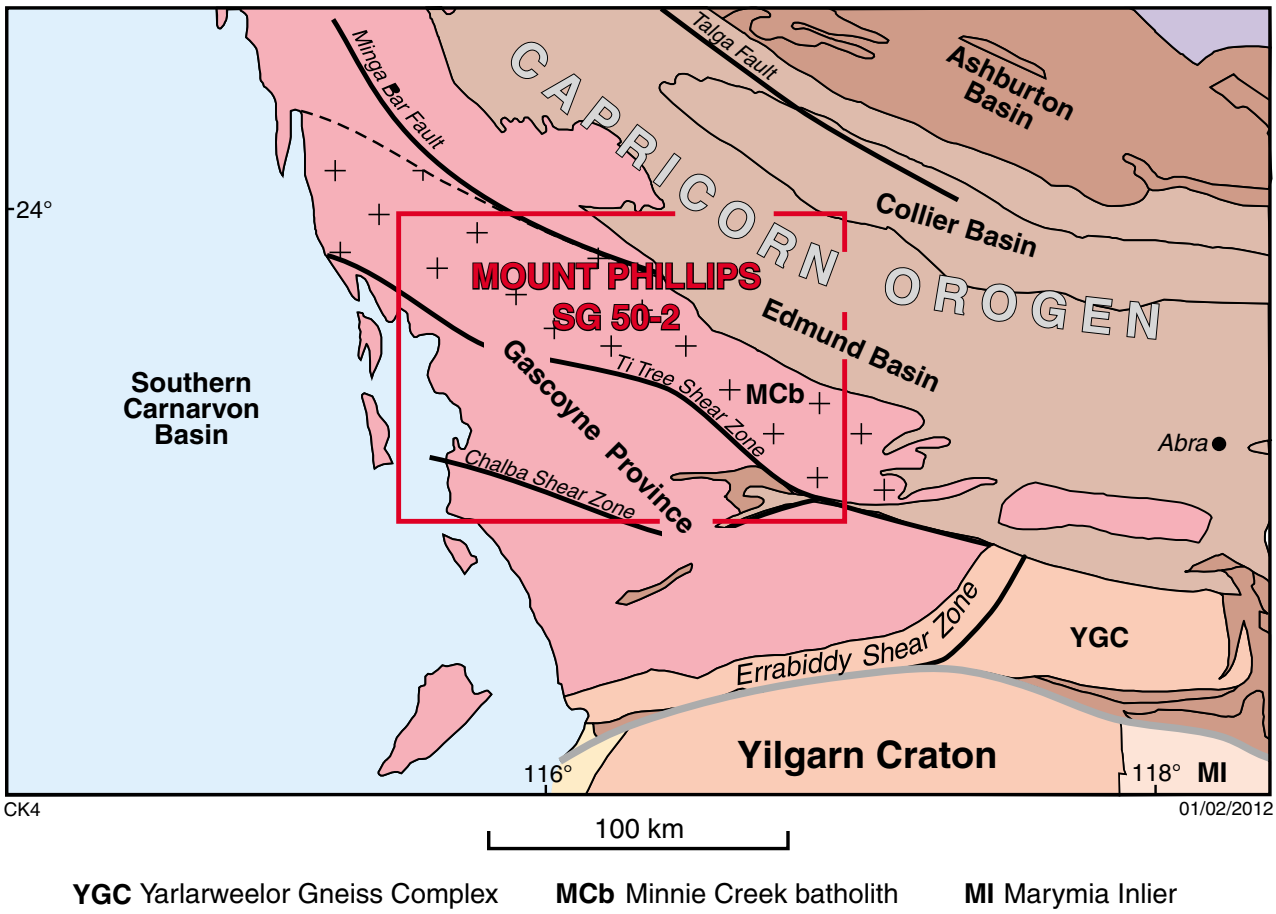

Figure 3. Simplified geology of part of the Gascoyne area showing outline of Mount Phillips Geological Series map sheet (SG 50-2)

abundance of mafic sills superseding the signature of the sedimentary rocks, whereas the regolith over the former metasedimentary units of the Gascoyne Province is characterized by its chemical diversity and areas of high pegmatite-element concentrations. Four areas of mineral potential were identified, including the central and south-western areas of the Gascoyne Province, the Edmund Group, and parts of the early- and late-stage granitic rocks (Sanders et al., 1997a).

The age of the landform elements and associated regolith is poorly constrained for the Gascoyne regions, as for most areas in Western Australia. Regolith on the Mount Phillips Geological Series map sheet is shown as Quaternary or undifferentiated Cenozoic, depending on whether or not the regolith is related to present-day processes (Williams et al., 1983a). In the absence of absolute age data, assigning regolith as either Quaternary or Cenozoic is based on the position of the unit in the landscape, its degree of induration, and the extent to which it has either been dissected by more recent processes or the relationship with overlying younger material. Thus, relict or residual units (R) are interpreted to be the oldest regolith units within the study area. Although these units have been assigned to the Cenozoic, it is possible they could be Mesozoic or older (Hocking et al., 1987; Pillans, 2005).

Mineral exploration

The Gascoyne region is considered prospective for unconformity-type, vein-type, granite-related, and calcrete-hosted uranium mineralization, as well as for gold and base metals (Cooper et al., 1998). The main regolith-focused exploration is for uranium, particularly in the drainage divides and in calcareous duricrusts. Over 45 uranium occurrences have been discovered on Mount Phillips since the early 1970s (Cooper et al., 1998).

Elevated concentrations of uranium characterize the contact of the Edmund Basin with the southern Gascoyne Province rocks, from Wyloo through to the Mount Phillips Geological Series map sheets (Cooper et al., 1998). Primary mineralization in mainly granitic rocks of the Gascoyne Province is the main source of uranium for secondary calcrete-hosted deposits, which are located within the paleovalleys of the Gascoyne River and its tributaries (Cooper et al., 1998).

Regolith landform units

Regolith landform units have developed due to multiple episodes of weathering, erosion, and deposition over an extended period over wide areas of the Gascoyne region. These units can provide critical information about the development of regolith through time and are the key elements in developing landscape evolution models. The main emphasis of this Record is understanding relict regolith units, which can result from in situ weathering of underlying bedrock, or which represent remnants of a previous landform like paleochannels, and their relationship with the modern day landscape. In addition, some younger regolith units will be investigated.

Geological provinces and regolith distribution

The results of the regolith mapping on Lockier (Johnson et al., 2011) and Pink Hills (Johnson et al., 2010a) show that there is a broad relationship between the distribution of regolith materials and landforms with the underlying bedrock geology and its physiographic expression.

Regolith profiles over the Gascoyne Province are characterized by in situ weathering of basement rocks, resulting in the development of saprock or saprolite. These commonly have an in situ ferricrete or siliceous capping, or are unconformably overlain by variably altered sedimentary deposits of different ages. Several generations of colluvium showing variable thickness, degree of compaction, and cementation and therefore different stratigraphic ages, are found throughout the area. They occur mainly towards the base of isolated hills and prominent quartz veins as well as over undulating plains of granitic rocks. The composition of the colluvium is closely related to the adjacent bedrock, and seldom contains exotic clasts. The modern day Gascoyne River and its tributaries follow older paleovalley systems (Van De Graaff et al., 1977; Magee, 2009), now preserved as relict elevated calcrete, silcrete and ferruginous duricrust. Alluvial channel and floodplain deposits of different generations

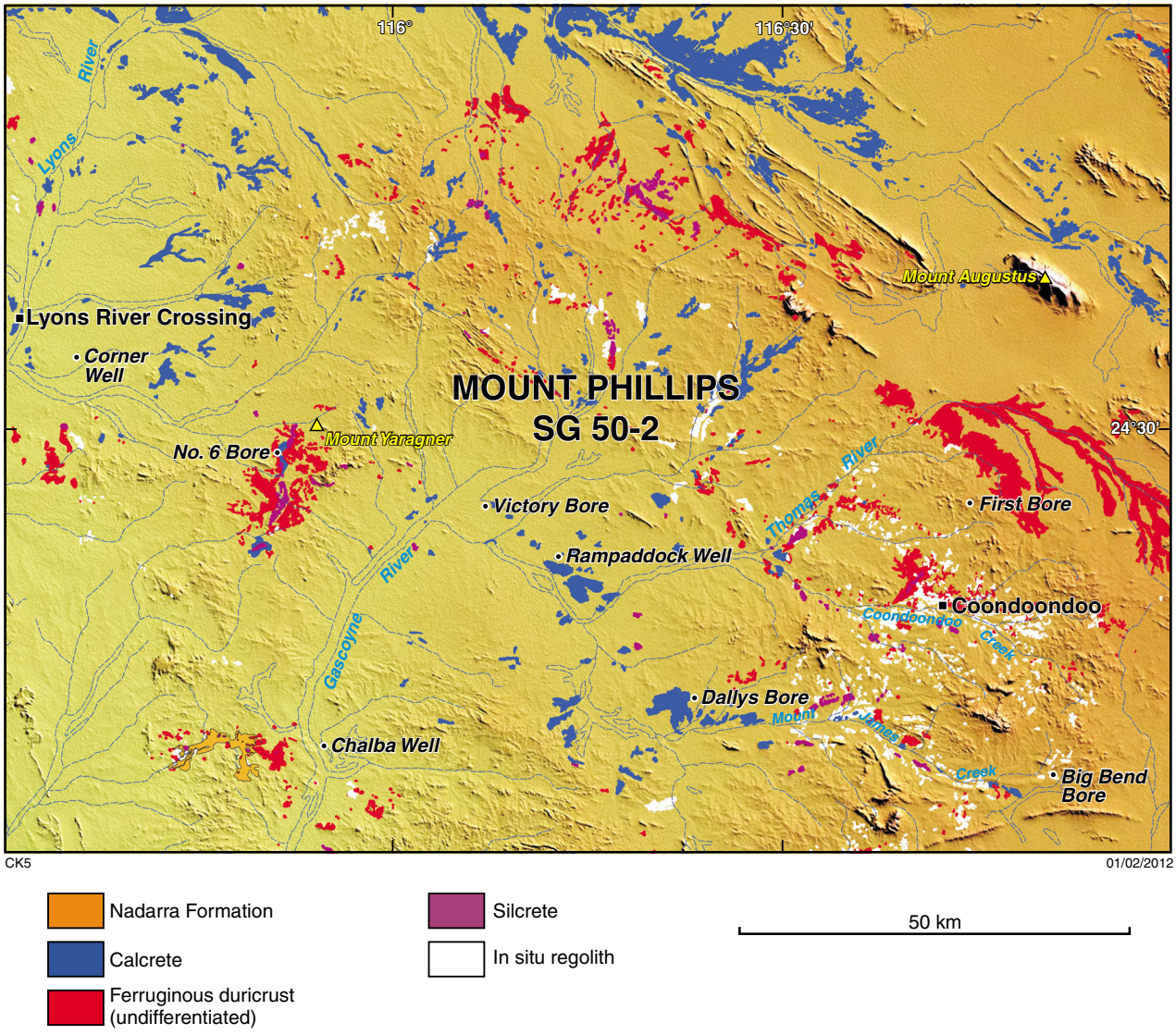

Figure 4. Occurrence of various regolith units and Nadarra Formation on Mount Phillips draped over a hill shaded Digital Elevation Model (SRTM3 DEM)

and variable thickness can be found within the Gascoyne River system and its tributaries.

Sedimentary rocks of the Edmund Group are associated with colluvium and sheetwash, which are widely underlain by transported ferruginous duricrust. Alluvial fans found on the flanks of synclines and older valley-fill calcretes are well exposed within the Lyons River valley.

Sheetwash, with a distinctive tiger bush pattern, is the main regolith type encountered over the gently westward-dipping sedimentary rocks of the Southern Carnarvon Basin. Relict regolith units are less common, reflecting both the shorter weathering history of these rocks and the highly erosive character of the Gascoyne River drainage system that results in less weathered rejuvenated outcrops.

Relict regolith units

Duricrusts

The term duricrust is used for regolith material indurated by a cement, or for the cement itself. It is found at or near the surface, or as a layer in the upper part of the regolith (Eggleton, 2001). The cement may be siliceous (silcrete), ferruginous (ferricrete), calcareous (calcrete), aluminous (alcrete), gypseous (gypcrete), manganiferous (manganocrete), dolomitic (dolocrete), salty (salcrete), or any combination of these. The main duricrust types encountered in the Mount Phillips Geological Series map sheet area are calcrete, silcrete, and ferruginous duricrust.

Widespread uncertainty and disagreement exists about the depositional processes and genesis of different duricrust types (Martin et al., 2007; Magee, 2009). The most widely accepted view is that for arid parts of Australia, silcrete formation probably occurred in two distinct Cenozoic episodes, each preceded by a period of ferricrete formation (summarized in Magee, 2009). Calcrete formation was related to the onset of arid conditions in the Neogene (c. 23 Ma) and likely represents the final phase of secondary duricrust deposition. Iron and silica mobilization continued, at variable rates, throughout much of the Cenozoic.

The study on the Gascoyne regolith has shown that the stratigraphic relationships between the different duricrust units is complex due to a combination of precipitation, overprinting and replacements processes, and weathering events. Interpretation is also hampered by the lack of absolute regolith ages.

Calcrete

Calcretes and their associated sediments are widespread in the arid regions of Western Australia and are important hosts for uranium mineralization (Butt et al., 1977) and groundwater resources (Magee, 2009).

Calcrete is a near surface, terrestrial accumulation of predominantly calcium carbonate resulting from the cementation of the soil profile, sediment, and bedrock by calcium carbonate. This process commonly involves displacement or replacement and takes place where vadose (subsurface water above the water table) and shallow phreatic (subsurface water below the water table) groundwaters become saturated with respect to calcium carbonate (Wright and Tucker, 1991).

Genetically, calcretes can be classified into groundwater and pedogenic types, but it is not always easy to distinguish between these two in the field as they have similar morphological and macroscopic features (Chen et al., 2002). The most common type of groundwater calcrete is 'valley calcrete', which is found as 1–30 m thick sheets along several ancient trunk valleys in Western Australia (Chen et al., 2002). It is formed by the in situ replacement of valley-fill debris by carbonate precipitated from percolating carbonate-saturated ground and soil water. Butt et al. (1977) subdivided calcretes into trunk-valley calcretes, playa lakes, and dissected calcretes based on uranium occurrences.

Calcretes on the Mount Phillips Geological Series map sheet area have previously been classified as dissected calcretes by Butt et al. (1977) and as valley calcretes by Williams et al. (1983a). Furthermore, Williams et al. (1983a) recognized two subtypes: dissected valley calcrete, common in the Gascoyne River drainage, and buried trunk-valley calcrete, found over Bangemall Supergroup rocks.

The majority of the calcretes in the Mount Phillips Geological Series map sheet area are relict and are being actively dissected. Calcite precipitation and cementation have only been observed in older alluvium exposed within cutbanks in modern-day river channels.

In some areas, calcrete overlies ferruginous duricrust hardpan (Williams et al., 1983a), and is itself commonly capped by silcrete. Dissected high-level calcretes that are unrelated to the present-day drainage systems are interpreted as part of a paleodrainage system (Williams et al., 1983a; Williams et al., 1983b; Hocking et al., 1987).

Calcretes are commonly opalized or have bands of chalcedony and opaline material that probably mark former water tables. This is common in granitic terrains of the Gascoyne Province, where high concentrations of dissolved silica in shallow groundwater are the result of feldspar weathering (Magee, 2009). Most calcretes show signs of surface reworking due to dissolution and re-precipitation of calcite and dolomite by rainwater.

In addition to these calcretes, the Cenozoic Nadarra Formation is found on Mount Phillips (Fig. 4; Williams et al., 1983a; Hocking et al., 1987). It is typically a silicified, silty, micritic lacustrine limestone that includes minor calcrete. The limestone is composed of structureless to poorly bedded, fine-grained calcilutite and variably calcareous to calcreted mudstone and siltstone, with minor fine-grained gritty and silty sandstone. The Nadarra Formation unconformably overlies lateritic duricrust, with a commonly irregular basal contact, and is inferred from stratigraphic constraints to be Miocene to Pleistocene (Williams et al., 1983a) or Pliocene to Pleistocene in age (Hocking et al., 1987).

In order to better understand the calcretes on Mount Phillips, 15 calcrete outcrops have been investigated, resulting in the recognition of five different calcrete types. Their subdivision is based on a combination of their interpreted genesis and geomorphological position in the present-day landscape. The calcrete types are groundwater calcrete mesas (valley-fill calcretes), younger groundwater calcrete, spring-associated calcrete mounds, calcrete layer over weathered bedrock, and pedogenic calcrete.

Groundwater calcrete mesas (valley-fill calcretes)

In Australia, groundwater calcretes are reported to have developed only north of about latitude 30°S, as their formation requires arid conditions with very high potential evaporation, as well as the periodic recharge of groundwater systems (Mann and Howitz, 1979). Irrespective of size, the shape of groundwater calcrete deposits is usually elongate and controlled by the drainage topography (Mann and Howitz, 1979). Generally groundwater calcretes are preserved along the main drainage channels and their margins, although some deposits are preserved over a wider area of the drainage system (Chen et al., 2002).

In some areas, such as in the Ashburton Valley, groundwater calcretes are dissected and preserved as perched remnants or mesas. Here calcretes form 5–10 m thick mesa-like cappings which stand some tens of metres higher than the level of the present valley floor and the surrounding plain (Mann and Howitz, 1979). These dissected calcretes represent the more resistant remnants of calcrete ribbons, which formed in older drainage systems. In some cases these systems flowed in the opposite direction to the present-day drainage (Mann and Howitz, 1979). These older valley-fill calcretes have been subsequently dissected and isolated by the incision of younger active stream systems.

On Mount Phillips, valley-fill calcretes can be found as mesas along and adjacent to the Gascoyne River valley and its tributaries, in particular the Thomas River and Mount James Creek (Figs. 2, 4).

Victory Bore locality, Yinnetharra Station (412770E 7278787N)

In the vicinity of Victory Bore on Yinnetharra Station, a string of dissected calcrete-topped mesas stand above the flat interfluve area between the Gascoyne and Thirty Three rivers. These mesas have previously been mapped as dissected valley-fill calcrete, in part replaced by opaline silica (Williams et al., 1983a). Two locations have been investigated.

Victory Bore locality: Location 1 (412515E 7278937N)

The calcrete 300 m northwest of Victory Bore is about 15 m thick and is mainly covered by colluvium (Fig. 5). Good outcrops are only found along the cliff face below the top of the mesa, where a 4 m thick section has been divided into four units (Units A–D; Fig. 6).

Unit A, exposed at the bottom of the cliff face, has a minimum thickness of 1 m, as its base is not exposed due to thick scree cover. The unit comprises a reddish, subhorizontally bedded, poorly sorted, fine- to coarse-grained ferruginized sandstone with isolated pebble layers (Fig. 7a). The sand fraction is dominated by angular to subangular quartz grains, which show few grain-to-grain contacts. The grains are surrounded by a clayey to silty ferruginous matrix that is partly replaced by carbonate. The carbonate itself seems to be dissolved in many places, giving the sandstone a secondary porous texture. Faint subhorizontal bedding with individual beds 1–2 cm thick have been observed.

Unit B, which conformably overlays Unit A, is characterized by a 1-m thick, light-red to whitish deposit of pervasively carbonate cemented, subhorizontally bedded, poorly sorted, fine to very coarse grained sandstone, which is pervaded with carbonate veins (Figs. 7b, c). The ferruginous matrix has been partly replaced by carbonate mud, and fibrous calcite growth structures are commonly found in thin section (Fig. 8a). Individual quartz grains are angular to subrounded and may be enclosed in an isopacheous calcite crust (Fig. 8b). The CaO content increases from 0.91% in Unit A (GSWA199527, Appendix 1) to 30.2% in unit B (GSWA199528, Appendix 1) indicating that the latter has been intensively overprinted by carbonate-rich groundwater as part of the post-depositional calcrete development.

Unit C erosively overlies Unit B and consists of a 75 cm thick, carbonate-cemented, horizontal to trough cross-bedded, poorly sorted, fine to very coarse grained, ferruginized sandstone. Towards the top of this unit, the sediment is cut by a network of numerous calcareous and siliceous veins, which are partly aligned along bedding surfaces. Several burrows and root casts are present in this unit indicating intensive bioturbation (Fig. 7b). Thin sections reveal that calcretization produced a mesh-like network of calcite microveins throughout the sediment (Fig. 8c). Two phases of vein filling are visible. An initial phase consists of thick, dendritic, sheaf-like calcite crystal aggregates with long axes orientated perpendicular to the fracture surface. A second phase comprises coarse-grained polygonal calcite grains (Fig. 8d).

Unit D is exposed at the top of the cliff section and is composed of carbonate-cemented, massive, moderately sorted, fine- to coarse-grained sandstone, up to 1.20 m thick. The base of Unit D is characterized by a distinctive layer of vugs lined with opaline silica (Fig. 7d). This layer possibly represents a former groundwater table, now over 25 m above the present-day floor of the Gascoyne River valley. Unit D is pervasively cross-cut by numerous calcareous and siliceous veins (Fig. 7e). In thin section, angular to subangular quartz grains are set in a microcrystalline carbonate matrix (Fig. 8e). Some quartz grains have been intensively fractured due to the growth of carbonate (Fig. 8f). The carbonate content of this unit (47.3% CaO; GSWA199530, Appendix 2) is the highest in this section, effectively making this uppermost unit more resistant to weathering, and protecting the underlying units from further erosion.

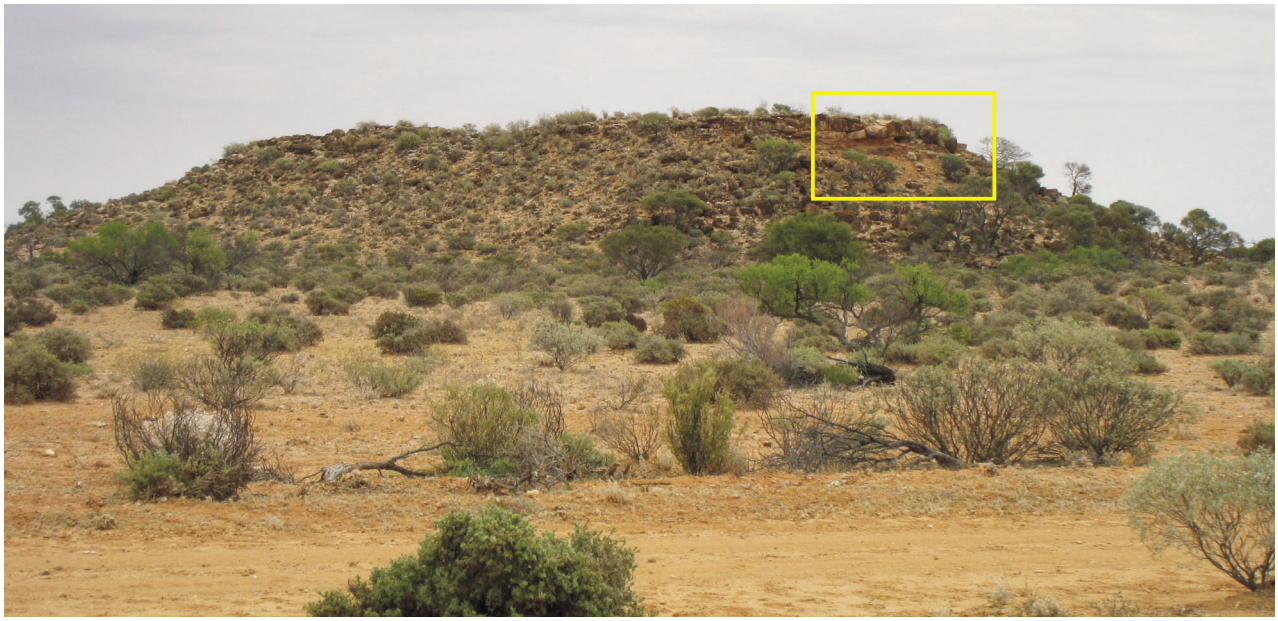

Figure 5. Calcrete-capped mesa at Victory Bore, Location 1, 6.2 km NNW of Yinnetharra homestead. The outcrop is part of a string of mesas that are located along the margin of the former Gascoyne River valley. Box indicates the location of the logged profile in Figure 6

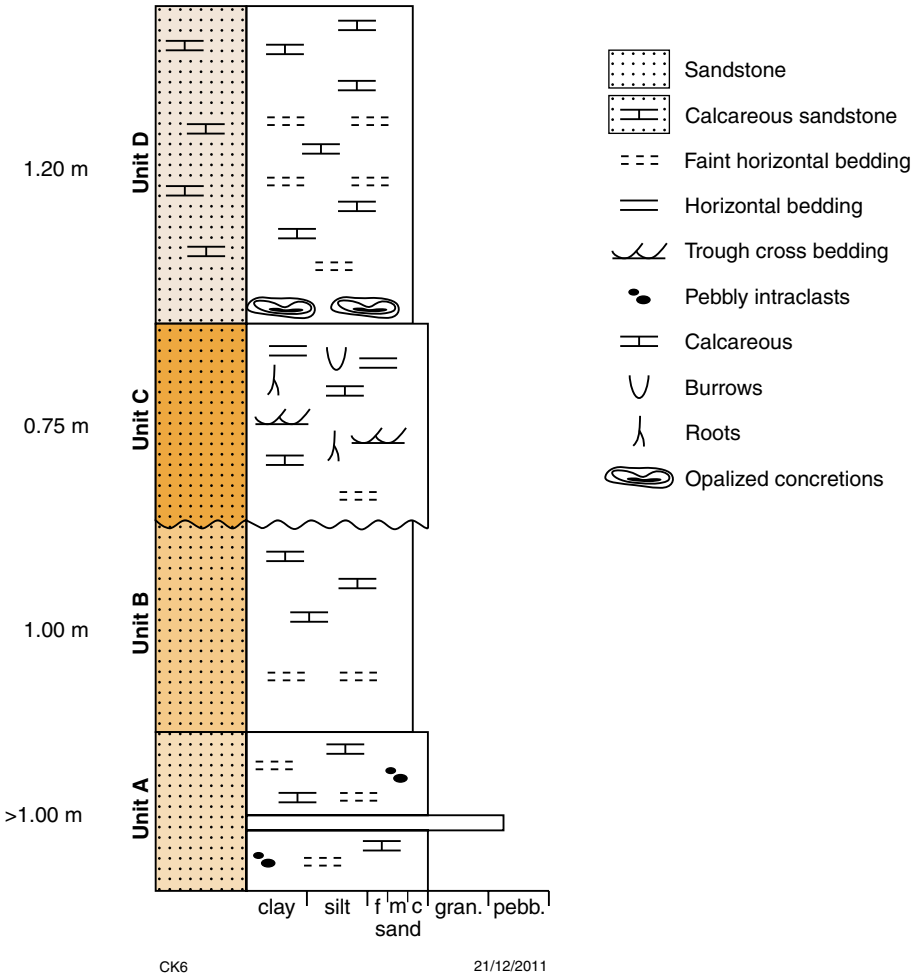

Figure 6. Measured section at Location 1, Victory Bore locality. Section location shown in Figure 5

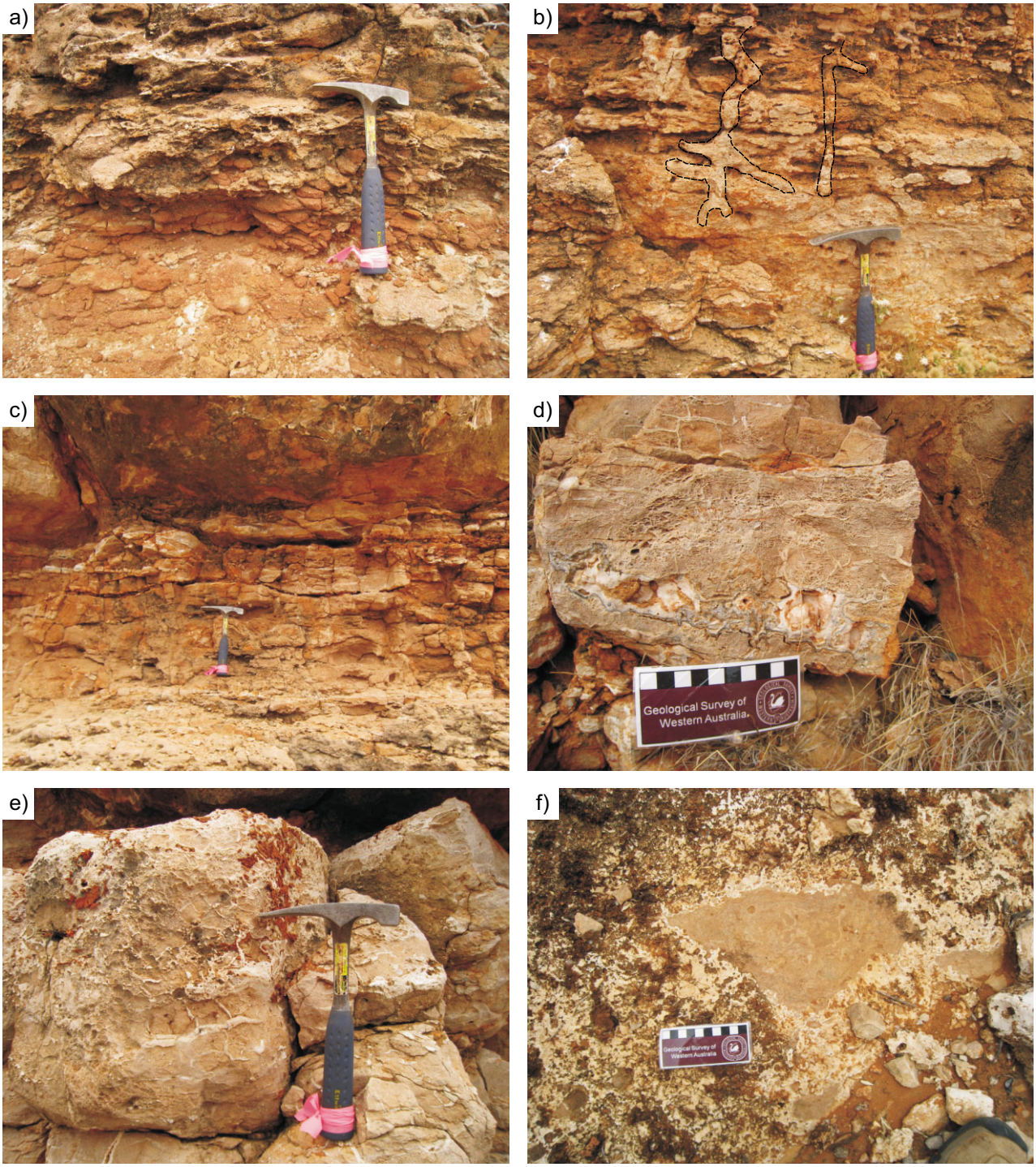

Figure 7. **Outcrop views of sedimentary units encountered in cliff section of Figure 5 at Victory Bore, Location 1: a) ferruginized bedded sandstones of Unit A overlain by carbonate-cemented sandstones of Unit B; b) calcified burrows (outlined) in Unit C, possibly representing ant nest with chambers; c) lateral expression of units B, C, D and their contacts; d) base of Unit D showing vugs lined with opaline silica, possibly representing former groundwater level; e) highly indurated sandstone with calcareous and siliceous veins; f) embedded calcrete clast at the top of the mesa outcrop (scale bar: 10 cm)**

The top part of the succession is not found in this section, but is preserved on the top of an adjacent mesa. There, grey, partly laminated, angular to subangular, 0.5 – 20 cm diameter clasts of partly silicified calcrete are surrounded by a whitish, medium-grained, silica- and carbonate-rich matrix (Fig. 7f). Some of the carbonate has been replaced by opaline silica. In thin section, chalcedony with radial fibrous growth was observed and probably formed due to the replacement of carbonate by opaline silica (Fig. 8g). Irregular-shaped vugs, filled with laminar chalcedony and coarse-grained quartz crystal mosaics, are also present within fine-grained calcareous matrix (Fig. 8h).

Victory Bore locality: Location 2 (412963E 7278854N)

A similar lithostratigraphic succession as at Location 1 is exposed about 100 m southeast of Victory Bore. Here, the exposure is poor due to a more extensive scree cover and a less pronounced cliff face along the mesa top. Greenish-red, carbonate-cemented sandstone crops out 3 m topographically lower than the lowest part of Unit A in Location 1. This sandstone is faintly bedded, poorly sorted, fine to very coarse grained, with isolated pebbles of angular to subrounded quartz, and platy angular feldspar clasts of up to 0.7 mm, in a clay to silty matrix. Some reworked angular rip-up mud clasts up to 5 mm diameter have also been observed. The sandstone is heavily mottled and characterized by red–green–white colour changes over short distances.

Units A–C are not as well exposed as at Location 1 but sandstones with comparable composition, texture, and degree of carbonate cementation have been observed.

At the top of the mesa, partly opalized, cellular silcrete crops out, and in many places is coated by <1 mm thick iron crust. The silcrete includes pockets of relatively unsilicified or partly silicified calcrete. The whole outcrop surface shows typical karst weathering with sharp edges and pockmarks due to carbonate solution (Fig. 9a). The thin section of a partly silicified calcrete shows that the original sediment was a poorly sorted, fine- to medium-grained sandstone (Fig. 9b) prior to calcretization and silicification. The sediment has been ferruginized and a remnant of this ferruginization is still visible in the iron-rich matrix in which very angular to subrounded quartz grains are embedded (Fig. 9b).

Laminated calcrete clasts (Fig. 9c) may have formed biogenically. In thin section, the lamination is formed by layers of small, densely packed micrite peloids set in a carbonate matrix (Fig. 9d).

The peloids are subround to round, 0.1 – 0.25 mm in diameter, and are either homogenous or display a faint internal structure with an occasional clast in the centre of some grains. The origin of these peloids is difficult to determine. They may represent fecal pellets, strongly micritized grains, or rounded fragments of reworked carbonate mud (Adams et al., 1984). Alternatively, they can also be directly produced by calcareous algae and cyanobacteria, or as a cement formed with the microbial involvement. Peloids are interpreted to be mainly indicative of a low-energy depositional environment (Tucker, 2001).

Interpretation

The succession at both of the Victory Bore locations provides a good insight into the development of valley-fill groundwater calcrete and shows that these sediments have undergone a complex depositional and weathering history.

Valley-fill calcretes are traditionally assumed to be a chemical precipitate within the fluvial sediments of an ancient drainage system (Butt et al., 1977; Mann and Howitz, 1979). Evidence of an alluvial origin of the deposits at the Victory Bore localities is evident throughout the succession. The sedimentology of the sandstones points to a short transport distance, as sorting is poor and most quartz grains are angular to subrounded. The sediment source must have been located close by and composed of a substantially weathered basement terrain, as few compositional components other than quartz are present. In the lower parts of the succession bedding is faint and thin, which may result from either unconfined sheetwash, or from low-energy stream processes, coupled with limited variation in sediment grain size and composition. Towards the top, bedding is more distinct and some trough-cross bedding is preserved. As bed thickness is still very thin, with individual beds from 2–15 cm thick, deposition in a wide fluvial channel environment is likely. Root casts and ant burrows in the upper part of the succession indicate a less energetic, subaerially exposed environment, such as a floodplain or abandoned channel (Fig. 7b).

Throughout the succession, ferruginization of sediments occurred prior to calcrete formation. This differs from the interpretation of Mann and Howitz (1979) regarding groundwater calcrete formation in Western Australia. They argued for initial carbonate precipitation within an alluvial valley fill during or shortly after sediment deposition. In the case of the sediments encountered in the Victory Bore locality, an extended period of weathering favouring ferruginization must have taken place prior to calcrete formation.

The different stages in the development of the studied succession are preserved in a slabbed sample (Fig. 10; GSWA199528). After initial ferruginization, the host sediments have been overprinted by calcrete. In thin section the presence of calcite cement around grain contacts (Figs. 8a,e, 9c) indicates an early phase of cementation in the vadose zone, where pores in the sediment were not completely water filled (Adams et al., 1984). During alternating episodes of wetting and drying, mobilization of intraformational waters transferred, concentrated, and deposited the carbonate within the ferruginized sediment. The sediment was brecciated and indurated by the influx of carbonate-bearing groundwater, resulting in carbonate cementation and the precipitation of calcite. Calcrete formation continued in the phreatic zone with the formation of calcrete pods and domes, some of which coalesced and caused upward displacement and the formation of surface mounds (Fig. 11). As carbonate is pushed above the water table, hardening and recrystallization proceeds. Secondary processes and silicification occurred, and surface reworking by weathering resulted in a hard, locally laminated, calcite cap (Mann and Howitz, 1979).

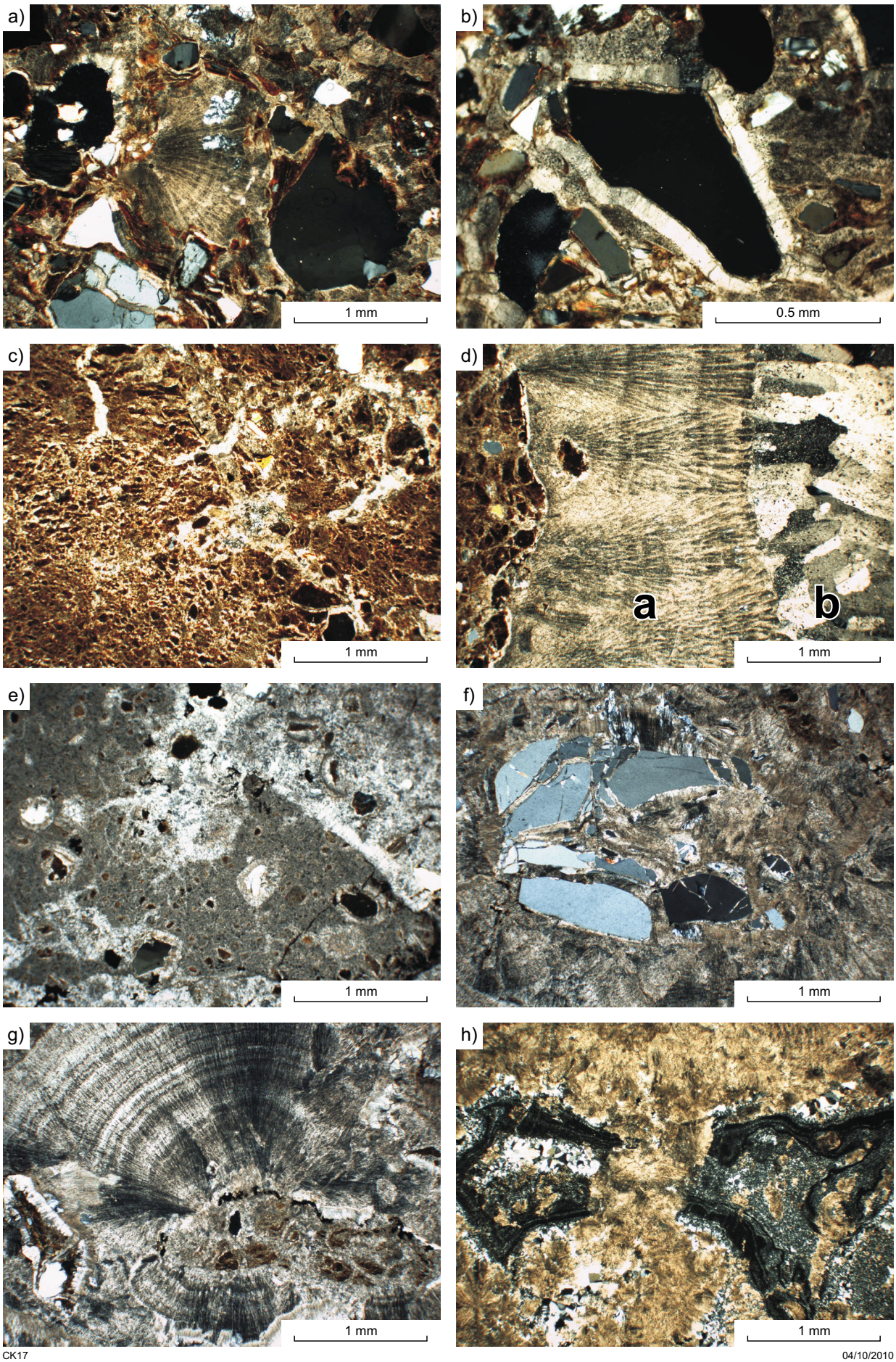

CK17

04/10/2010

Figure 8. **(facing page) Photomicrographs (crossed polars) of calcrete samples from Victory Bore, Location 1: a) angular quartz grains in a ferruginous matrix, partly replaced by carbonate mud and fibrous calcite (GSWA199528); b) isopachous calcite crust around a quartz grain (GSWA199528); c) angular quartz grains in a muddy ferruginous matrix. Calcretization has produced a mesh-like network of calcite micro veins (GSWA199529); d) two-phase vein filling showing (a) 1 mm thick dendritic sheaf-like calcite crystal aggregates with long axes orientated perpendicular to fracture surface, and (b) coarse-grained polygonal calcite mosaic growth in second phase (GSWA199529); e) angular to subangular quartz grains in a microcrystalline carbonate matrix (GSWA199530); f) quartz grain in the centre has been fractured by the growth of calcite (GSWA199530); g) chalcedony with radial fibrous growth formed due to replacement of carbonate by opaline silica (GSWA199526); h) irregular-shaped vugs filled with laminar chalcedony and coarse-grained quartz crystal mosaics in a fine-grained calcareous matrix (GSWA199526).**

No. 6 Bore locality, Eudamullah Station (383256E 7286817N)

No. 6 Bore locality: Location 1 (383507E 7286675N)

Calcrete crops out in an older, approximately 10-m high erosional terrace along the southern bank of a tributary of Onslow Creek, 300 m east of No. 6 Bore. Metre-scale, rectangular calcrete blocks have broken off the terrace, with each block characterized by distinctive pockmarked weathering (Fig. 12a, b). Locally silicified areas are more resistant to weathering. They are characterized by intervals of carbonate-cemented, orange-coated, moderately sorted, very fine to medium grained sandstones. Weathering also accentuates bedding within the calcrete (Fig. 12a). The whitish calcrete has a massive crystalline to sugary texture and is riddled with silcrete and calcite veins. Moderately sorted, very fine to medium grained sand layers are common within the calcrete. In thin section, spherical peloids show botryoidal overgrowths of fibrous calcite

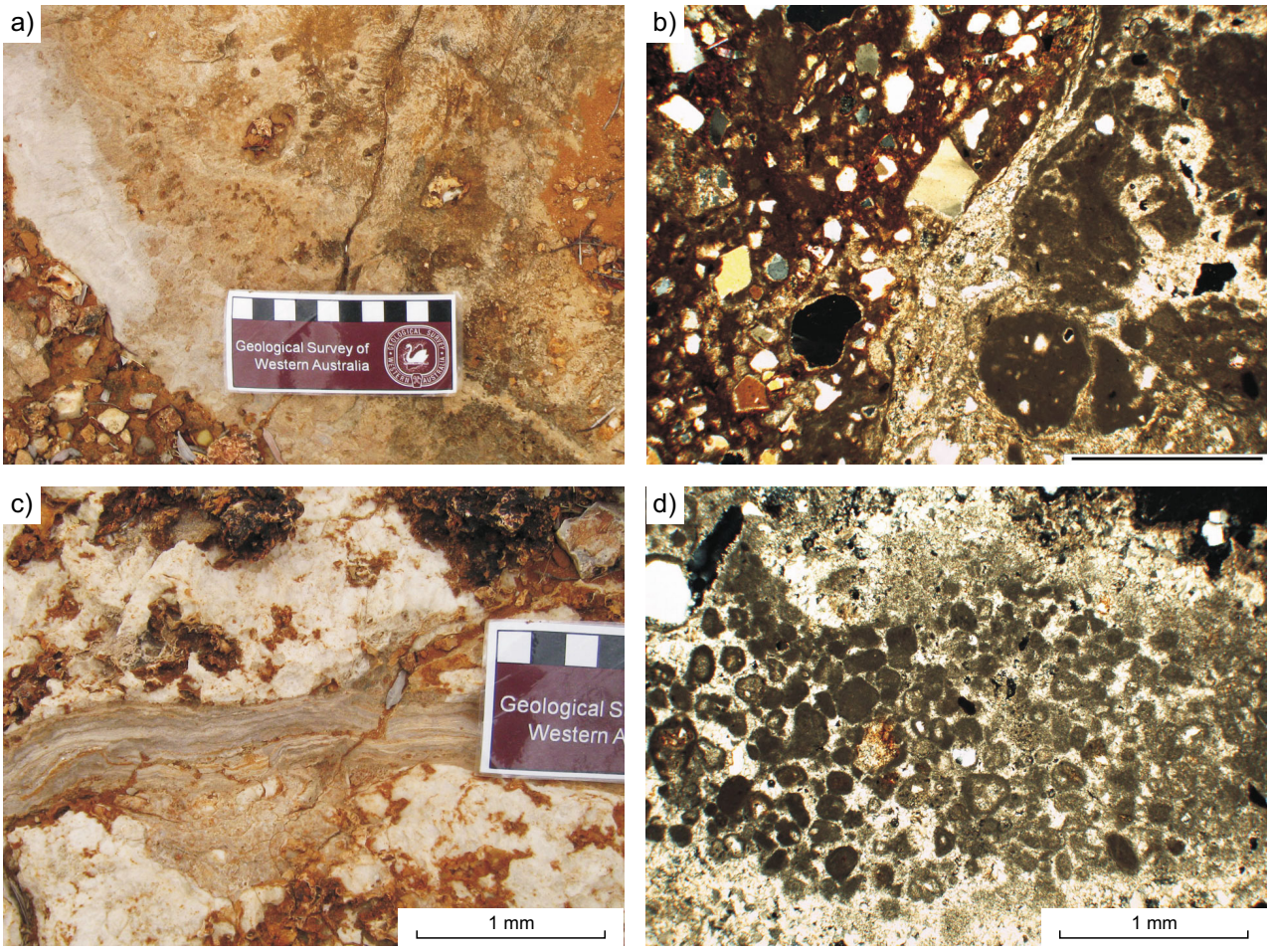

Figure 9. **Outcrop views and photomicrographs from calcrete-topped mesa of Location 1 at Victory Bore: a) calcrete with typical surface weathering crust; b) photomicrograph (crossed polars) of calcrete showing angular to subrounded quartz grains embedded in a ferruginous (left) and calcareous (right) matrix, which is broken up by carbonate veins (GSWA199531); c) laminar calcrete clast (centre) surrounded by massive calcrete; d) photomicrograph (crossed polars) of laminated calcrete showing that the lamination is the result of layers of small, densely packed peloids in a carbonate matrix (GSWA199532)**

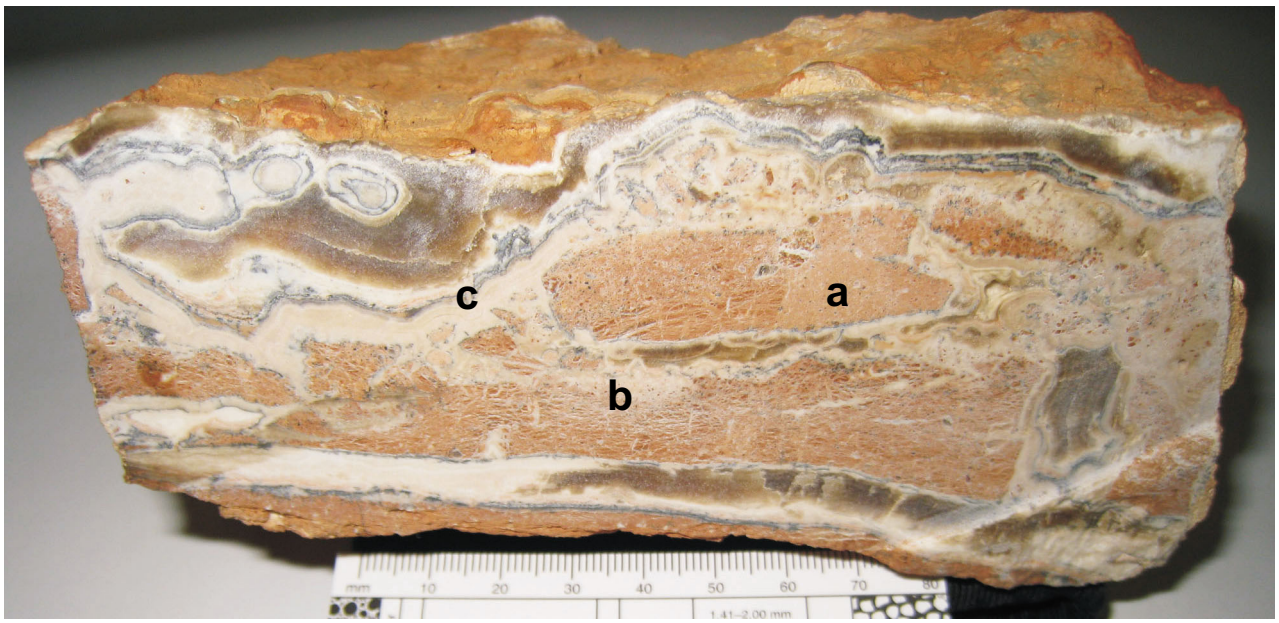

Figure 10. Polished rock slab from base of Unit D, Location 1, Victory Bore, showing the regolith relationships encountered in the mesa outcrops along the paleovalley of the Gascoyne River: (a) sedimentation-bioturbation-ferruginization; (b) calcretization; (c) silicification and replacement by opaline silica.

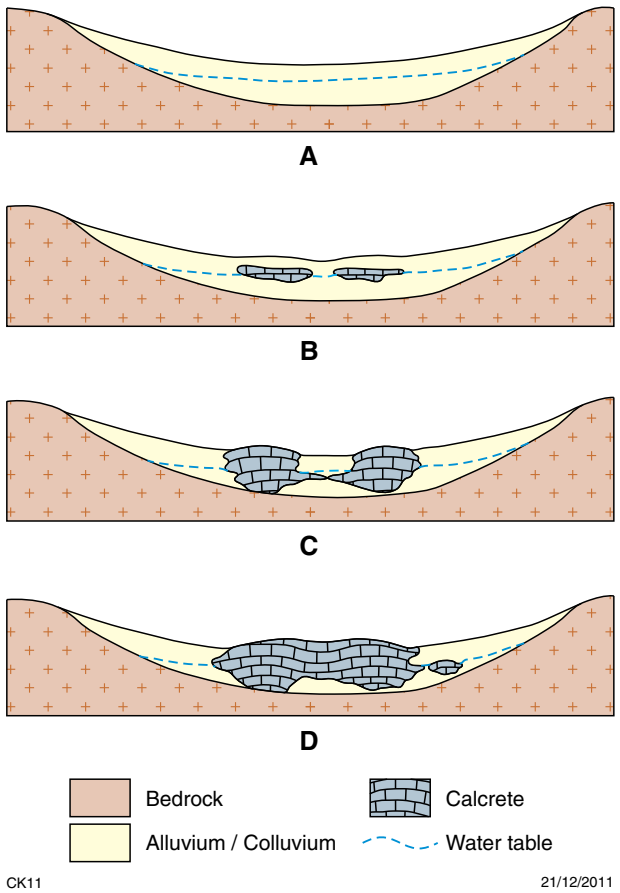

Figure 11. Stages in development of groundwater calcrete (modified from: Mann and Howitz, 1979)

(Fig. 12c). The calcrete is also composed of fan-shaped, radial-fibrous crystal aggregates with veins of polygonal quartz mosaic (Fig. 12d).

The calcrete was originally either overlain or capped by a silcrete, which has been weathered and eroded and is now mainly preserved as a surface lag. Remnants of the orange-red moderately sorted very fine to medium grained sand are present in some of the silcrete clasts.

Dallys Bore locality, Yinnetharra Station (434775E 7253390N)

Thirty three kilometres to the southeast of the No. 6 Bore locality, in the vicinity of Dallys Bore on Yinnetharra Station, a 20 km^2 calcrete plateau extends north from the convergence of Mount James Creek and the Gascoyne River. The plateau is marked by a 10–15 m high escarpment on its western margin. Calcrete outcrops are limited as most of the exposure has been weathered into blocks up to 50 cm in diameter, resulting in an irregular surface scree and upper surface. The calcrete blocks have a characteristic iron-coated pockmarked weathering surface, giving them a cellular appearance (Fig. 13a). Patches of carbonate-cemented, fine to medium grained, moderately sorted sand surrounded by iron-rich massive calcrete and cauliflower-shaped calcite growths (Fig. 13b) occur within the calcrete. The calcrete also contains angular quartz crystals set in a microcrystalline ferruginous carbonate matrix, which has been impregnated by fine-grained silcrete (Fig. 13c). The silcrete has partly replaced radiating carbonate crystals, as well as filling free spaces in the calcrete (Fig. 13d).

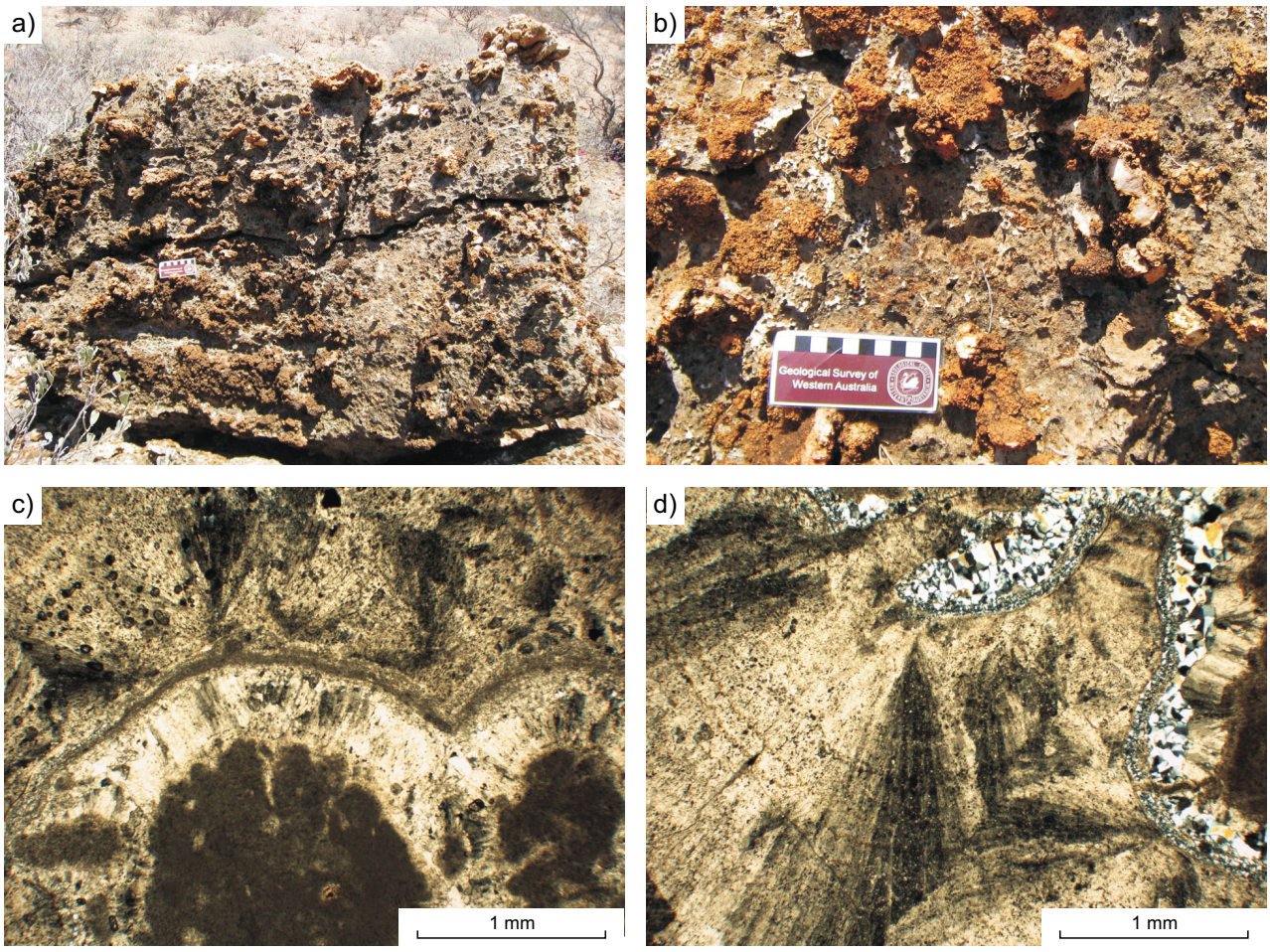

Figure 12. Outcrop views and photomicrographs of valley-fill calcrete at No. 6 Bore, Location 1: a) 1-m high block of pockmark-weathered calcrete; b) detail of pockmark-weathering of calcrete due to varying degrees of silicification in calcrete (scale bar: 10 cm); c, d) photomicrographs of calcrete (crossed polars, GSWA199508); c) spherical peloids showing botryoidal overgrowth of fibrous calcite; d) calcrete composed of fan-shaped, radial-fibrous crystal aggregates with veins of polygonal quartz mosaics

Interpretation

The calcrete encountered at No. 6 Bore Location 1 and Dallys Bore also represent valley-fill groundwater calcretes. Ferruginization prior to calcretization is evident, as well as subsequent silification of the calcrete in the upper parts of the stratigraphy.

Younger groundwater or valley-fill calcrete

Big Bend Bore locality (478558E 7243628N)

Calcrete and calcareous alluvium crop out in a small, 2 x 4 km drainage basin approximately 5.5 km west-southwest of the abandoned Big Bend Bore in the headwaters of Mount James Creek. The basin is surrounded by sandstones and siltstones of the Edmund Group and metasedimentary siliciclastic rocks of the Mount James Supergroup, and granitic rocks of the Moorarie Supersuite (Johnson et al., 2010a). It has an unnamed creek running along its centre, and another creek runs parallel to a small NW–SE-trending ridge composed of metasandstone and metasiltstone of the Yilgatherra Formation (Edmund Group). Both creeks are incised up to 3 m into calcrete, with reworked calcrete clasts found in the contemporary channel deposits (Fig. 14a). Scours and associated push bars are a common feature within the creek beds. Older calcareous fluvial sediments with reworked calcrete gravel layers are exposed along the banks of the central creek (Fig. 14c).

The calcrete crops out along the creek banks and as individual elongated ridges (Fig. 14b). It is whitish grey, with a cellular (Fig. 14d) to nodular weathering pattern but appears more massive on fresh surfaces. Carbonate-cemented plant roots (rhizomorphs) are common. Some fine- to coarse-grained quartz grains and 0.1 – 2 cm angular to rounded reworked calcrete clasts and nodules

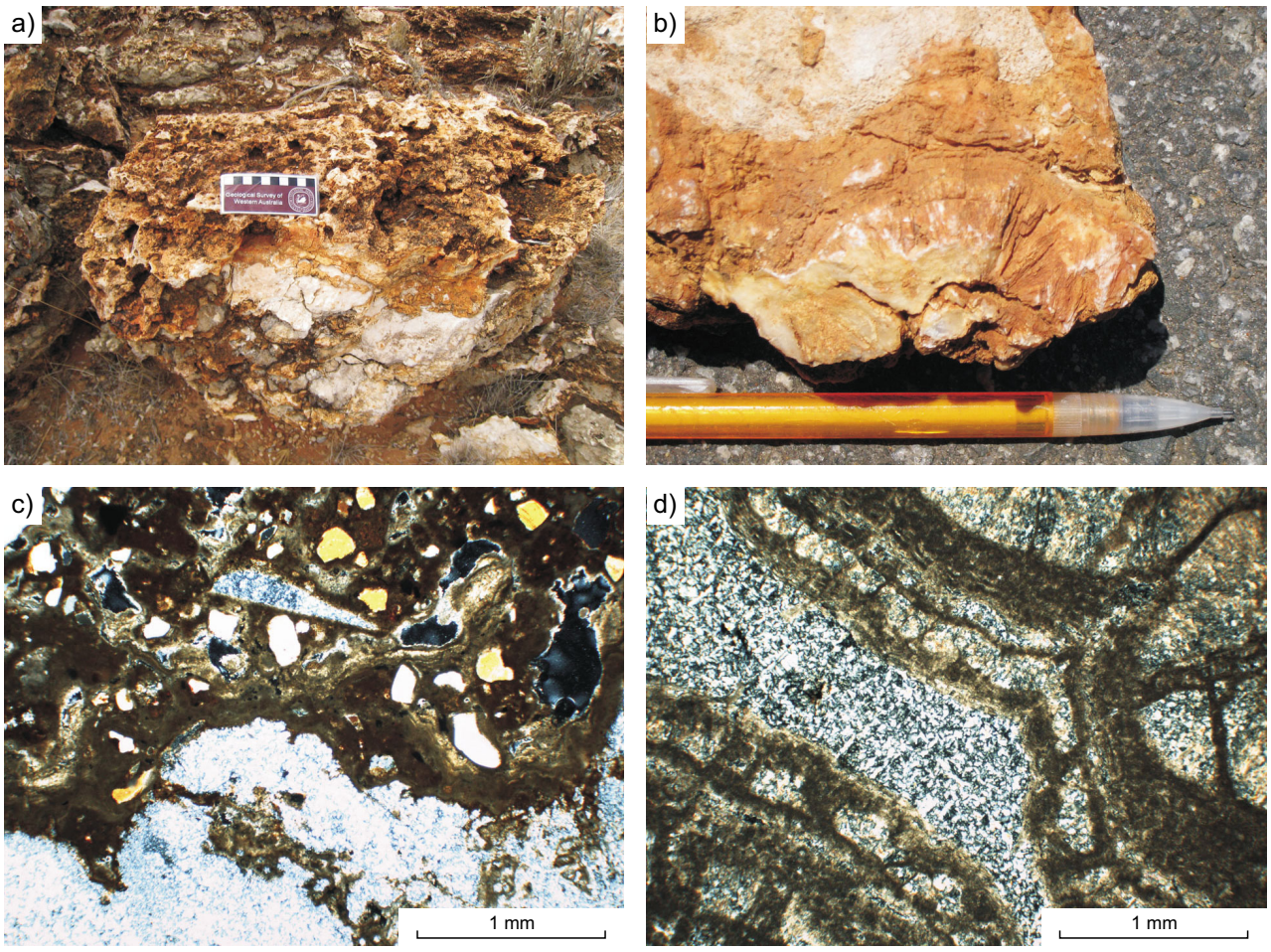

Figure 13. Outcrop views and photomicrographs of valley-fill calcrete at Dallys Bore: a) weathered calcrete block (scale bar: 10 cm); b) cauliflower-shaped calcite growth within calcrete; c, d) photomicrographs of calcrete (crossed polars, GSWA199535); c) calcrete composed of angular quartz crystals set in a microcrystalline ferruginous carbonate matrix (upper part) impregnated by fine-grained silcrete (lower part); d) silcrete partly replacing radiating carbonate crystals and filling voids in calcrete

are set in an indurated crystalline calcareous matrix. Iron-coated hollows 0.1 – 2 cm in diameter were also observed. In thin section, the calcrete shows solution cavities (Fig. 14e). Concentrically layered, spherical, peloid-like carbonate grains of unknown origin set in a carbonate-rich microcrystalline matrix (Fig. 14f) were also observed.

Interpretation

The calcrete at the Big Bend locality shows compositional similarities but also differences from the previously described valley-fill groundwater calcretes. The calcrete has formed due to calcretization of alluvial sediments along tributaries in the headwaters of Mount James Creek. No ferruginization prior to calcrete development and subsequent silification of the calcrete is evident from the outcrops. The calcrete outcrops are also morphologically in a different landscape position and are much more closely related to the present-day drainage. Therefore, it is suggested that these calcretes are the product of a different, more recent phase of calcrete development then the earlier discussed valley-fill groundwater calcretes.

Spring-associated calcrete mounds

No. 6 Bore locality, Eudamullah Station

No. 6 Bore locality: Location 2 (383542E 7286347N)

A 2-m high, 5 x 5 m calcrete mound unconformably overlies carbonate-cemented ferruginized sandstones approximately 440 m southeast of No. 6 Bore on Eudamullah Station. The calcrete is composed of light brown to green, poorly sorted, fine to very coarse grained sand with angular to subrounded quartz grains and minor lithic fragments. Although weathering has broken the calcrete into 10–40 cm diameter subangular to rounded boulders (Fig. 15a,b), faintly inclined subhorizontal bedding is still preserved. The bedding may reflect the build up and growth of the calcrete mound over time as it appears to dip moderately outwards from the central part of the outcrop. Individual calcrete boulders have a net-like, pockmarked structure with voids and tubes. Imprints of fine laminar lines have been observed in some of the tubes and represent hollow casts of calcified plant material. The

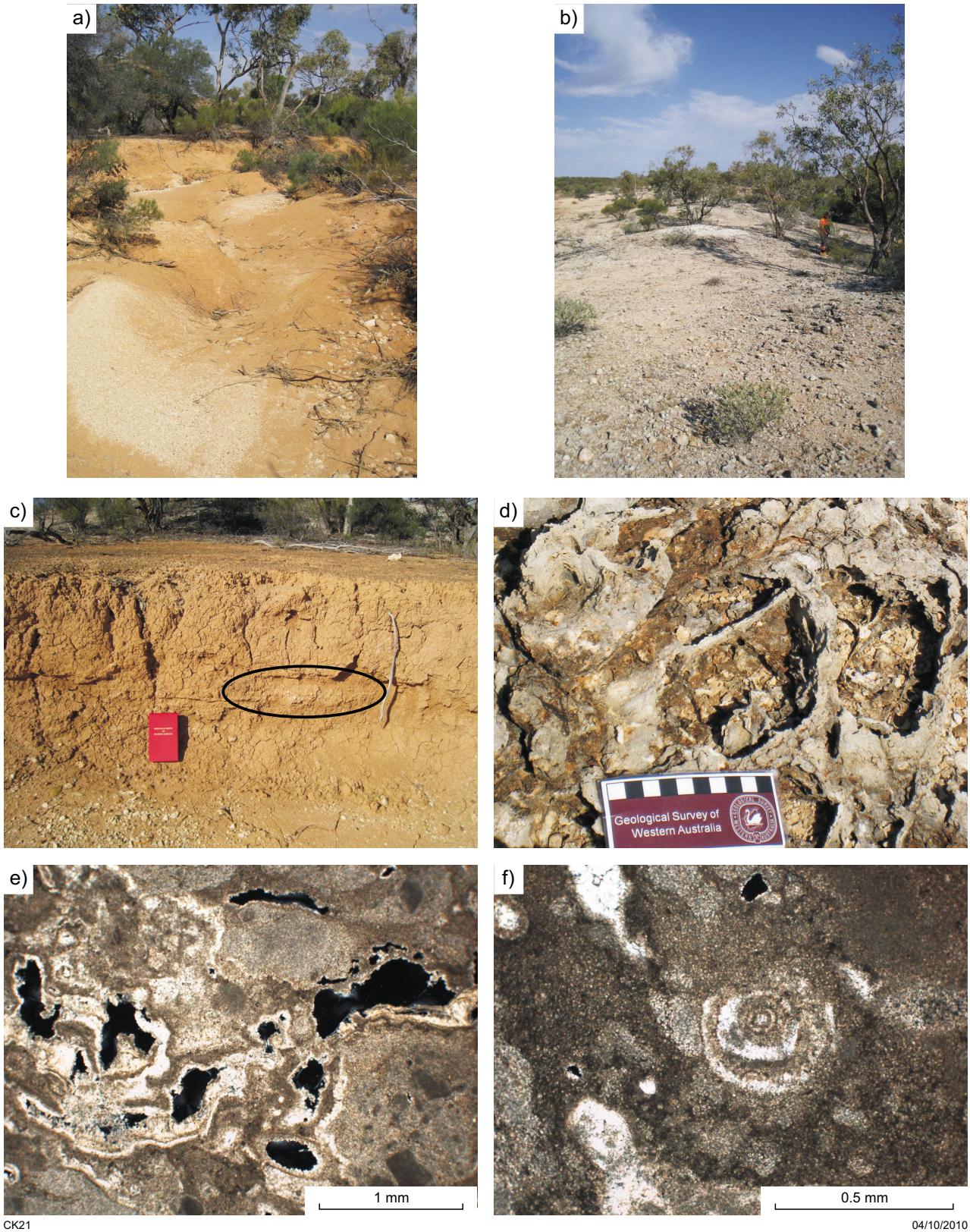

Figure 14. Outcrop views and photomicrographs of younger valley-fill calcrete at Big Bend Bore: a) reworked older alluvium and calcrete; scour and push bars within modern creek (flow direction towards viewer); b) calcrete ridge parallel to small creek, view towards east; c) older calcareous fluvial sediment with thin reworked calcrete gravel layers (ellipse). Field book for scale is 21 x 13 cm; d) detail of cellular calcrete (scale bar: 10 cm); e), f) photomicrographs of calcrete (crossed polars, GSWA199556); e) cellular calcrete with solution cavities; f) concentrically layered, spherical, peloid-like carbonate grain of unknown origin in carbonate-rich microcrystalline matrix

calcrete has a greyish-white fine-grained calcareous matrix in which some medium to very coarse grained angular to subangular quartz grains are embedded.

In thin section, the calcrete is composed of a loosely interlocking network of peloids (Fig. 15c). The peloids are 0.05 – 0.1 mm in diameter, semiround to round, and are either homogenous or show signs of a faint internal structure. The latter are indicative of microbial and/or bacterial involvement in the formation of the calcrete. Irregular cavities that give the calcrete a microporous texture (Fig. 15d) are probably due to partial dissolution of calcite during weathering. These calcretes are likely to form groundwater aquifers or act as possible hosts to mineralization.

Interpretation

The mound shape, inclined bedding, and calcified plant material are indicative of a spring-associated calcrete. Here, the mound-like shape has been accentuated by the increased resistance to erosion of the calcrete, in comparison to the surrounding material. Calcrete formation has also extended into the adjacent ferruginized sandstone, which shows an increase in the degree of carbonate cementation towards the calcrete mound.

Thin calcrete layers over weathered bedrock

Chalba Well locality, Lockier Station (389677E 7248808N)

About 750 m south of Chalba Well, along an elevated older terrace of the Gascoyne River, granitic gneisses of the Halfway Gneiss (Sheppard et al., 2010) are brecciated and partly overlain by whitish-grey calcrete (Fig. 16a). The calcrete contains fine- to coarse-grained quartz grains and rounded silcrete clasts up to 1 cm in diameter. Calcrete nodules up to 5 mm across are also present. In thin section, the calcrete contains angular altered bedrock fragments cemented by microcrystalline carbonate (Fig. 16b).

Interpretation

The calcrete formed by carbonate precipitation during flooding of the terrace at times of high discharge events. The calcrete is thin and only blankets the outcropping weathered basement rocks.

Pedogenic calcrete

Pedogenic calcrete results from the accumulation of carbonate in the soil moisture zone, due to movement of percolated rain water and/or soil water, or also as a product of biological activity such as a root respiration (Chen et al., 2002). Pedogenic calcretes are not common in the Mount Phillips Geological Series map sheet area as there is a general lack of soils in which calcrete can form. Pedogenic calcretes have been found to be mainly associated within desert soils developed in sheetwash and older floodplain deposits. Exposures are present in the vicinity of Landor Homestead on the Landor 1:100 000 Geological Series map sheet, which is part of the Glenburgh 1:250 000 Geological Series map sheet.

Landor Homestead locality, Landor Station (490344E 7220466N)

Landor Homestead locality: Location 1 (493981E 7231946N)

Boulders of nodular calcrete of various sizes have been excavated during road construction along the Landor to Mt Augustus Road 12 km to the north-northeast of Landor Homestead (Fig. 17a). The surface of the road coincides with the top of a calcrete horizon, which is covered on both sides of the road by sheetwash plains with a tiger bush vegetation pattern. The sheetwash consists of red, faintly bedded, poorly sorted, clay to coarse-grained sand, with abundant angular to subrounded calcrete clasts up to 5 mm in diameter. The top of this nodular pedogenic calcrete horizon has been encountered about 50 cm beneath the top of the sheetwash plain, approximately at the same level as the top surface of the nearby gravel road. The white nodular calcrete is composed of individual subangular to rounded carbonate nodules, which are between 0.1 and 1 cm in size. In thin section, the nodular calcrete shows an isopachous calcite rim, lining isotropic carbonate nodules that are cemented by coarse-grained calcite crystal aggregates (Fig. 17b).

Landor Homestead locality: Location 2 (493485E 7216395N)

Five hundred metres south-southeast of Landor Homestead, in the vicinity of Warri Well, a well preserved 1.3 m high pedogenic calcrete profile is exposed in a road metal quarry (Fig. 18). The calcrete has developed in older fluvial deposits and is best developed in the lower parts of the profile. Three different horizons can be distinguished. The lowest 40 cm of the profile is characterized by white, 1–3 cm thick friable calcrete layers, which become thinner towards the top. The calcrete layers at the base are subhorizontally bedded but bedding becomes more undulating towards the top. Orange-red, carbonate-cemented, moderately sorted, fine- to coarse-grained sand is common between and within the individual bedding layers and becomes more abundant towards the top. In the overlying unit, the calcrete layers become thinner and less distinct and sand layers dominate. Towards the top, the calcrete layers are replaced by individual 0.3 – 3 cm in diameter, angular to subrounded calcrete clasts. The uppermost horizon is orange-red, carbonate-cemented, moderately sorted, fine- to coarse-grained silty sand, with isolated calcrete nodules up to 3 mm in diameter.

Interpretation

The presence of well-developed horizons within the alluvial and/or sheetwash deposits clearly shows that the calcrete has developed as part of a soil profile and can therefore be classified as a pedogenic calcrete. Observed calcrete thickness is limited by the degree of the soil profile development but the extent of the calcrete can be quite widespread, e.g. below vast sheetwash areas.

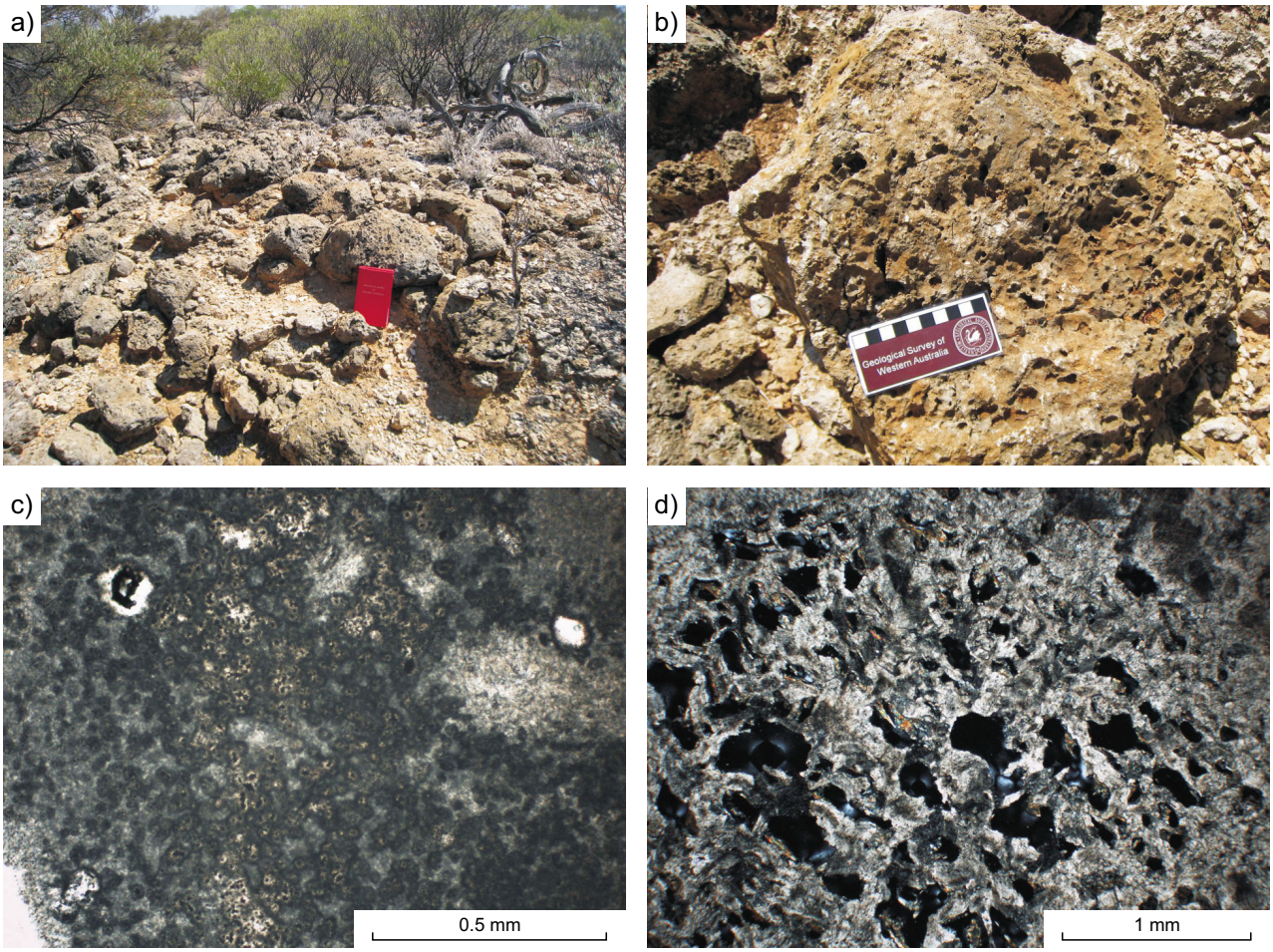

Figure 15. Outcrop views and photomicrographs of spring-associated calcrete at Location 2, No. 6 Bore locality: a) calcrete mound outcrop showing weathered calcrete boulders intercalated with a more massive calcrete layer giving rise to faint bedding (field book for scale is 21 x 13 cm); b) detail of calcrete boulder with tube hollows from calcified plants (scale bar: 10 cm); c, d) photomicrographs of calcrete (crossed polars, GSWA199505); c) loosely interlocking network of peloids; d) porous fine-grained calcrete with irregular cavities (black)

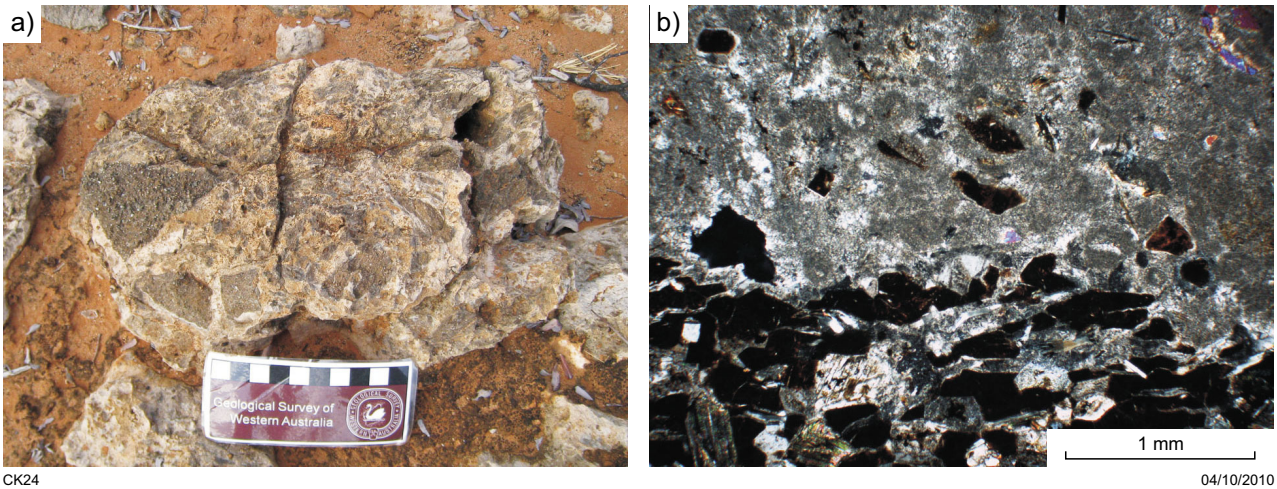

Figure 16. Outcrop view and photomicrograph of a thin calcrete layer overlying a weathered bedrock boulder of the Halfway Gneiss at Chalba Bore: a) calcrete inundating weathered bedrock clasts (scale bar: 10 cm); b) photomicrograph of calcrete (crossed polars) showing angular altered bedrock fragments cemented by microcrystalline carbonate (GSWA199521)

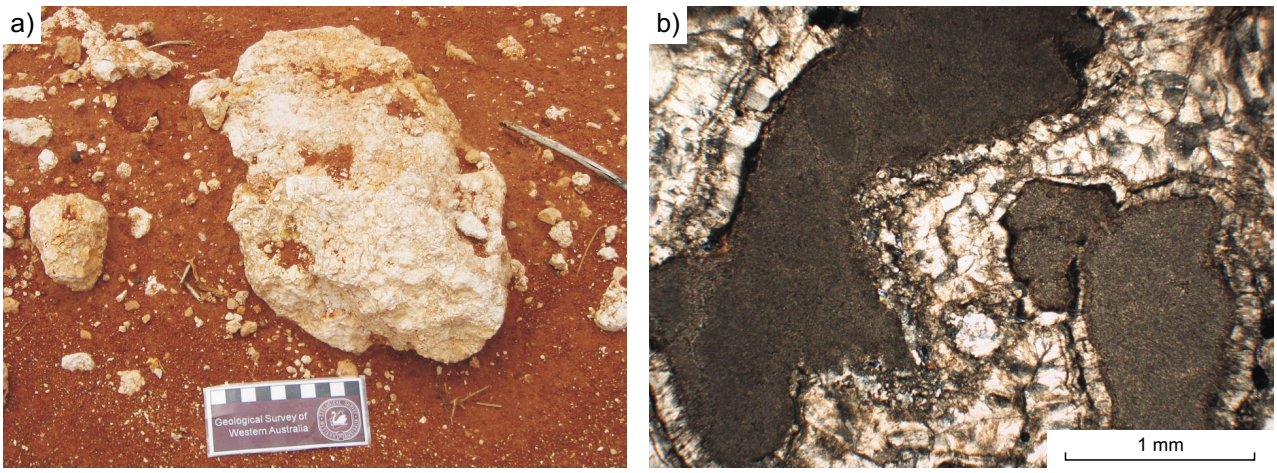

Figure 17. Outcrop view and photomicrograph of pedogenic calcrete at Location 1, Landor Homestead locality: a) pedogenic nodular calcrte boulder (scale bar: 10 cm); b) photomicrograph of nodular calcrete (crossed polars) showing an isopachous calcite rim lining isotropic carbonate nodules, which are cemented by coarse-grained calcite crystal aggregates (GSWA199560)

Figure 18. Pedogenic calcrete profile at Location 2, Landor Homestead locality, showing a decrease in calcrete development from bottom to top (scale bar: 10 cm)

Summary

Occurrences of calcrete examined from various parts of the Gascoyne area illustrate the interplay of time, climate, host material, carbonate source, landscape position, sedimentation and erosion rate, overprinted by local conditions. This has resulted in a highly diverse suite of calcrete types. Due to the lack of dating no absolute ages can be assigned to the different calcretes, so the correlation of outcrops is based on similar morphology and landscape position (e.g. calcrete mesas along the Gascoyne River paleovalley). The source for the carbonate is most probably a combination of in situ weathering of bedrock and aeolian dust (Glassford and Semeniuk, 1995).

Silcrete

Silcrete is defined as a strongly silicified, indurated regolith, generally of low permeability, commonly having a conchoidal fracture and a vitreous lustre (Eggleton, 2001). Silcrete has been widely cited as being indicative of an alkaline, arid or semi-arid environment (Summerfield, 1982); however, recent studies have shown that silcrete is not indicative of any particular climate (Webb and Golding, 1998).

Silcretes in Western Australia have developed through silicification of a variety of host materials, especially calcrete and older alluvial deposits. Due to their resistance to weathering and erosion, silcretes are commonly preserved in sites of topographic inversion, including ridge crests, tops of mesas, and as cappings on erosional plains. Silcretes play a critical role in the preservation and redistribution of economic mineral deposits and groundwater aquifers (Arakel et al., 1989).

Silicified calcretes form highly permeable aquifers and are prime sources of low salinity water throughout Australia's arid zones (Arakel et al., 1989). They also can bear significant concentrations of uranium and vanadium. By forming a thin microcrystalline silica coating around carnotite grains, uranium ores can be preserved (Arakel et al., 1989).

Silcretes in the Mount Phillips Geological Series map sheet area are commonly found indurating and capping calcretes. Williams et al. (1983a) interpreted the silcretes as part of an old, possibly quite extensive, duricrust surface, remnants of which are still preserved as silcrete surface lags and silcrete-rich colluvium throughout the study area.

No. 6 Bore locality, Eudamullah Station

No. 6 Bore locality: Location 3 (383476E 7286222N)

Silcretes form the top of a 15 m high hill about 500 m southeast of No. 6 Bore on Eudamullah Station. Here, the silcrete overlies calcrete but the contact is not exposed. The silcrete is weathered into 5–50 cm blocks, forming the colluvium on the hillslope. The silcrete is vuggy to cellular or massive white and is partly replaced by opaline silica. In some areas vugs have a bright orange-red, millimetre-thick iron coating (Fig. 19a). In outcrop, some individual quartz grains can still be seen within milky white and translucent, bluish-grey areas in massive silcrete (Fig. 19c). Photomicrographs reveal that the bluish-grey translucent parts of the silcrete are composed of fine-grained, chert-like aggregates of 5–20 µm quartz crystals, whereas the milky white areas represent isotropic, cryptocrystalline pale yellow-brown silica, that appears black under cross-polarized light (Fig. 19d).

Partly silicified calcrete boulders located halfway down the hillslope, indicate that the upper part of the calcrete has been overprinted by the formation of silcrete. In the lower third of this hilly outcrop, calcrete is underlain by ferruginized sandstone, which is partly covered by silcrete-dominated colluvium.

Rampaddock Well locality, Yinnetharra Station (419455E 7273483N)

Rampaddock Well locality: Location 1 (417896E 7273081N)

A 15 m high silcrete-topped mesa (Fig. 20a) forms part of a string of mesas which parallel the Gascoyne River 1.6 km west of Rampaddock Well and 2.2 km east of the Yinnetharra Homestead. These outcrops have previously been mapped on the Mount Phillips 1:250 000 Geological Series map sheet as 'calcrete (and kankar) which are in part replaced by opaline silica' (Williams et al., 1983a). Several of these mesas have been investigated during the present study. An extensive silcrete layer occurs on top of the mesas, which is now preserved as a gravel lag of 1–20 cm angular silcrete clasts and scattered minor calcrete clasts, surrounded by a moderately sorted, fine- to medium-grained, red sandy matrix (Fig. 20b). A thick colluvial layer mainly composed of silcrete clasts covers the flanks of the mesa with only rare exposures of underlying units.

Rampaddock Well locality: Location 2 (416632E 7275057N)

A silcrete-topped mesa, located 2.2 km northwest of Location 1, has a gravel lag of 0.5 – 20 cm sized, partly iron-coated, angular to subrounded silcrete clasts, embedded in a red, moderately sorted, fine- to medium-grained sandy matrix (Fig. 20c). No calcrete clasts were observed in this outcrop.

Victory Bore locality, Yinnetharra Station

Victory Bore locality: Location 2 (412963E 7278854N)

In many places, cellular, partly opalized, silcrete, coated by an iron crust up to 1 mm thick, crops out (Fig. 21a, b) on the top of a mesa, 170 m northeast of Victory Bore (Victory Bore locality Location 2 described in calcrete section), with remnants of calcrete still present (Fig. 9b).

Interpretation

Studies of inland silcretes of central South Australia show that silcretes can be divided into two groups:

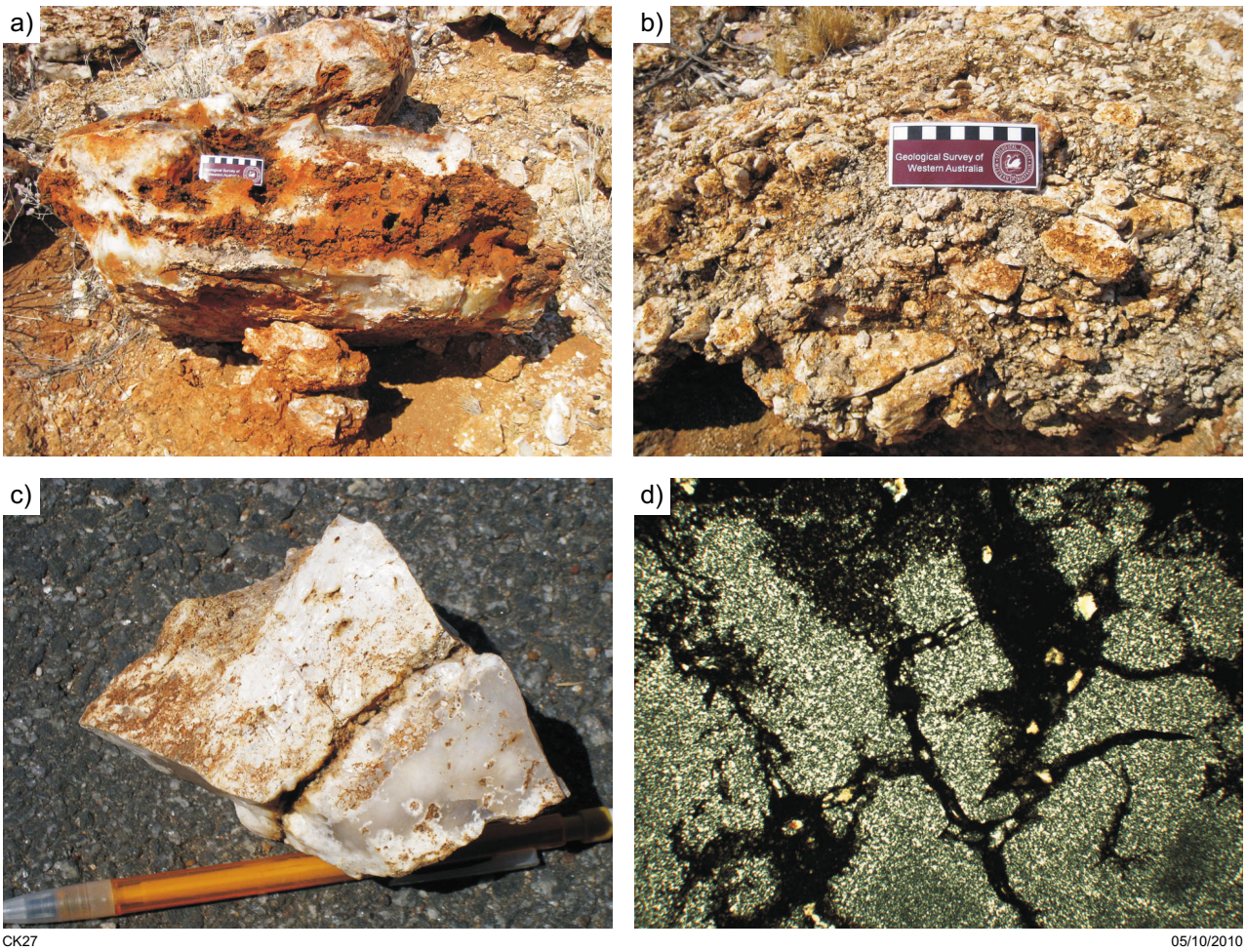

Figure 19. Silcrete examples from No. 6 Bore locality, Location 3: a) silcrete block showing cellular structure and strong iron coating; b) brecciated silicified calcrete (scale bar: 10 cm); c) detail of silcrete sample showing milky white and translucent, bluish-grey areas within silcrete (pen: 15 cm); d) photomicrograph (crossed polars, GSWA199503) of c): bluish-grey translucent silcrete is composed of fine-grained, chert-like aggregates of 5–20 µm quartz crystals, whereas the milky white areas represent isotropic, cryptocrystalline pale yellow-brown silica that appears black in this view

pedogenic and groundwater (Webb and Golding, 1998). Pedogenic silcretes show typical soil features such as columnar and nodular textures, whereas groundwater silcretes have massive textures and formed at or close to the water table. Only groundwater silcretes have been observed in the Mount Phillips Geological Series map sheet area. In most cases the silcretes are associated with underlying calcrete. Silicification of calcrete is common throughout large areas of Australia, and involves the filling of voids and replacement of calcite by opaline and quartzose silica (Arakel et al., 1989). This can take place as a late diagenetic event in the vadose or phreatic zones. Silicification in the Mount Phillips area is laterally and vertically irregular. It seems to have formed originally as patchy lenses in the upper part of the calcretes lining solution pipes and filling cavities. Silica has also cemented irregular joint networks of brecciated calcrete, resulting in its cellular appearance in some outcrops (Fig. 21a, b).

Ferruginous duricrust

Nomenclature: Laterite – Ferricrete

Laterite is the product of weathering, and commonly exhibits the characters of all, or at least the upper part, of an in situ regolith profile, also called laterite profile. Laterite commonly has a hard, often prominent, ferruginous surface expression, with some degree of chemical and mineralogical differentiation. In recent years there has been increased discussion around the usage of the word ‘laterite’ as the term is used in different ways in the literature. Due to these differences several authors have suggested abandoning the term ‘laterite’ (Pain and Ollier, 1992; Bourman, 1993). Eggleton (2001) suggests using the non-generic term 'ferricrete', which is defined as ‘an indurated material formed by the in situ cementation of regolith by iron oxyhydroxides, mainly goethite and/or

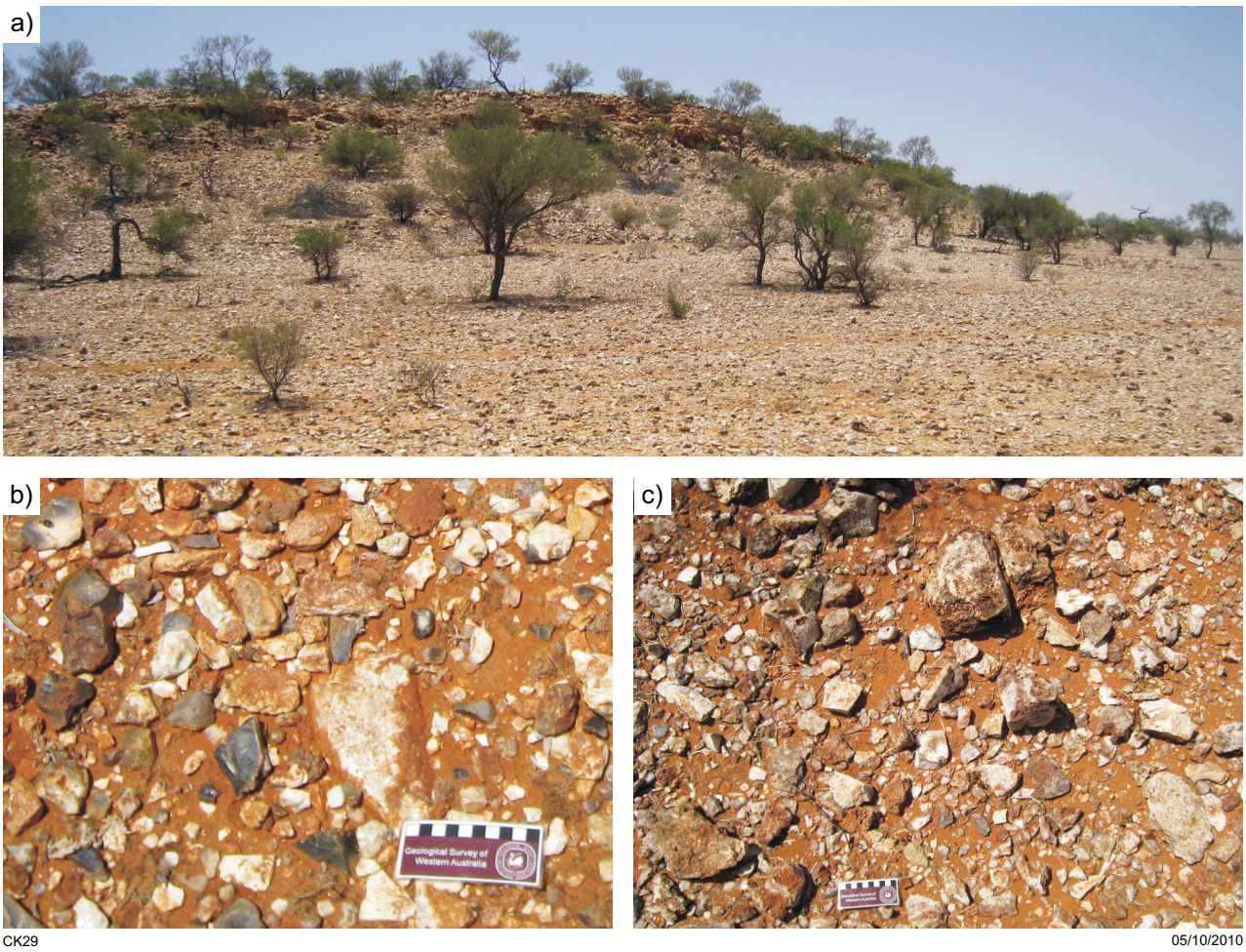

Figure 20. Outcrop views of silcrete-topped mesa with gravel lag at Locations 1 and 2, Rampaddock Well: a) silcrete-topped mesa with thick silcrete colluvial cover (Location 1); b) gravel lag on top of mesa composed of silcrete and less common calcrete clasts in an orange-red sandy matrix (scale bar: 10 cm); c) gravel lag on mesa top (Location 2) composed of silcrete clasts in a red sandy matrix (scale bar: 10 cm)

hematite' instead (Eggleton, 2001, p. 33). In this record the non-generic term 'ferruginous duricrust' is preferred. A more genetic classification is achieved by using it in combinations with the terms 'transported' and 'in situ'.

Ferruginous duricrust on the Mount Phillips Geological Series map sheet area

Ferruginous duricrust is common on the Mount Phillips Geological Series map sheet area, where it has been previously subdivided into hardpan-consolidated and semi-consolidated colluvium and alluvium; silt, sand, gravel, and rubble, commonly dissected (Czc); and laterite and ferruginous deposits (Czl) (Williams et al., 1983a).

Two distinctive types of ferruginous duricrust have been recognized on Mount Phillips — transported ferruginous duricrust and in situ ferruginous.

Transported ferruginous duricrust

Iron-cemented transported material such as alluvium and colluvium is commonly referred to as hardpan. A hardpan is defined as a 'relatively hard, impervious layer in the regolith lying at or near the surface' (Eggleton, 2001, p. 47) or as a partially cemented duricrust with 'less than 70% cemented material, generally with an open texture' (Eggleton, 2001, p. 28). It results from the cementation of soil particles by the precipitation of relatively insoluble materials, most commonly silica, iron oxide, calcium carbonate, and organic matter (Eggleton, 2001).

The best known hardpan in Western Australia is the Wiluna Hardpan (Bettany and Churchward, 1974), also termed the Menzies Formation by Glassford and Semeniuk (1995). Figure 22 shows its inferred extent. Eggleton (2001) described it as a red-brown hardpan with a coarsely laminated appearance. It consists of a variety

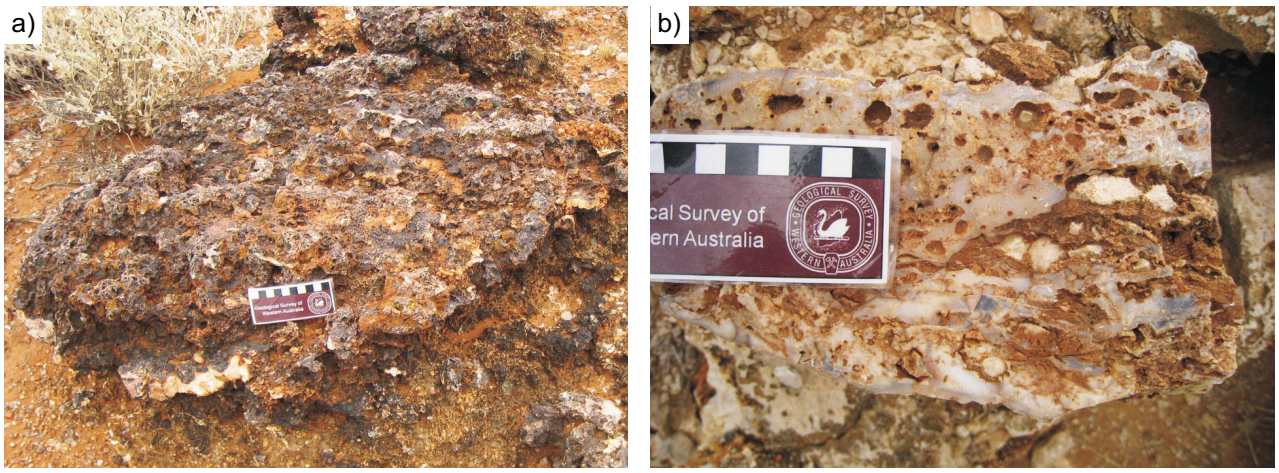

Figure 21. Outcrop views of iron-coated silcrete at Location 2, Victory Bore: a) iron-coated silcrete block on top of mesa; b) detail of block in a), showing cellular nature of the silcrete

of transported or residual host materials, including soil, colluvium, pisolitic horizons, and brecciated saprolite, set in a porous, red-brown, earthy matrix and cemented by silica, clay, and iron oxyhydroxides. The deposits are found close to or along large drainages where they represent cemented older alluvium, consisting of horizontal- and cross-bedded sand, and imbricated gravel. Paleocurrent directions accord with present stream directions (Bettany and Churchward, 1974). Maximum thickness is estimated to be over 30 m. Brewer et al. (1972) concluded that the Wiluna Hardpan was formed from colluvium with a high proportion of lateritic debris that had been eroded from an older laterite or hardpan. Bettenay and Churchward (1974) suggested a Late Tertiary or Early Quaternary age for the Wiluna hardpan deposits.

Elias and Williams (1980) described hardpan in the Gascoyne area as partially consolidated colluvium, which forms dissected remnants of talus aprons on valley sides in the Ashburton River area, and elsewhere occurs in the banks of incised watercourses and probably also extends under much of the younger colluvial deposits. The hardpan is 15–35 m thick, orange or reddish-brown and consists of sand, pebbles, and cobbles in a finer grained, ferruginous clay matrix (Williams et al., 1983a; Williams et al., 1983b; Martin et al., 2005). On Mount Phillips, the consolidated hardpan unit is described as an old colluvium–alluvium deposit composed of crudely bedded silt, sand and pebbles (Williams et al., 1983a). The hardpan is strongly dissected and outcrops are found in broad valleys or adjacent to erosional bedrock outcrops such as the Lockier Ranges.

Transported ferruginous duricrust is found throughout the Mount Phillips Geological Series map sheet area. These deposits preserve a wide variety of sedimentary characteristics, which give new insights into their depositional history.

First Bore locality, Cobra Station (472454E 7279812N)

A well-exposed section of ferruginious duricrust is located between Pink Hills Creek and an unnamed tributary of the Thomas River, 6.7 km east northeast of First Bore on Cobra Station. The unnamed creek has eroded into flat lying sediments and exposed a fining-upward succession of three sedimentary units, coinciding with three distinct terraces, over a distance of one kilometre. Due to the character of the outcrop, exact thicknesses could not been measured and only minimum thickness estimates are provided here (Fig. 23).

First Bore locality: Location 1 (479006E 7281140N)

The lowermost Unit A is exposed along a small creek. It has a minimum thickness of about 5 m and is composed of a partly mottled, pisolitic, carbonate-cemented, subhorizontally bedded, moderately to well-sorted, very fine to medium grained sandstone (Figs. 23, 24a, b). The whitish-beige sandstone has ochre- and red concentric stains throughout. The original sediment is overprinted by intense pisolite development forming concentric iron-rich nodules, 0.5 – 1.5 cm in diameter. Weathering results in a distinctive pisolitic surface lag (Figs. 24b, c).

First Bore locality: Location 2 (479489E 7281598N)

Unit A is overlain by a reddish-green, ferruginized, subhorizontally bedded, poorly sorted fine-grained to pebbly sandstone, termed unit B (Figs. 23, 25a), which has a minimum thickness of 10 m. The sandstone has thin individual mud layers and mud cracks on the top of bedding surfaces (Fig. 25b). Unit B shows intense bioturbation, with abundant burrows and roots. Calcrete nodules are common in root casts (Fig. 25c). Semicircular

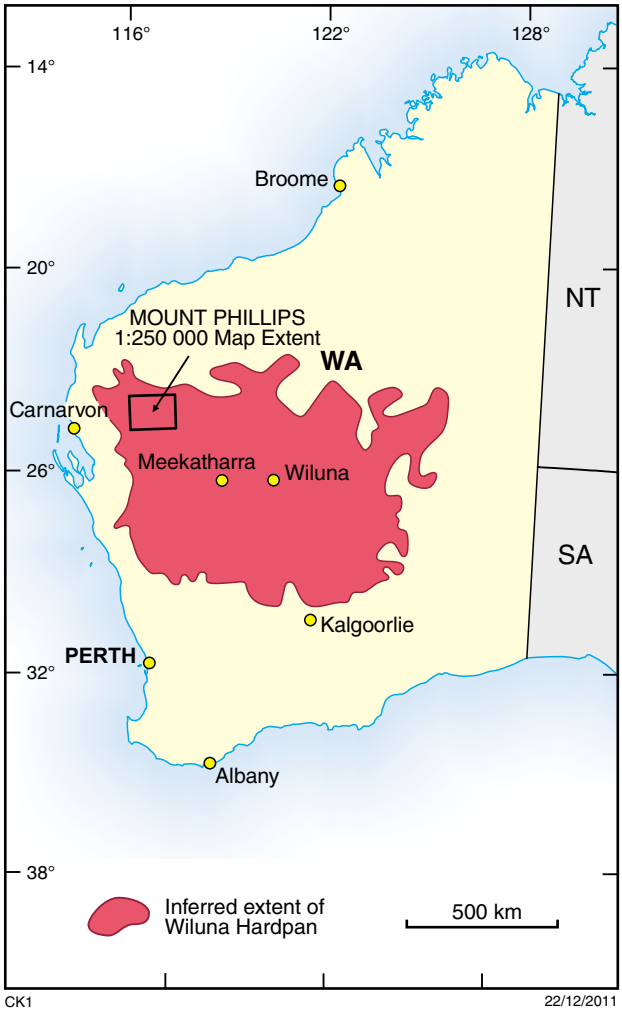

Figure 22. Inferred extent of the Wiluna Hardpan (modified after: Bettenay and Churchward, 1974) and location of the Mount Phillips Geological Series map sheet area

to circular, cylindrical, stump-like features spaced 10 cm to 1 m apart are also abundant (Fig. 25d, e). A cross section through one of these features reveals an abundance of burrows (Fig. 25f). Some are open and passively filled with the reworked surrounding material and are most likely to have been produced by ants or termites (personal communication Stephen Hasiotis, 2010). Others are mainly backfilled burrows made by beetle larvae ('AMB burrows' in Hasiotis, 2002) and indicate a high degree of bioturbation after deposition in a subaerial environment.

First Bore locality: Location 3 (479150E 7282293N)

Concentric weathering features similar to the previous section but much larger, were observed 800 m to the NW along the breakaway (Fig. 25g). These features are up to 1.5 m in diameter, and protrude up to 15 cm above the ground surface. They are composed of orange-red, weakly horizontally bedded, moderately sorted, fine- to coarse-grained ferruginized sandstones, which show incipient pisolite development throughout. The surrounding sediment is of a similar composition but is less cemented and therefore more prone to weathering. It is covered by a thin surface lag comprising clasts of reworked ferruginous duricrust, pisolites and some milky quartz.

First Bore locality: Location 4 (479739E 7281748N)

The top-most unit, Unit C has a minimum thickness of 5 m. It is characterized by red, iron-and carbonate-cemented, quartz-rich, subhorizontally bedded, poorly sorted, clay-rich, silty to fine-grained sandstone, with individual pebble layers composed of 0.3 – 1.5 cm pisolites (Fig. 26a). On top surfaces, polygonal mud cracks with diameter varying from 5–65 cm are common (Fig. 26b). Bioturbation is a common feature and several horizons are strongly mottled.

Interpretation

The minimum cumulative thickness of the succession at First Bore locality is about 20 m. It represents a fining-upward alluvial succession, from shallow fluvial channel deposits at the base to floodplain deposits towards the top. The occurrence of mudcracks in the middle and upper units indicates alternating wet and dry periods. The intense bioturbation also indicates long periods with minimal inundation or minimal disturbance of the floodplain. This suggests episodic deposition and reworking in a seasonal climate. The whole succession is intensively overprinted by ferruginization.

The First Bore succession shows many similarities with descriptions of the Wiluna Hardpan. Bettenay and Churchwald (1974) indicated that the extent of the Wiluna Hardpan includes Mount Phillips and adjacent map sheet areas (Fig. 22). Other transported ferruginized sandstone units encountered at the Victory Bore locality (Location 1) or No. 6 Bore Paleochannel (see paleochannel section) are associated with overlying calcrete and silcrete. This association has not been encountered in the succession at First Bore and also has not been described from the Wiluna Hardpan.

The position of transported ferruginized duricrust deposits within the contemporary landscape suggests they are either part of elevated calcrete or silcrete-topped mesas, or else they form terraces and cutbanks along modern drainage channels. Correlation between these regolith units is difficult as they lack absolute ages.

In situ ferruginous duricrust as part of an in situ regolith profile

In comparison to the transported ferruginous duricrust, in situ ferruginous duricrust is part of a regolith profile that has developed due to intensive weathering over bedrock. It is part of the pedolith and is also commonly termed 'lateritic duricrust' (Eggleton, 2001). In an idealized regolith profile (Eggleton, 2001) the 'lateritic duricrust' is overlain by lateritic gravel, soil, and a lag (Fig. 27).

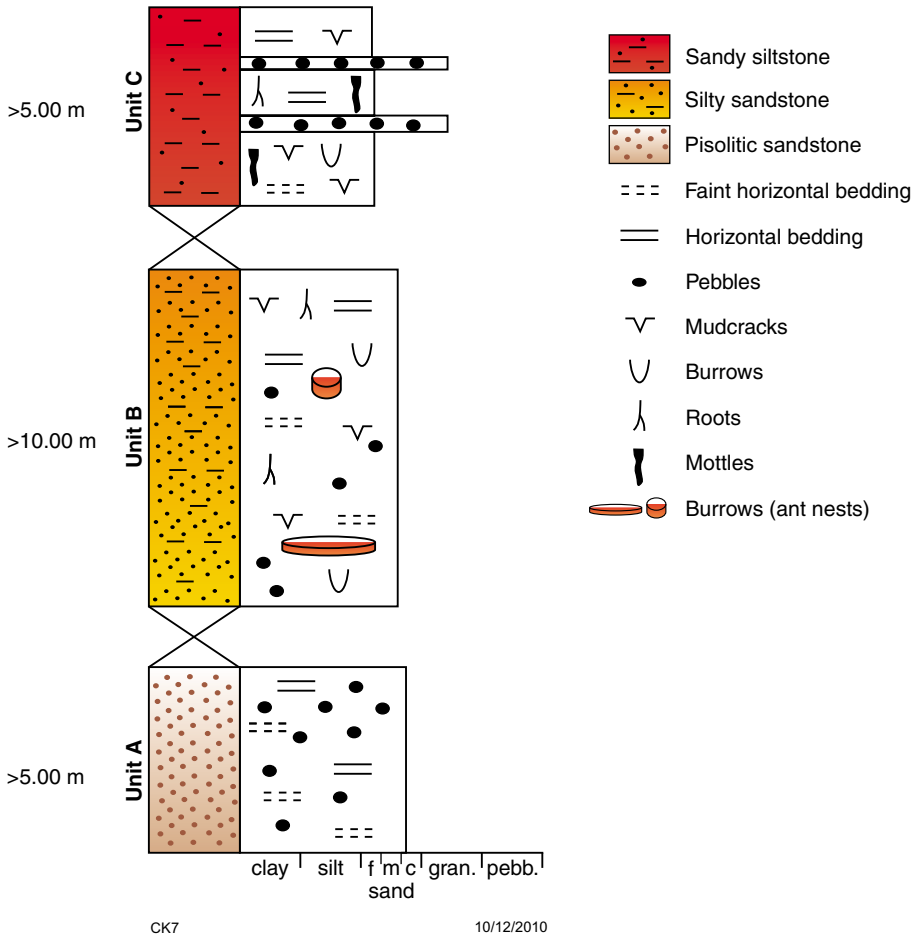

Figure 23. Composite graphic log of measured sections of transported ferruginous duricrust at Locations 1–4, First Bore locality

No. 6 Bore locality, Eudamullah Station

No. 6 Bore locality: Location 4 (385857E 7289201N)

A 10-m thick in situ regolith profile is exposed in breakaways along tributaries of Onslow Creek 3.6 km northeast of No. 6 Bore on Eudamullah Station. The outcrops mimic the outline of a paleodrainage system, which is now incised by contemporary drainage (Fig. 28). Exposures of the regolith profile are limited, as the slopes of the breakaways are covered by colluvium.

The base of the profile is characterized by a bright white saprolite composed mainly of angular quartz and kaolinite and some minor muscovite flakes. The grain size of the quartz grains ranges from fine-grained sand to granules. About half of the quartz grains are smoky quartz, indicating that the original bedrock was exposed to radioactivity (Holden, 1925). Towards the top of the saprolite, the amount of mottling increases with individual mottles showing orange-yellowish staining (Fig. 29). Upper parts are slightly silicified and more resistant to weathering, giving the appearance of a silicified caprock. The contact between the saprolite and the overlying pedolith is not exposed; however, the original bedrock on which the in situ regolith profile has developed is most probably gneissic to schistose biotite metamonzogranite and metasyenogranites of the 1680–1620 Ma Durlacher Supersuite (Sheppard et al., 2010).

Three major horizons are present within the pedolith (Fig. 29). The lower horizon is representative of the arenose zone and shows no evidence of any primary rock fabric. Ferruginization increases upwards and the contact with the overlying middle horizon is gradational. This middle horizon is a partly mottled, pisolitic, in situ ferruginous duricrust. It has a distinct red and white layering that is especially well developed in the upper part. In addition, pisolites become more abundant towards the top. The uppermost horizon is a consolidated in situ ferruginous duricrust, formerly classified as ‘lateritic duricrust’ (Williams et al., 1983a), that forms a conspicuous capping on top of the outcrop. The two uppermost horizons are part of the ‘lateritic residuum’ of the in situ regolith profile (Fig. 27).

Outcrops similar to those at the No. 6 Bore locality have also been found in the headwaters of a tributary to Mount

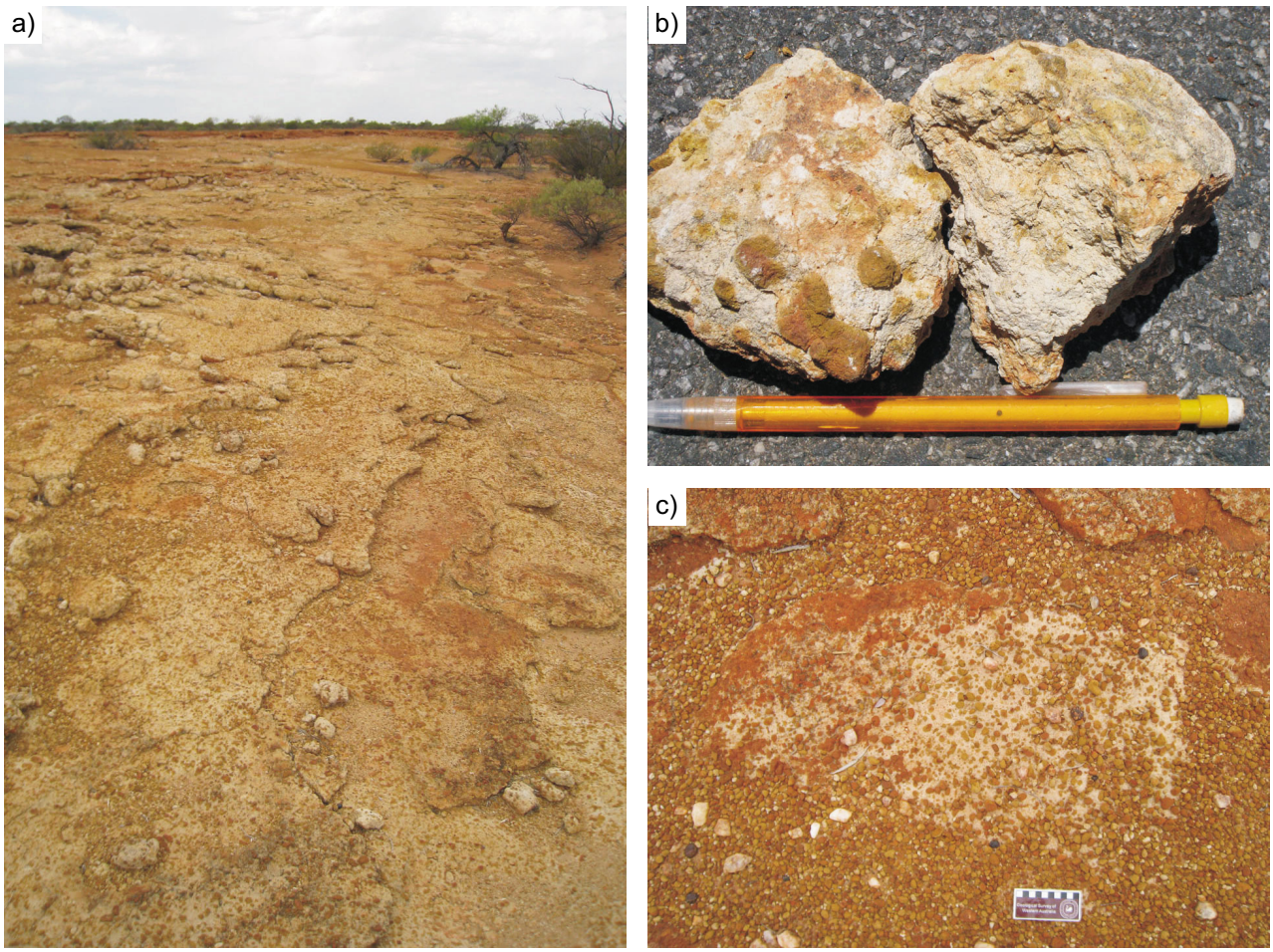

Figure 24 Outcrop views of lower Unit A, measured section at Location 1, First Bore locality: a) outcrop of basal part of Unit A next to small creek, showing distinct bedding surfaces; b) detail of sandstone showing the intensive overprinting by weathering and incipient formation of pisolites (pen: 15 cm); c) pisolitic gravel as surface lag (scale bar: 10 cm)

James Creek, near Deep Well on Dalgety Downs Station (see paleochannel section, Fig. 30).

Relationship between transported and in situ ferruginous duricrust

Thick regolith profiles are typical of large parts of Western Australia (Anand, 2005). Due to its genetic relationship with the underlying weathered bedrock and saprolith, there should be a geochemical relationship between in situ ferruginous duricrust and the parent bedrock. Conversely, this relationship should be less well defined between bedrock and transported ferruginous duricrust.

Paleodrainages, paleochannels and their associated deposits

Most of the contemporary rivers of inland Western Australia follow ancestral drainage systems with valleys infilled by alluvium and occasionally calcrete (Magee, 2009). These deposits are characterized by unconsolidated sediments or semiconsolidated sedimentary rocks, which were deposited within the channels and floodplains of paleodrainage systems (Eggleton, 2001). They can be buried, such as the paleovalleys of the Yilgarn Craton (de Broekert and Sandiford, 2005), or inverted, like some of the Channel Iron Deposits of the Pilbara Craton (Morris and Ramanaidou, 2007).

Two types of paleochannel deposits have been investigated on Mount Phillips: 1) branching in situ ferruginous duricrust; 2) inverted, partly silicified paleochannel deposits. Both are characterized by their distinct surface expression and both occupy an inverted position in the contemporary landscape.

Branching in situ ferruginous duricrust paleochannel deposits

On the Mount Egerton 1:250 000 Geological Series map sheet, Muhling et al. (1978) reported elongated, branching ironstone bodies that lie across valleys and hills, independent of the present-day topography. These

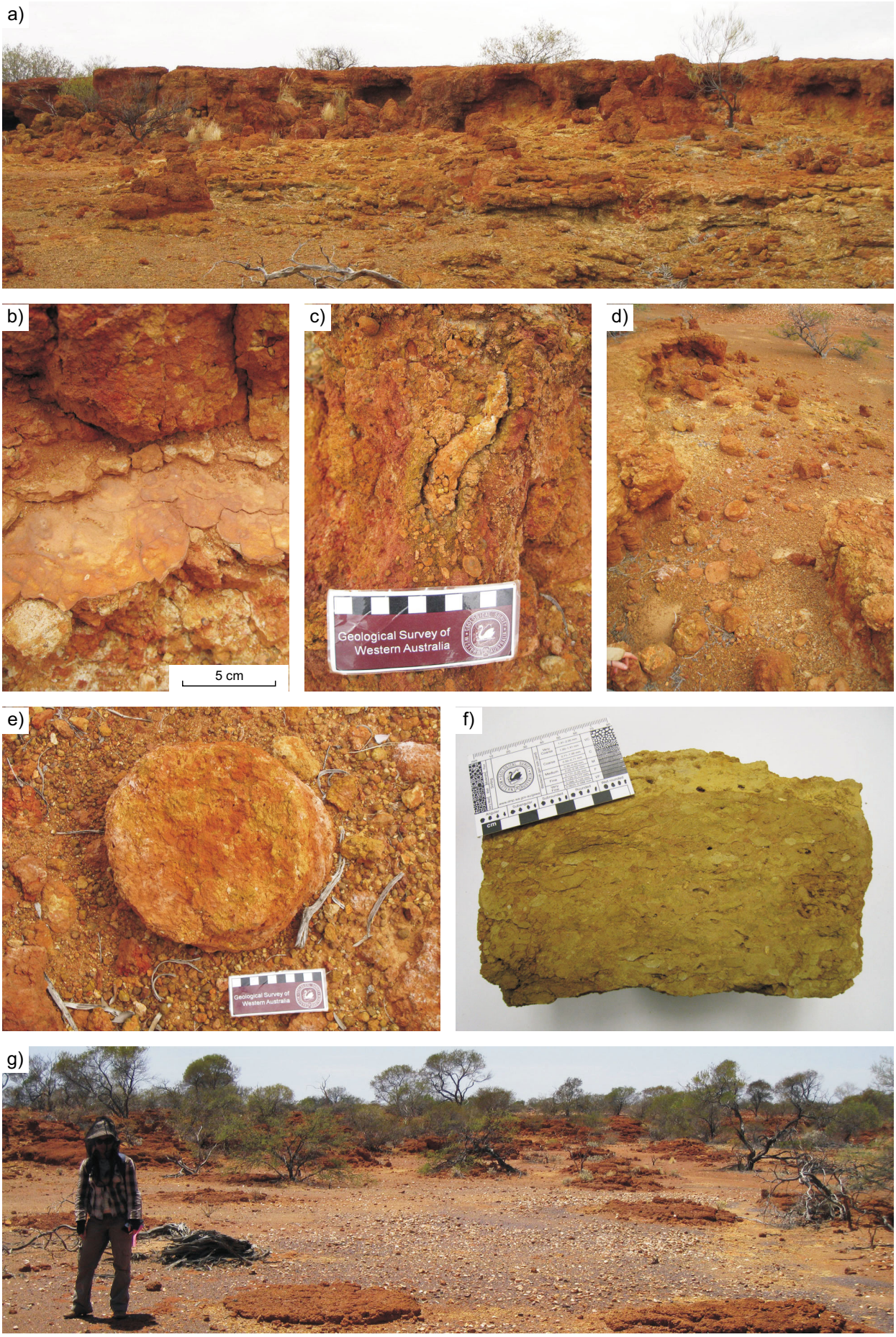

CK32 06/10/2010

Figure 25 (facing page) Outcrop views of Unit B measured section at Locations 2 and 3, First Bore locality: a) exposures along breakaway; b) thin mudcracked layers on top of bedding surfaces; c) root cast filled with calcrete and calcrete nodules; d) semiround to round, cylindrical 'tree stump-like' weathering features; e) detail of d) showing the top of a weathering feature; f) dissected sample of e) revealing internal complexity caused by different types of burrows (scale bar: 8 cm); g) large concentric weathering features, probably representing paleo-ant nests

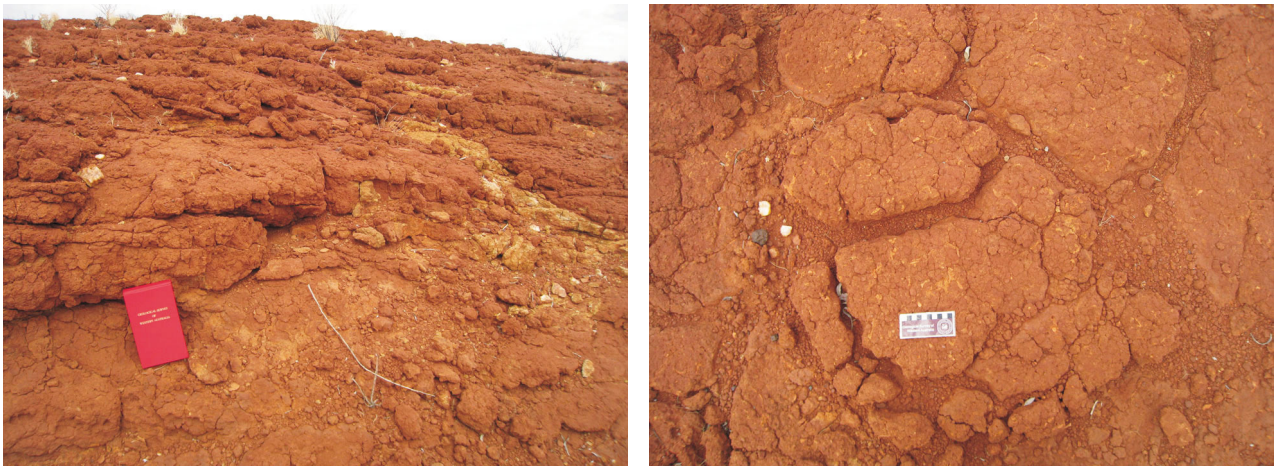

CK33 06/10/2010

Figure 26. Outcrop views of Unit C measured section at Location 4, First Bore locality: a) crumbly weathered, transported ferruginous duricrust, showing some faint bedding (field book for scale 21 x 13 cm); b) mudcracks developed on top of bedding surfaces (scale bar: 10 cm)

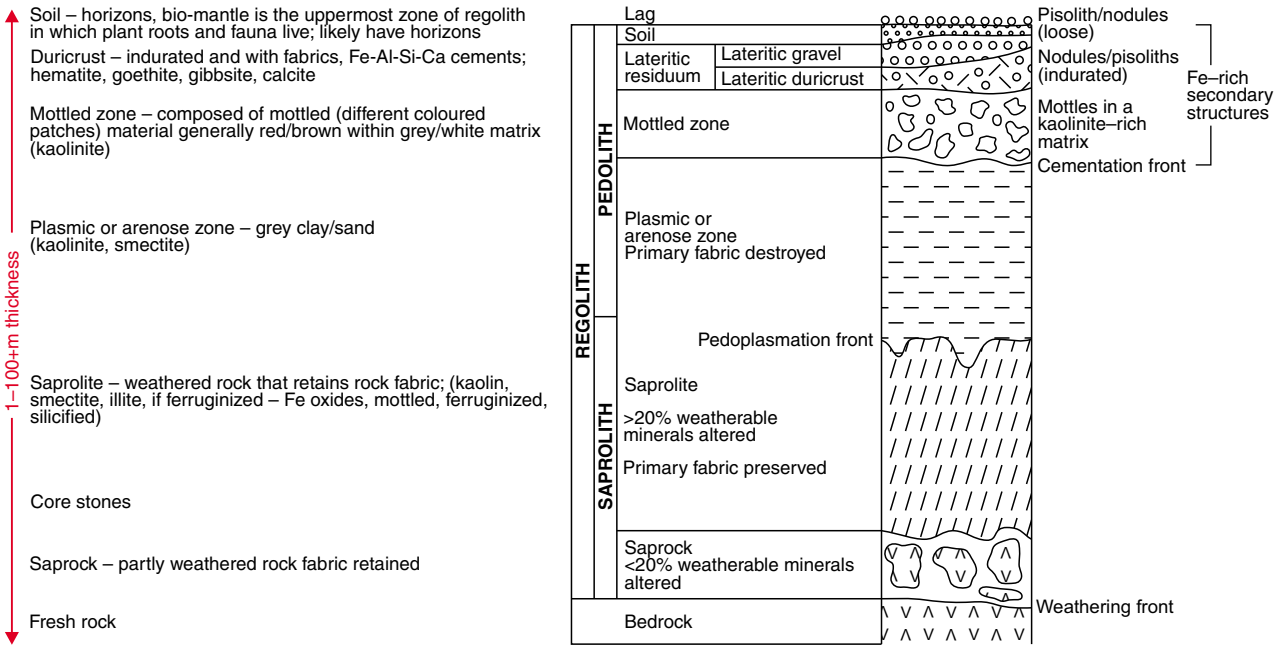

CK43 22/12/2011

Figure 27. Idealized in situ regolith profile (modified from: Eggleton, 2001)

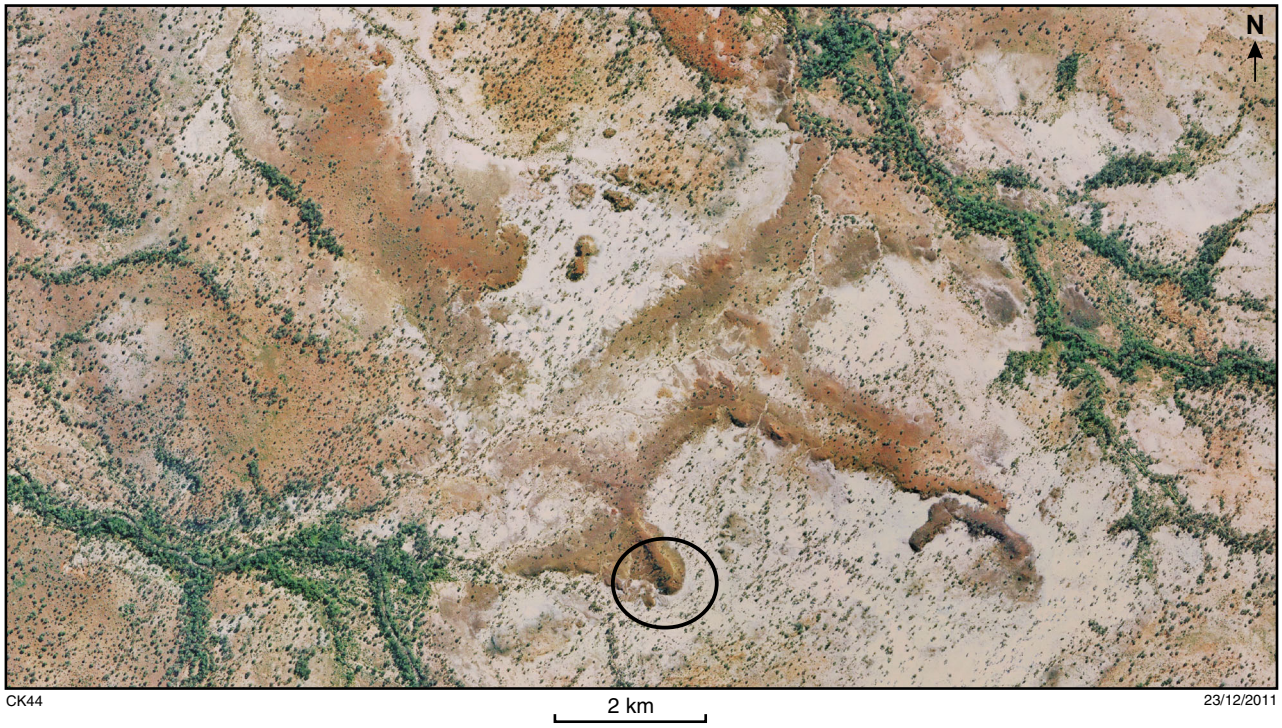

Figure 28. Tilted orthophoto showing in situ ferruginous duricrust outcrops mimicking a paleodrainage pattern at Location 4, No. 6 Bore locality. Circle indicates location of measured regolith profile (Fig. 29)

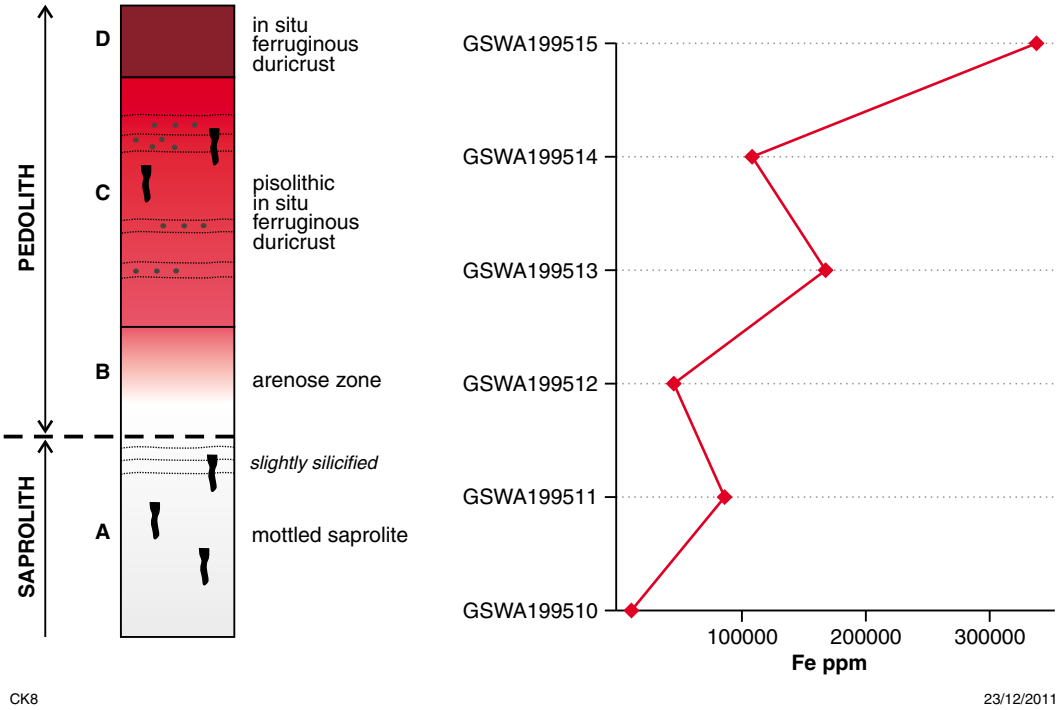

Figure 29. Composite log of the in situ ferruginous duricrust profile at Location 4, No. 6 Bore locality

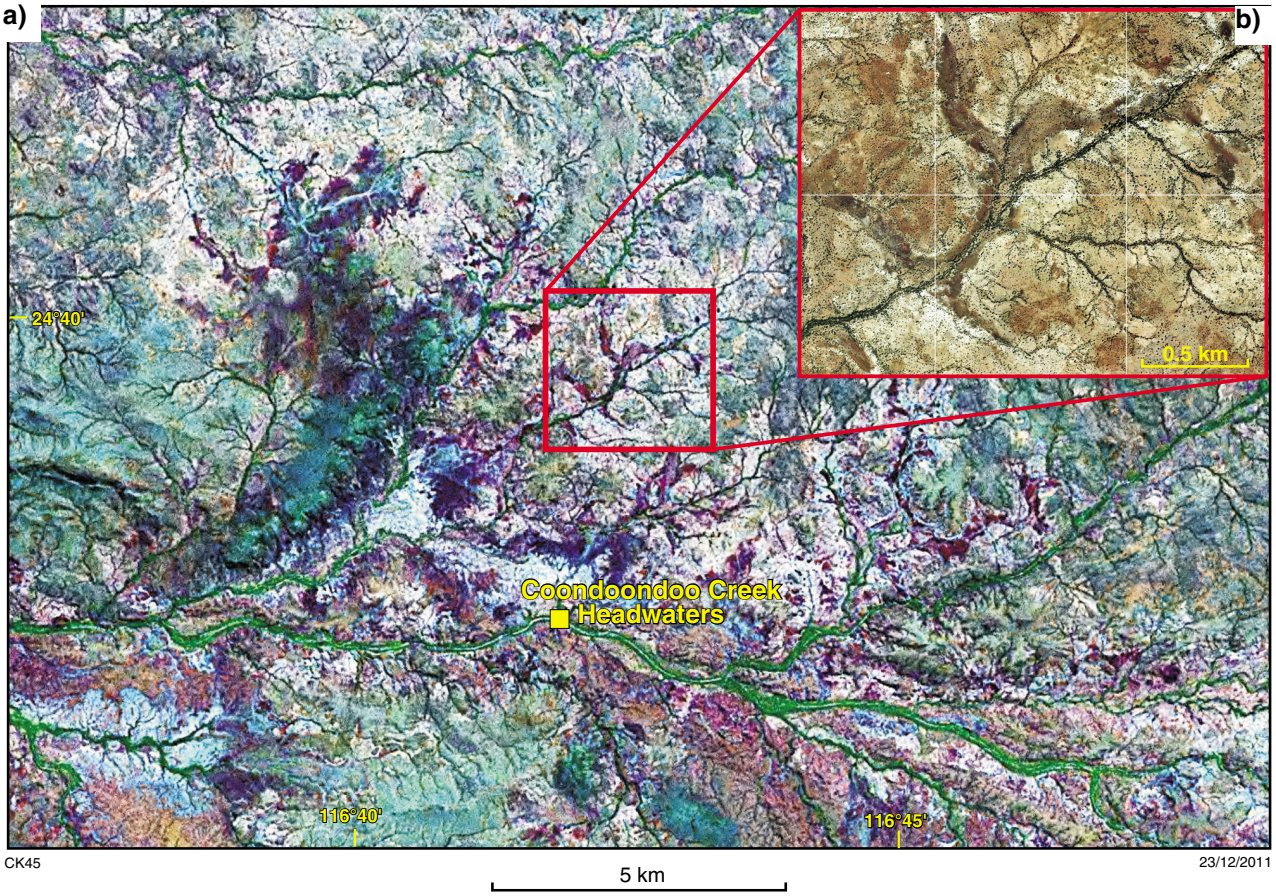

Figure 30. a) Landsat ETM7 image of Coondoondoo Creek headwater locality showing branched and elongated in situ ferruginous duricrust outcrops mimicking a paleodrainage system; b) orthophoto showing detail of a)

ironstone bodies have been interpreted to represent ancient streams. Similar features have been encountered in several locations on Mount Phillips, such as the No. 6 Bore locality (Eudamullah Station, Location 4) described above. At this locality, the top of the in situ regolith profile consists of a consolidated ferruginous duricrust which forms a pronounced capping. An aerial view (Fig. 28) shows a well-defined channel feature with breakaways along its outer margin and side branches that are incised by several smaller creeks.

Coondoondoo Creek headwaters locality, Dalgety Downs and Mount Phillip Stations (467375E 7274609N)

Throughout the headwaters of Coondoondoo Creek and its tributaries (Miniearra and Middle Springs creeks), dark areas on orthophotos and Landsat TM5 images (Fig. 30a, b) surrounding the present-day drainage channels and their interfluves preserve the morphology of an older dendritic drainage system. These areas are clearly unrelated to the current drainage system and are composed of ferruginous duricrust (Fig. 31); part of an in situ regolith profile developed over metamonzogranites of the Rubberoid Granite (Johnson et al., 2010a).

No. 6 Bore locality, Eudamullah Station

No. 6 Bore paleochannel

A well-defined 15 km long and up to 2 km wide sinuous channel-like feature extends northwards from Marloo Bore (378269E 7269613N) to Teddy Bore (387276E 7293758N) on Eudamullah Station. It forms a prominent feature on a 741 (RGB) Landsat TM5 image and on the Ternary Radiometric Image (TRI), especially in terms of the uranium band (blue; Fig. 32d).The regolith in this locality has previously been mapped as calcrete and kankar, partially replaced by silica, whereas adjacent areas consist of laterite and ferruginous deposits (Williams et al., 1983a). The outline of the mapped calcrete deposits also shows a distinct channel shape but these have not been investigated further.

A topographic cross section reveals this feature is inverted (Fig. 33), with the central part 10–15 m higher than the surrounding plains. Small drainage channels are incised along both margins, accentuating its channel-like shape (Fig. 32b). Two surface calcrete samples from one paleochannel location have 11.5 ppm and 20.7 ppm U (Appendix 2: GSWA199503 and 199508) indicating a minor increase of uranium in comparison to samples

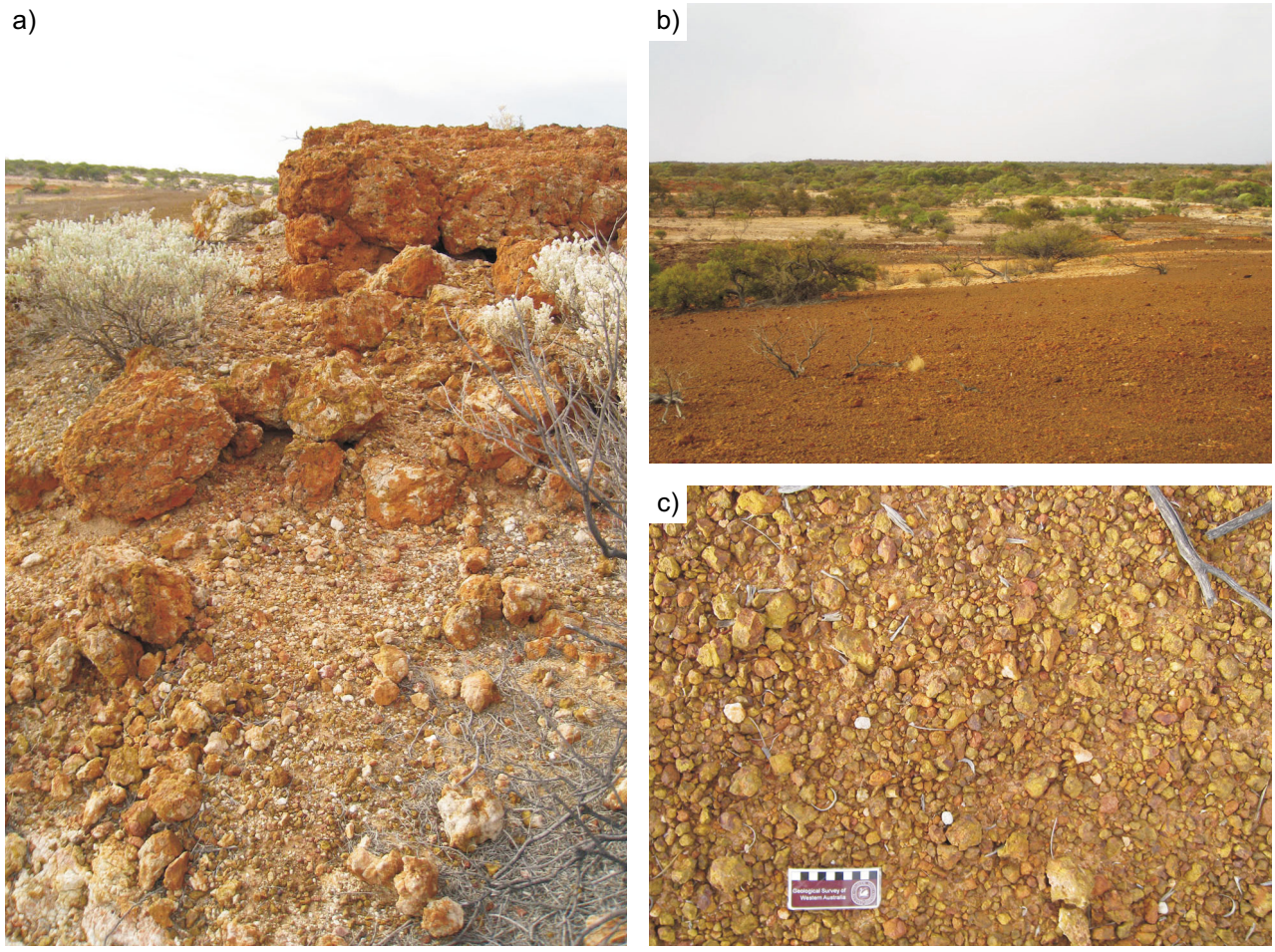

Figure 31. Outcrop view of in situ ferruginous duricrust at the Coondoondoo Creek headwater locality: a) breakaway on the margin of an elongate, branching in situ ferruginous duricrust outcrop; b) view along the top of a paleochannel; c) gravel surface lag on top of paleochannel in b)

from other calcretes and duricrusts of adjacent areas (see Appendix 2).

Field observations of the deposits associated with the paleochannel feature, coupled with studies of remote sensed images, DEM and radiometric data reveal a complex depositional and weathering history. On the Landsat AGSO ratio image (Fig. 32b) yellow areas west and east of the channel-feature represent ferruginous duricrust deposits. Bluish-purple and greenish-purple colours in its northern and central parts are reflecting areas of calcrete, and silicious and quartzose material is displayed in red.

In situ ferruginous duricrust has only been encountered along tributaries of Onslow Creek (3.6 km northeast of No. 6 Bore, Location 4), where it is part of an in situ regolith profile mirroring a paleodrainage pattern. Variably weathered, transported ferruginous duricrust is found adjacent to this material along its western and eastern margin, as well as in the lower parts of small creeks and gullies, along the margin and in the central parts of the paleochannel.

About 800 m south of No. 6 Bore, highly weathered sandstones crop out along a cutbank of a small creek. They are green and white coloured, with reddish iron stains, very poorly to poorly sorted, and fine to coarse grained. Subrounded to rounded quartz and silcrete pebbles, up to 1.6 cm, in a clay to silt matrix are also present. The sandstones are subhorizontally bedded with individual beds up to 5 cm in thickness. Some beds are partially silicified and bedding surfaces are commonly iron stained. One hundred metres to the north of this outcrop, sandstones are overlain by a pisolitic ferruginous duricrust with 0.5 – 3 cm diameter pisolites in a fine to very coarse grained hematitic matrix. A surface lag of angular to subrounded silcrete clasts up to 15 cm and 0.5 – 1 cm well-rounded pisolites covers the underlying sediments.

The ferruginous duricrust is overlain by poorly exposed groundwater calcretes (valley-fill type), commonly only

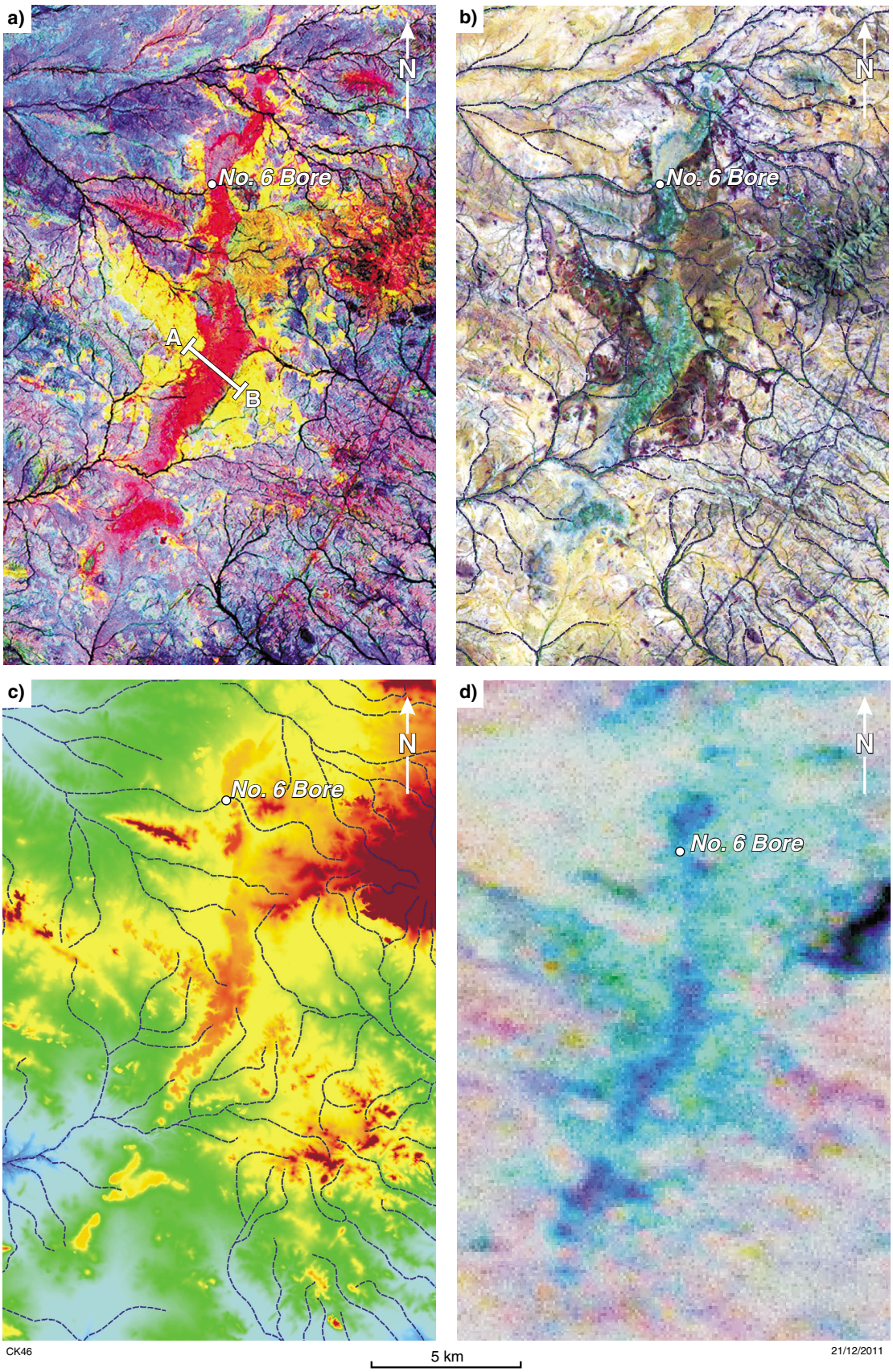

Figure 32. Remotely sensed images of the No. 6 Bore paleochannel on Eudamullah Station: a) Landsat TM5 AGSO ratio image showing the low, sinuous, channel-like feature (red) with a rim of transported ferruginous duricrust (yellow). A – B is line of section shown in Figure 33; b) Landsat TM5 false colour composite (741 RGB) overlain with present drainage; c) Digital Elevation Model (DEM) with 10 m contour interval; d) ternary radiometric image (TRI; potassium, thorium, uranium as red, green, blue respectively)

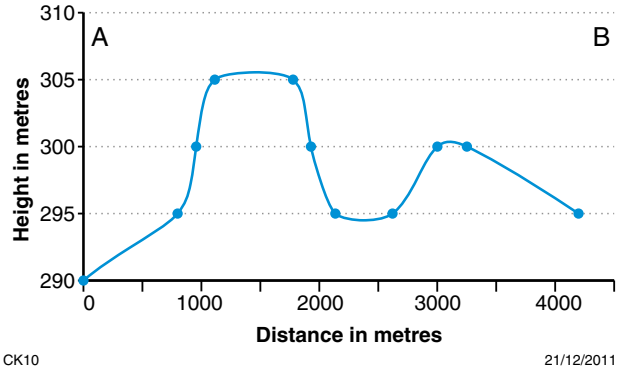

Figure 33. Topographic cross section of the No.6 Bore paleochannel showing its inverted and dissected character. Location of cross section indicated on Figure 32a

seen as blocks within scree. The calcretes are partly silicified or replaced by opaline silica. The whitish to grey calcrete has a nodular appearance, with 1–3 cm diameter subangular to subrounded calcrete clasts set in a massive carbonate matrix. An extensive 0.7 x 2 km calcrete plateau is preserved to the north of the paleochannel. Here, poorly exposed calcrete is partly silicified and overlain by a surface lag composed of weathered calcrete clasts. The calcrete is generally overlain by cellular to massive, white to translucent silcrete with locally ferruginized voids (Fig. 18a), although the contact between the two regolith types is seldom exposed. The silicified calcrete and the overlying silcrete form the most elevated and inverted paleochannel.

A spring-associated calcrete mound, located 500 m south-southeast of No. 6 Bore (No. 6 Bore locality, Location 1), is believed to be younger than the valley-fill calcrete as it crops out within a small creek, which is incised into the transported ferruginous duricrust and the overlying valley-fill calcrete.

Interpretation

Due to its distinct shape and the outcropping regolith material, this sinuous channel-like feature is interpreted as a paleochannel, which has been inverted due to weathering and erosion of the surrounding land surface. It is informally named No. 6 Bore paleochannel after No. 6 Bore, the only bore directly located within the paleochannel feature. Figure 34 shows a schematic interpreted cross section of the No. 6 Bore paleochannel.

Alluvium

Alluvium is present along and within present-day drainage systems on Mount Phillips. The modern fluvial channels and associated floodplains are ephemeral and only active after heavy rain. The planform channel morphology of the Gascoyne and Lyons rivers is straight to slightly sinuous, with multiple anastomosing channels. Usually only one main channel is active during runoff. Individual channels are flat bottomed and can be, as in the case of the Gascoyne River, up to 120 m wide. Material deposited within the channels and floodplains include clay, silt, sand, and gravel in variable proportions. The channel surface commonly shows some reworking by eolian deflation between the periods of fluvial runoff. Modern-day channels are incised into older alluvial deposits. The tributaries also carry a substantial amount of sediment and are incised to different degrees into the underlying, typically strongly weathered bedrock.

Lyons River crossing locality, Eudamullah Station (349642E 7300771N)

Near the confluence of Onslow Creek and Lyons River on Eudamullah Station the main channel of the Lyons River is incised up to 2 m into older deposits, exposing two older generations of fluvial deposits (Fig. 35). In the lower 60 cm of the cutbank, a semi-consolidated, upward fining, light-brown to mottled, carbonate-cemented, planar to cross-bedded, poorly sorted, fine- to coarse-grained pebbly sand is exposed (Fig. 35b). It contains calcified to slightly silicified root casts up to 30 cm long and 3 cm in diameter (Fig. 35c). This unit is erosively overlain by an 80 cm thick succession of massive to trough cross-bedded, poorly to moderately sorted fine- to very coarse-grained pebbly sand. Individual troughs are about 5 m long and 0.1 – 0.2 cm thick. Some clast imbrication is visible at the base of troughs (Fig. 35d) and root casts and reworked calcrete nodules are common. The succession is overlain by fine-grained modern floodplain deposits.

This fluvial succession records an episodic history of erosion and deposition, which in turns reflects changes in discharge and sediment supply caused by changes either in climate or base level in the catchment areas. No age data are available for these deposits but Denman et al. (1985) suggested that the modern course of the Gascoyne River was established during a wet phase between 40 000 to 25 000 BP.

Sheetwash

Sheetwash deposits are the result of sediment transport by episodes of thin, continuous sheetflow over relatively smooth surfaces (Eggleton, 2001). On Mount Phillips and adjacent areas sheetwash deposits are mainly associated with the low hillslope terrain of the Edmund and Carnarvon basins, which are weakly dissected by present-day drainage. Large sheetwash areas are characterized by a banded mosaic vegetation pattern (‘tiger bush’; Wakelin-King, 1999) which represents a combined soil/sediment and vegetation response to the effects of an arid climate on gently sloping plains of between 0.5 and 2º (Dunkerley and Brown, 1995). Bands of vegetation, separated by bare ground, are aligned roughly parallel to the contour lines (Eggleton, 2001). Banded mosaic sheetwash deposits are present in the foreland around Mount Augustus and Bore Paddock Hills, and on the interfluve areas of some Gascoyne and Lyons River tributaries.

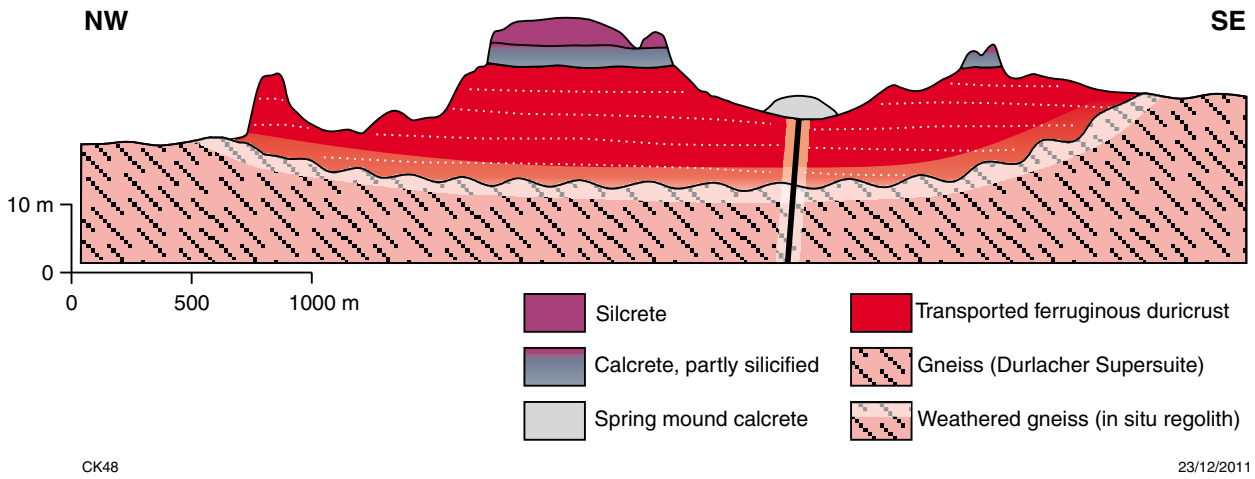

Figure 34. Schematic NW to SE cross section of the No. 6 Bore paleochannel

Corner Well locality, Eudamullah Station (356461E 7298898N)

A large area of banded mosaic sheetwash occurs in the western part of the Eudamullah 1:100 000 Geological Series map sheet area in interfluve areas along the lower reaches of Onslow and Calbajacka creeks (Fig. 36a). This area is characterized by pattern of alternating vegetated and unvegetated sheetwash deposits (Fig. 36b).

The vegetated sheetwash deposits are orange-red, crumbly, moderately sorted, silt to medium-grained sands and have been intensely bioturbated by ants and termites (Fig. 36c). Plant fragments are common. The unvegetated areas are characterized by faintly subhorizontal bedding, poorly sorted, clay to coarse-grained sand with isolated pebbles. Individual beds are less than 1 cm thick. The sediment is mainly composed of iron-coated quartz grains, with minor silcrete and quartzite pebbles at the surface. Mudcracks are present on the surface in small depressions, and 1–3 cm long mud chips occur in the subsurface, accentuating the bedding of the sheetwash deposit (Fig. 36d).

At other locations (e.g. Location 1of the Landor Homestead locality), pedogenic calcrete has formed within sheetwash deposits. In these cases, sheetwash deposits are composed of red, faintly bedded, poorly sorted, clay to coarse-grained sand. Small angular to subrounded calcrete clasts of up to 5 mm are common within the sheetwash, indicating the presence of pedogenic calcrete in the subsurface.

Colluvium

Colluvium is present across the entire Mount Phillips Geological Series map sheet area and is typically associated with hillslopes and prominent topographic highs, such as Mount Augustus. Colluvium consists mainly of locally derived quartz, lithic fragments, and silcrete and ferruginious duricrust fragments, set in a dominantly silty to sandy, and in some cases gravelly, matrix. The composition of the colluvium is highly dependent on its source and in most cases correlates with underlying or nearby exposed bedrock or regolith.

At least three generations of colluvium are inferred, based on the degree of induration and incision. Where a relative age assignment was not possible colluvium is unassigned and undivided. The oldest generation is composed of weakly cemented and compacted silt, sand, and gravel. In many areas it is deeply dissected by present-day drainage. Partly consolidated silt, sand, and gravel make up the second oldest generation of colluvium, which is also partly dissected by the present-day drainage. The youngest colluvium is characterized by quartz and lithic fragments in an unconsolidated silt and sand matrix. The thickness of the colluvium varies considerably and ranges from a single layer gravel lag, to a deposit several metres in thickness. A deflation lag, in places with ventifacts, has developed on the top of many colluvial units, indicating post-depositional periods of eolian deflation and abrasion (Fig. 37).

Discussion

Australia's paleoclimatic and weathering history — implications for the Gascoyne region

The weathering history, and hence the regolith and landscape, of an area is closely related to climatic variations through time (Fig. 38). Deep weathering has affected most rock types and geological provinces across the Australian continent (Anand, 2005). Lithology, structural features, landscape position, and the overlying sediments play an important role during the weathering process. The weathering depth and regolith thickness

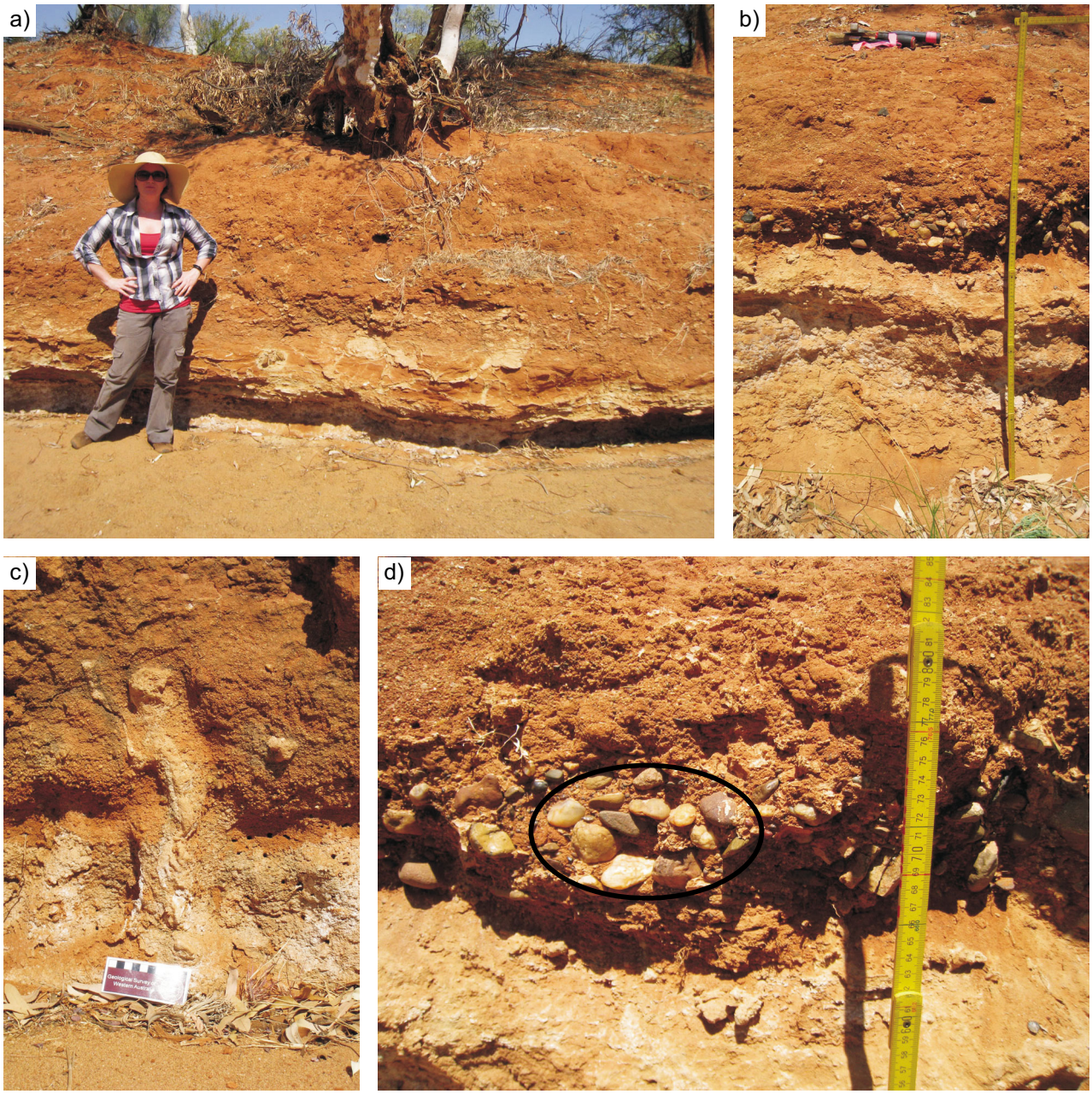

Figure 35. **a) Outcrop view of the alluvial succession exposed in a cutbank of the Lyons River at the Lyons River crossing locality (person for scale 1.55 m); b) carbonate-cemented fluvial sands unconformably overlain by trough cross-bedded channel deposits (scale measure: 1.20 m); c) calcified to slightly silicified root cast at base of succession; d) detail of scour eroded into carbonate-cemented fluvial sands. Quartz and silcrete pebbles show some imbrication (circled). Scale measure is 35 cm**

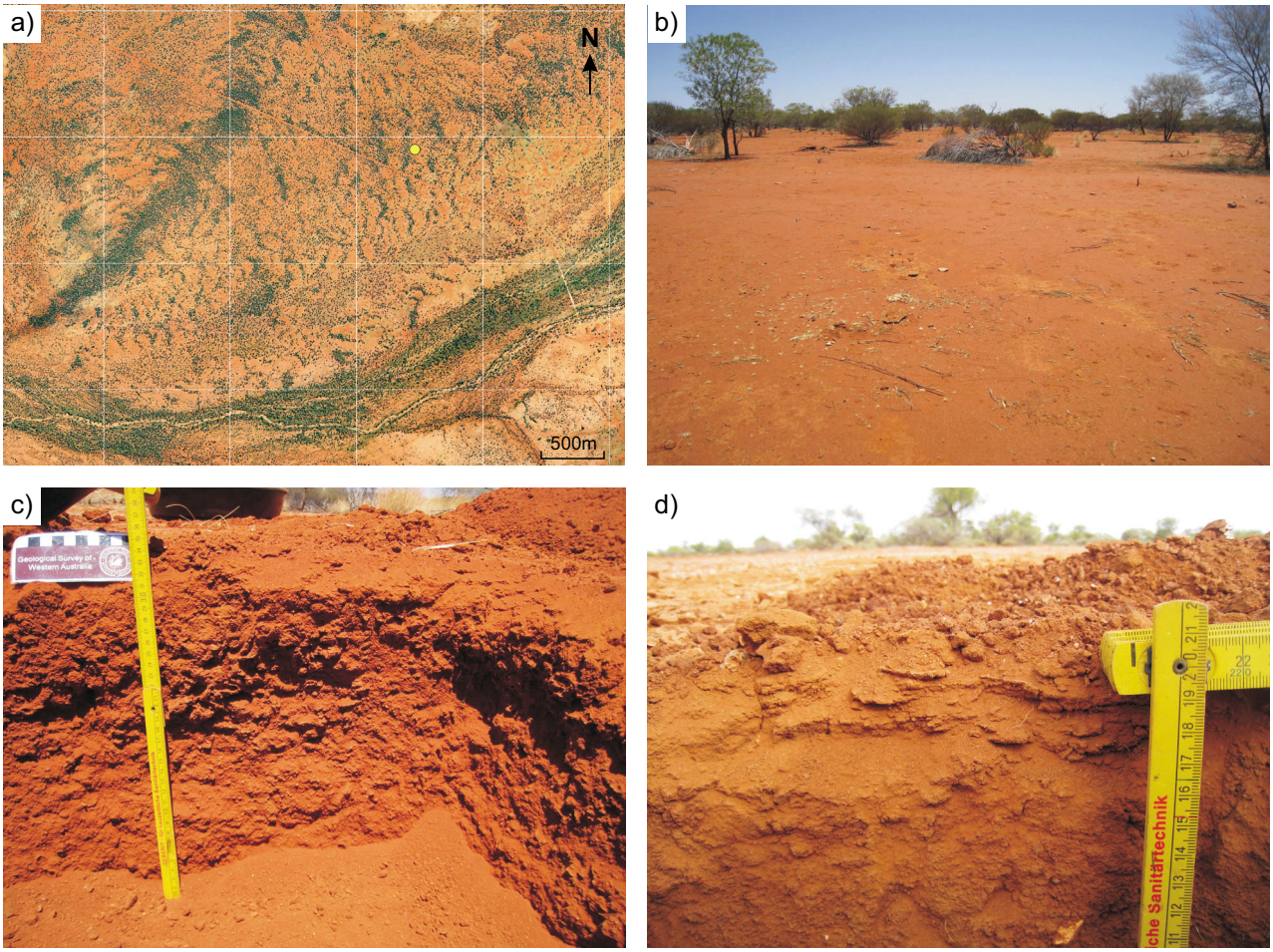

Figure 36. Orthophoto and outcrop views of tiger-bush patterned sheetwash, Corner Well locality: a) orthophotograph showing dark vegetated bands alternating with lighter unvegetated areas; b) surface view of a) looking from an unvegetated area towards an area of low bushes and acacias. Note that vegetated areas do not appear as densely vegetated as in the aerial view; c) trench into vegetated sheetwash showing intensely bioturbated, massive to crumbly silt to medium-grained sand; d) trench profile showing thin layers with some development of mudcracked surfaces preserved in the upper 5 cm. The lower part of the profile is more massive due to compaction and bioturbation.

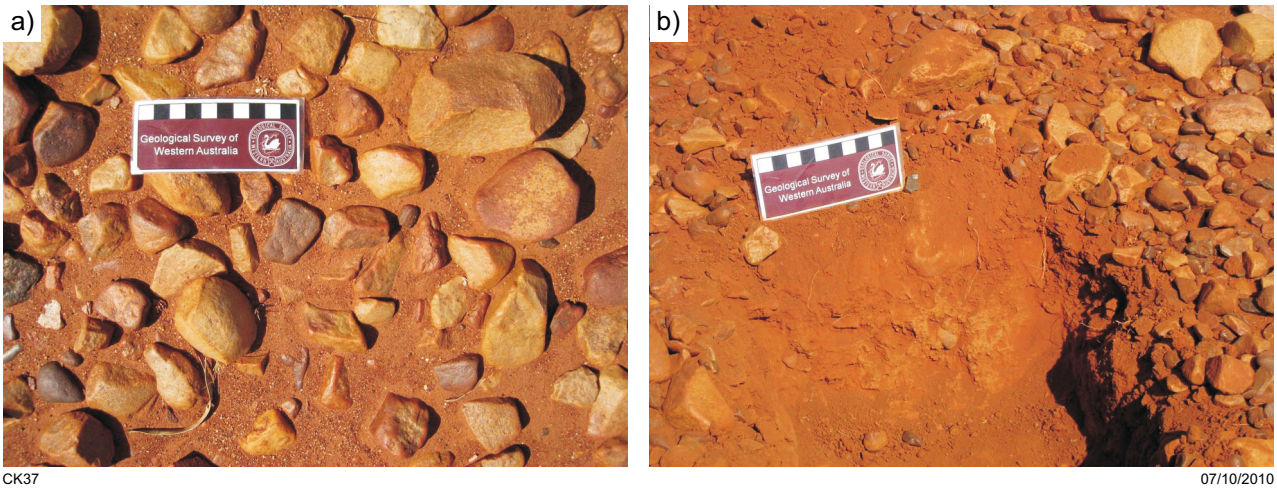

Figure 37. Alluvial fan surfaces along the northeastern foothills of the Bangemall Anticline: a) gravel lag of subrounded to rounded quartzite, abraded by wind erosion to form ventifacts; b) trench into alluvial fan surface showing quartzite-rich colluvium in a sand-rich matrix

vary considerably but can be up to 200 m in some areas (Anand, 2005). In the Gascoyne region, regolith depth of up to 136 m has been recorded near Mt Dalgety (Barranco Resources, 2009 confidential WAROX report). In general, weathering is deeper in topographic lows and on paleoplains than on erosional plains and hilly areas.

The types and distribution of regolith in the Gascoyne region reflect the variety of climatic conditions this region has experienced throughout the Cenozoic, Mesozoic, and Paleozoic (Fig. 38) (Van De Graaff et al., 1977; Cockbain and Hocking, 1990). However, the paleoclimatic history and the Cenozoic stratigraphy of the Gascoyne region are poorly understood, as is the case for many parts of Western Australia.

Pillans (2005) discussed a broad geochronological framework for the Australian regolith, and carried out paleomagnetic dating of hematite from approximately 30 sites throughout Australia, with a focus on the Yilgarn Craton (Fig. 39). There is a distinct bimodality in the data, pointing to events around 50–60 Ma, 10 Ma and <1 Ma, with some evidence of Mesozoic or even earlier weathering. Vasconcelos (2008) noted three main peaks, corresponding to the Cretaceous – Tertiary (65–70 Ma), the Late Eocene – Oligocene boundary (35 Ma) and the Early to Middle Eocene (20–13 Ma).

The driving force for climatic change during the Paleogene and Neogene was Australia's separation from Antarctica, which commenced in the latest Early Cretaceous, and resulted in an overall global cooling since the latest Early Eocene (Anand, 2005). At the beginning of the Paleogene, Australia was 25° south of its current position and has since continued to move about 3000 km north through a series of different climatic zones, which have themselves changed position during the Cenozoic (Fig. 38).

In the Paleocene and Eocene, a warm and wet climate resulted in much of the land being covered by rainforest. Warming culminated in the 'maximum Tertiary warmth' during the early Early Eocene, when very warm to hot temperatures were recorded for most parts of Australia (Macphail, 2007). This period was associated with wet to very wet conditions across the Australian continent (Macphail, 2007).

Very warm to hot conditions persisted in northwestern Australia throughout the Middle to Late Eocene, and similar conditions first developed in north-eastern Australia during the Oligocene and Miocene. Temperatures in northern Australia probably remained very warm to hot throughout the Neogene, due to rapid northward drift of the continent, despite a global cooling trend (Macphail, 2007). During the Oligocene, overall temperatures became cooler and closer to present-day temperatures (Frakes and Kemp, 1972) before they became warm to hot again in the Early Miocene.

At the Early to Middle Eocene boundary, variable and wetter conditions resulted in an increase in fluvial discharge, triggering deep and widespread fluvial incision, which is evident as the 'inset valleys' of the paleodrainage systems of the Yilgarn Craton (de Broekert and Sandiford, 2005). Wet to very wet conditions persisted into the Middle to Late Eocene, except that rainfall became more variable and possibly less reliable in central and south-western Australia and more uniformly distributed or more reliable during summer months in southeastern Australia (Macphail, 2007).

By the Oligocene to Middle Miocene, subhumid conditions prevailed in northwest Australia, with limited evidence for a decrease in rainfall in central and southwestern Australia. Rainfall remained high in the northeast, central south and southeast mainland Australia, and in Tasmania (Macphail, 2007).

By the Middle Miocene, the permanent southern ice cap formed, the temperatures started to cool again, and aridity increased markedly from the Late Miocene. The fauna progressively adapted to the changing environment, rainforests contracted, and desert conditions became established in the centre of Australia.

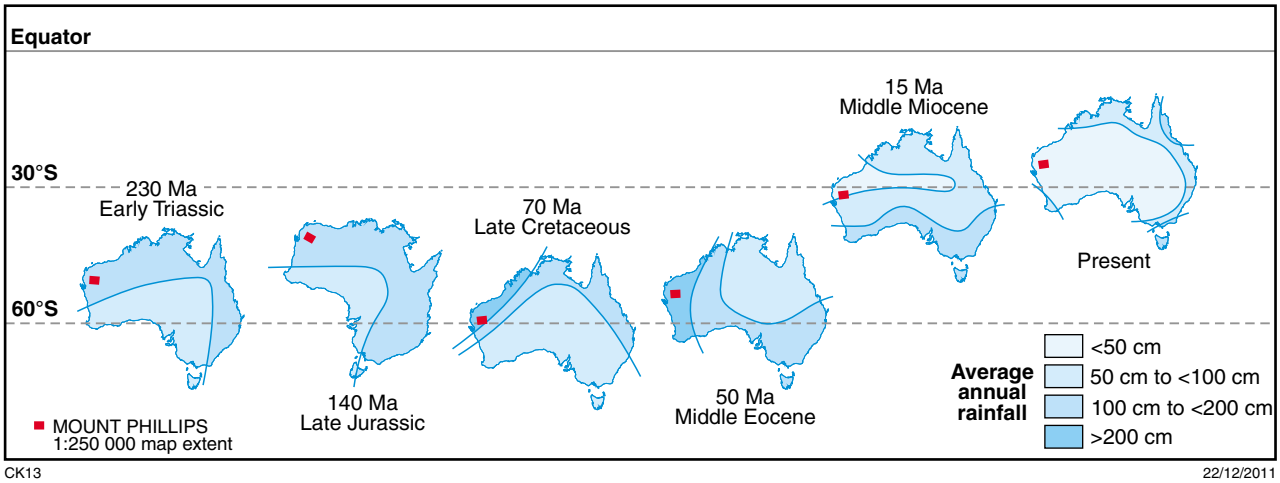

Figure 38. Paleoclimatic reconstruction of Australia from the Early Triassic to present (modified from: Anand, 2005) showing changes in latitude. Red square is outline of Mount Phillips 1:250 000 Geological Series map sheet

During the Early Pliocene, aridity increased markedly in association with global cooling. Three arid periods (at 2.9, 2.59, and 2.56 Ma) have been recorded from the Yallalie site in southwest Western Australia (Macphail, 2007). By the Late Pliocene, most elements of the modern bioclimatic regimes were in existence (Macphail, 2007).

Periods of alternating aridity and humidity during the Pleistocene were caused by global glacial minima and maxima culminating in maximum aridity during the last glacial maximum between 17 500 to 16 000 BP (Bowler, 1976).

Towards a landscape evolution model for the Mount Phillips 1:250 000 Geological Series map sheet area

Western Australia has a long and complex weathering and landscape evolution history, some of which took place under climatic conditions quite different from the present. However, little is known about the absolute age of regolith or the timing of regolith-forming processes (Pillans, 1998, 2005) in large part due to the lack of suitable regolith minerals for isotopic dating, and the lack of fossils in much of Australian's regolith. Nevertheless, a number of dating methods have been successfully applied to the Australian regolith (Pillans, 1998, 2005) and are helping to build the framework for reconstructing the evolution of Western Australia's regolith-dominated landscape (Tables 4 and 5).

The current regolith study of the Gascoyne region shows that several episodes of weathering including ferruginization, calcretization, silicification and erosion have occurred, leading to the complex regolith distribution of the current landscape. Due to the lack of absolute ages only relative age is assigned (Table 6).

With the exception of the Southern Carnarvon Basin, most of the bedrock on Mount Phillips must have been subaerially exposed or episodically exhumed since at least the Precambrian (Butt et al., 1977; Taylor, 1994; Pillans, 2005). This resulted in continuous weathering and the formation of extensive in situ regolith profiles over Gascoyne Province and Edmund Basin rocks. In the south-western part of the study area, where Upper Carboniferous and Lower Permian sedimentary rocks of the Southern Carnarvon Basin are exposed, subaerial exposure started during the Permian (Taylor, 1994; Pillans, 2005).

Development of deep weathering profiles and ferruginization was widespread in Australia during the Lower to Upper Cretaceous to early Paleogene (McGowran, 1979). Williams et al. (1983a) and Elias and Williams (1980) reported a 'Tertiary' land surface, which, due to active erosion, is only preserved as 'laterite' remnants along watersheds. Williams et al. (1983a) also included calcrete and silcrete as part of this 'old duricrust surface'. The current study has shown that two distinct types of ferruginous duricrust (in situ and transported) are found in the Mount Phillips Geological Series map sheet area and that there is no conclusive evidence that these are either stratigraphically equivalent or related. In situ ferruginous duricrust is part of the in situ regolith that developed over bedrock, mainly within the Gascoyne Province, whereas transported ferruginous duricrust is the result of widespread ferruginization of alluvial sediments in ancestral river valleys and alluvial plains.

Transported ferruginous duricrust is the result of intense post-depositional ferruginization of alluvial sediment that was originally deposited on wide plains and in wide semiconfined valleys (Fig. 40a). The deposits are primarily composed of reworked weathered bedrock. After deposition these sediments were intensely bioturbated and modified by soil-forming processes, cementation, weathering, and erosion.

This was followed by an extensive period of ferruginization that resulted in a more subdued landscape (Fig. 40b). Erosion of this landscape led to the development of an ancestral paleodrainage system (Fig. 40c, Fig. 41). The sediments deposited within the channels were ferruginized (Fig. 40d) followed by the development of calcrete along the ancestral river courses (Fig. 40d). Calcretization partly affected the underlying transported older ferruginous duricrust (e.g. outcrops at Victory Bore locality). The calcretes in turn have been overprinted by extensive silicification and replacement by opaline silica (Fig. 40e), which resulted in the development of an extensive silcrete. Subsequent rejuvenation and erosion led to landscape inversion and the formation of silcrete-capped mesas, mainly along the valleys of the ancestral drainage systems and inverted paleochannels that are unrelated to any present drainage pattern (Fig. 40f).

Ferruginization and deep weathering is generally associated with higher temperatures, higher rainfall, and the development of transgressional sedimentary sequences, whereas silicification is associated with cooling, accompanied by more arid continental conditions and regressional sequences (McGowran, 1979). Calcrete development is dependent on a variety of factors, such as the presence of carbonate, groundwater, and a suitable host material

Three episodes of ferruginization and two episodes of silicification have occurred in Australia leading to episodic duricrust development (McGowran, 1979). Intense weathering and ferruginization resulted in the development of deep weathering profiles during the Early to mid-Cretaceous to Early Tertiary. Two other episodes of ferruginization occurred in the Early Miocene between 25 and 15 Ma, and resulted in the formation of an inferred Australia-wide peneplain during the Pliocene (McGowran, 1979).

On Mount Phillips also, three phases of ferruginization are recognized. The first resulted in the development of the in situ ferruginized regolith profiles over bedrock, mainly within the Gascoyne Province (Fig. 23). A second phase of ferruginization has affected the mainly alluvial and colluvial sediments that are widespread in the study area. These represent potential correlatives to the Wiluna Hardpan deposits (Fig. 40a, b). The third phase of ferruginization followed the incision and

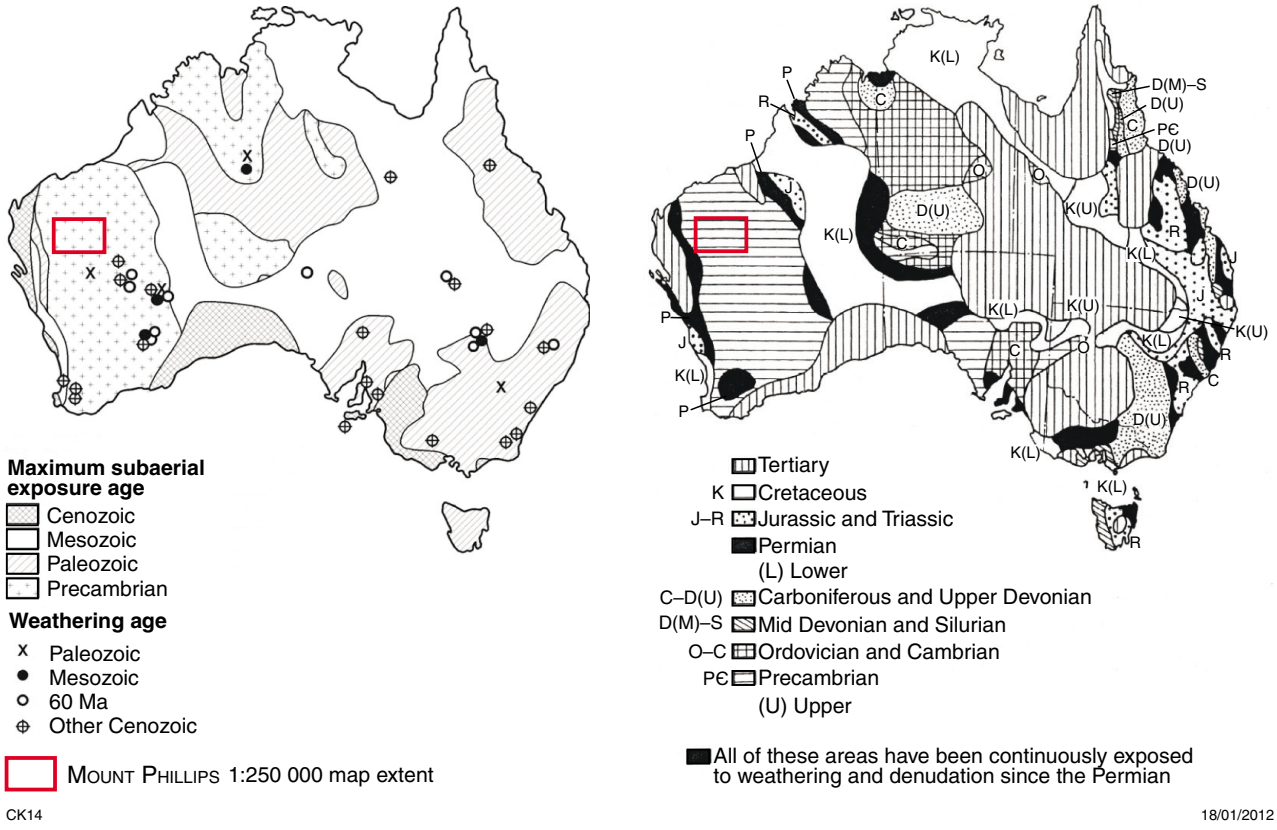

Figure 39. Exposure and paleomagnetic ages of Australian regolith: left) maximum duration of subaerial exposure and paleomagnetic ages determined on Australian regolith (from Pillans, 2005); right) age of exposure of land surfaces (modified from: Macphail, 2007 p. 35)

Table 4. Summary of paleomagnetic ages (Ma) from weathered regolith in Western Australia (from: Pillans, 2005)

	Paleomagnetic ages (Ma)					
Location	*0–20*	*20–50*	*50–65*	*65–250*	*>250*	*Reference*
Perth Basin	X					Schmidt and Embleton, 1976
Jarrahdale bauxite mine	X					Anand and Paine, 2002
Boddington Au mine	X					Anand and Paine, 2002
St Barbara's Au mine	X				X	Pillans, unpublished
Wiluna	X	X				Pillans, unpublished Schmidt and Williams, 2002
Lawlers Au mine	X		X		X?	Anand and Paine, 2002
Bronzewing Au mine	X		X			Anand and Paine, 2002
Murrin Murrin Ni mine				X		Anand and Paine, 2002
Mt Percy Au mine	X		X	X		Pillans and Bateman, 2000
Kanowna Belle Au mine			X			Anand and Paine, 2002
Lancefield Au mine	X	X	X		X	Pillans, unpublished

Table 5. Evolution of the western part of the Australian continent (modified after: Macphail, 2007)

Time slice	*Temperature*	*Rainfall*	*Seasonality*
Paleocene	upper mesotherm	subhumid–humid	strong
65 – 54.8 Ma	(18–24°C)	(600–1200 mm pa)	(rainfall)
	very warm	dry to wet	
Early Eocene	upper mesotherm	perhumid	strong
54.8 – 49 Ma	(18–24°C)	(>1200 mm pa)	(rainfall)
	very warm	very wet	
Middle to Late Eocene	mesotherm range	humid–perhumid	variable
49 – 33.7 Ma	(14–24°C)	(900–1200 mm pa)	(rainfall)
	warm to very warm	wet to very wet	
Oligocene to Middle Miocene	lower mesotherm	subhumid–humid	variable
33.7 – 11.2 Ma	(14–18°C)	(600–1200 mm pa)	(rainfall)
	warm	dry to wet	
Late Miocene to Pliocene	mesotherm range	subhumid–humid	strong
11.2 – 1.78 Ma	(14–24°C)	(600–1200 mm pa)	(rainfall)
	warm to very warm	dry to wet	

deposition of fluvial sediments within the ancestral valleys of the paleodrainage system of the Gascoyne River (Fig. 40c, d; Fig. 41). Only one phase of silification has been encountered (Fig. 40e) following the periods of ferruginization and calcretization of the dominantly colluvial and alluvial sediments, and prior to the phase of erosion leading to today's topographic landscape surface expression.

Silicified calcretes are exposed up to 35 m above the present valley floor of the Gascoyne River, and this suggests that uplift must have rejuvenated the river systems after extensive calcrete development and subsequent silicification. This process has also been discussed by Butt et al. (1977). As a result, the sediments have been eroded and elevated in the form of mesas or inverted paleochannels (Figs 4, 40, 41). The surface heights from the top of the silicified calcrete mesas decrease from the intersection of the Thomas and Gascoyne rivers downstream to McGregor Well, from 330 m AHD to 280 m AHD over a distance of 50 km, resulting in a surface gradient of 0.09%. The same gradient exists along the modern-day channel floor of the Gascoyne River.

Butt et al. (1977) identified a number of terraces along the western part of the Gascoyne River and its tributaries that reflect a complex history of deposition and erosion. Two of these terraces were calcretized and were termed by Butt et al. (1977) 'lower' and 'upper' terrace. The upper terrace is capped by silicified calcrete or silcrete and forms the prominent mesas within the Gascoyne paleovalley.

Denman et al. (1985) stated that the modern courses of the lower Gascoyne and Wooramel Rivers were established during a wet climatic phase between 40 000 to 25 000 BP. This was followed by major eolian reworking during an arid phase between 25 000 to 16 000 BP.

At least three generations of fluvial deposits have been encountered within the modern-day Lyons River, a major tributary of the Gascoyne River. The formation of the younger valley-fill calcretes and pedogenic calcretes most probably fall within this period (e.g. Big Bend Bore and Landor Homestead localities). No absolute ages are available for these deposits but the sedimentary succession indicates several episodes of erosion and deposition, which in turn reflects changes in discharge and sediment supply resulting from either change in climate or base level in the catchment areas.

Conclusions

The wide variety of regolith types present in the Mount Phillips Geological Series map sheet area reflect the complex landscape evolution of this part of the Gascoyne region. The nature of the in situ regolith units are closely related to the types of underlying bedrock. Differential rates of erosion and weathering during the Cenozoic resulted in a variety of different weathering styles on Archean to Phanerozoic rocks. Ferruginization and silicification of these rocks formed resistant rises, hills, and mesas. Relief inversion occurred in places over paleosurfaces. Weathering products are retained where the rate of weathering is greater than the rate of erosion.

Most of the transported relict regolith units, and some of the older alluvial and colluvial regolith units, have been cemented and lithified during alternating episodes of wet and dry climatic conditions, involving processes such as infiltration, desiccation, bioturbation, cementation, and mineral transformation.

Because there are no absolute ages for any regolith unit on Mount Phillips and neighbouring areas, only an interpretative simplified relative stratigraphy has been developed. Correlation with other regolith units such as the Wiluna Hardpan is problematic.

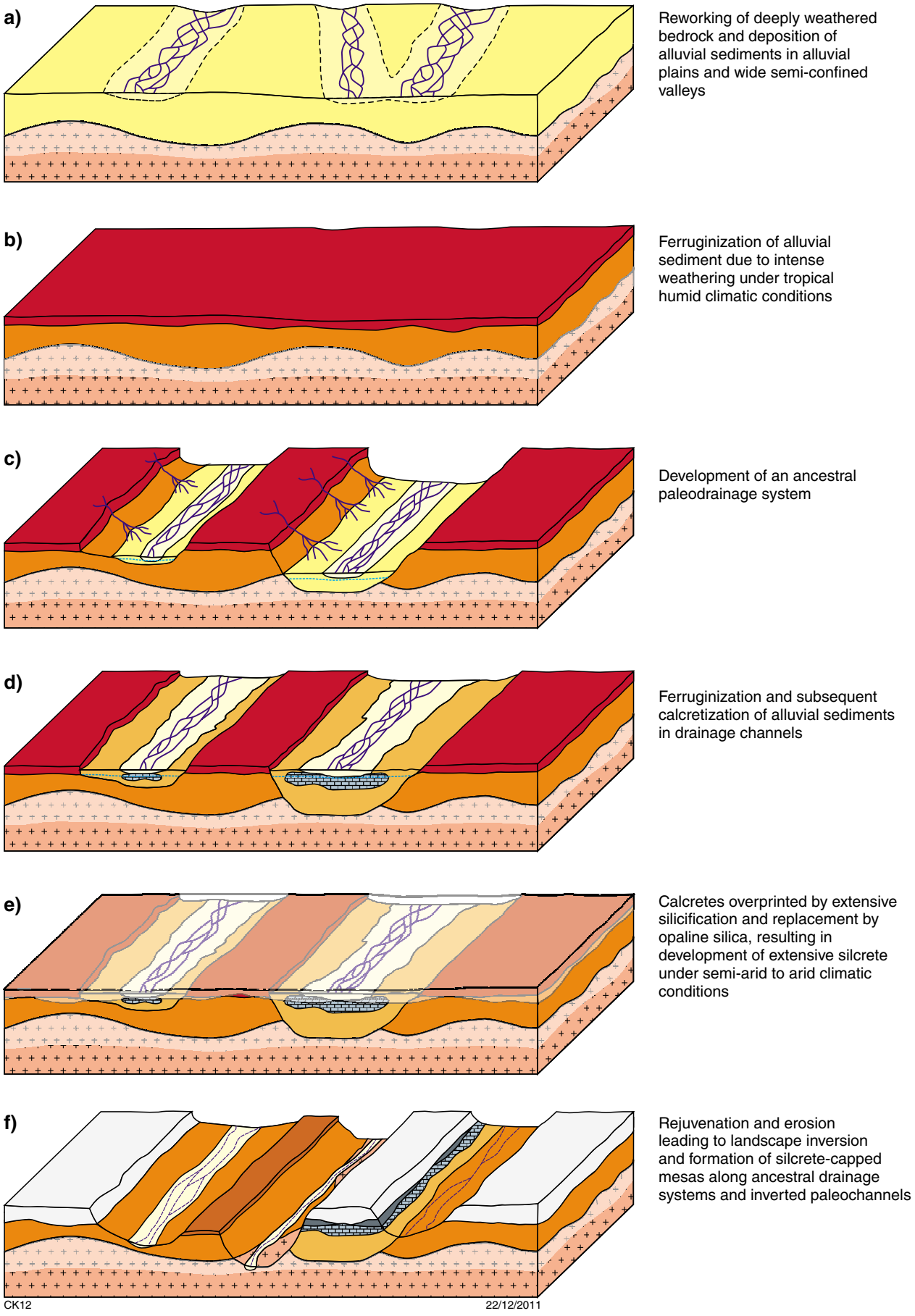

Figure 40. Landscape evolution model for the Mount Phillips 1:250 000 Geological Series map sheet

Table 6. Comparison of interpreted regolith and regolith ages, and weathering processes, from parts of the Gascoyne region and adjacent areas

			Australia	*Carnarvon Basin*	*Mount Phillips*	*Glenburgh*	*Winning Pool and Minilya*	*Kennedy Range*	*Wooramel*	*Edmund*	*Turee Creek*	*Mount Egerton*	*Robinson Range*
	Reference		McGowran 1979	Hocking et al. 1987	Williams et al. 1983a	Williams et al. 1983b	Hocking et al. 1985a	Hocking et al. 1985b	Denman et al. 1985	Martin 2005	Thorne et al. 1991	Muhlig et al. 1978	Elias and Williams 1980
Cenozoic	*Holocene*												
Cenozoic	*Neogene*	*Pleistocene* L			↑		valley calcrete (?)	25-16k BP later dunefields	25-16k BP major aeolian reworking 40-25k BP modern river courses			calcrete	
Cenozoic	*Neogene*	*Pleistocene*		calcretization laterization*		Nadarra Fm.			calcretization				
Cenozoic	*Neogene*		ferruginization		Nadarra Fm.		duricrust calcrete		paleodrainage				
Cenozoic	*Neogene*		silification	laterization*		duricrust	2nd ferruginization and silification		duricrust main phase of ferruginization and silification				
Cenozoic	*Neogene*					Pindiliya Fm.	Cape Range Group	Trealla Lst.	Pindilia Fm.				
Cenozoic	*Neogene*		ferruginization				1st ferruginization and silification		Trealla Lst.				
Cenozoic		*Oligocene* L											
Cenozoic		*Oligocene* E											
Cenozoic		*Eocene* L					Merlingleigh Sst.	Merlingleigh Sst.	Giralia Calcarenite				
Cenozoic		*Eocene*											
Cenozoic							Cardabia Group						
	Tertiary undiff. comments				undiff.: consolidated hardpan; calcrete; old duricrust surface (incl. laterite)		marine sedimentation			Tertiary undiff. ferruginous material, consolidated colluvium, calcrete, limonite	Hamersley surface late Mesozoic to early Tertiary		Tertiary landsurface (laterized plateu)

*equivalent to ferruginization

Winning Pool SF 50-13	Edmund SF 50-14	Turee Creek SF 50-15
Kennedy Range SG 50-1	Mount Phillips SG 50-2	Mount Egerton SG 50-3
Wooramel SG 50-5	Glenburgh SG 50-6	Robinson Range SG 50-7

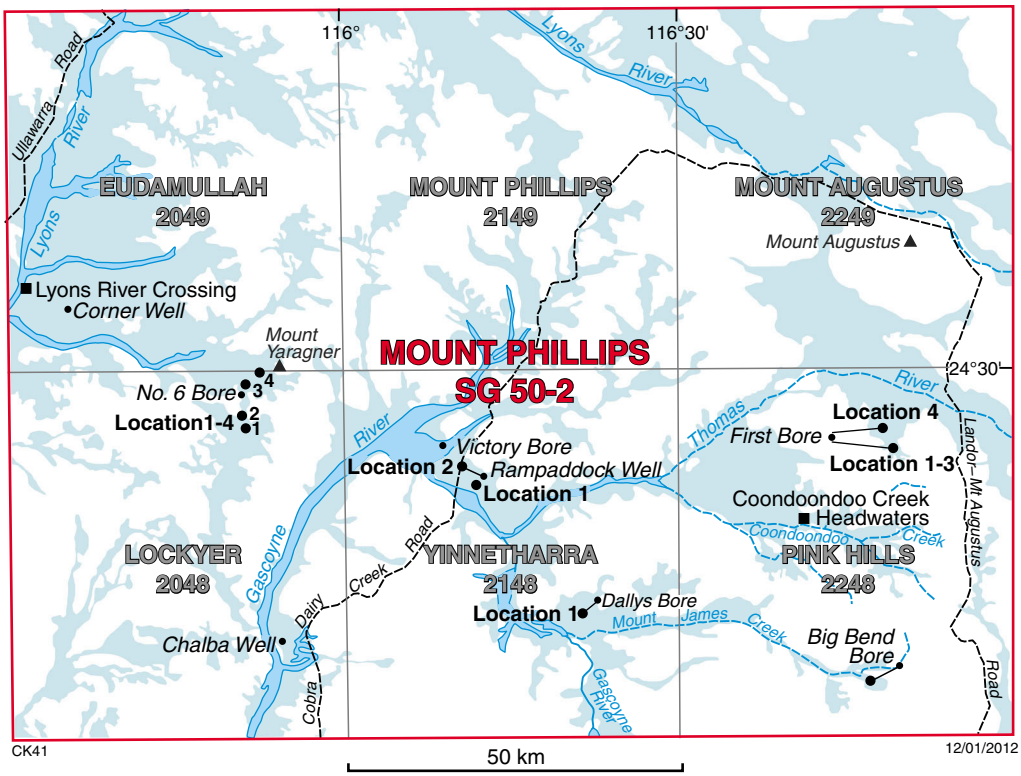

Figure 41. Reconstructed paleodrainage network (light blue) for the Mount Phillips 1:250 000 Geological Series map sheet (based on field observation and MRVBF data from Geoscience Australia, 2011) overlain by major modern river network (dark blue)

References

Adams, AE, MacKenzie, WS and Guilford, C 1984, Atlas of sedimentary rocks under the microscope: Pearson Education Ltd, Harlow, UK, 104p.

Anand, RR 2005, Weathering history, landscape evolution and implications for exploration, *in* Regolith landscape evolution across Australia *edited by* RR Anand and P de Broekert: CRC LEME, Perth, Western Australia, p. 2–40.

Anand, RR and de Broekert, P (editors) 2005, Regolith landscape evolution across Australia: CRC LEME, Perth, Western Australia, 345p.

Anand, RR, Churchward, HM, Smith, RE, Smith, K, Gozzard, JR, Craig, MA, and Munday, TJ 1998, Classification and atlas of regolith–landform mapping units (2nd edition): CRC LEME, Open File Report 2 (unpublished).

Arakel, AV, Jacobson, G, Salehi, M and Hill, CM 1989, Silification of calcrete in palaeodrainage basins of the Australian arid zone: Australian Journal of Earth Sciences, v. 36, no. 1, p. 73–89.

Bettany, E and Churchward, HM 1974, Morphology and stratigraphic relationships of the Wiluna hardpan in arid Western Australia: Australian Journal of Earth Sciences, v. 21, no. 1, p. 73–80.

Bourman, RP 1993, Perennial problems in the study of laterite: a review: Australian Journal of Earth Sciences, v. 40, no. 4, p. 387–401.

Bowler, JM 1976, Aridity in Australia: age, origins and expression in aeolian landforms and sediments: Earth-Science Reviews, v. 12, p. 279–310.

Brewer, R, Bettenay, E and Churchward, HM 1972, Some aspects of the origin and development of the red and brown hardpan soils of Bulloo Downs, Western Australia: CSIRO, Division of Soils, Technical Paper 13, 13p.

Butt, CRM, Horwitz, RC and Mann, AW 1977, Uranium occurrences in calcrete and associated sediments in Western Australia: CSIRO Minerals Research Laboratories, Report FP16, 67p.

Butt, CRM, Robertson, IDM, Scott, KM and Cornelius, M (editors) 2005, Regolith expression of Australian ore systems: CRC LEME, Perth, Western Australia, 431p.

Chen, XY, Lintern, MJ and Roach, IC (editors) 2002, Calcrete: characteristics, distribution and use in mineral exploration: CRC LEME, Belconnen, Australian Capital Territory, 160p.

Cockbain, AE and Hocking, RM 1990, Geological evolution — Phanerozoic, in Geology and mineral resources of Western Australia: Geological Survey of Western Australia, Memoir 3, p. 750–755.

Commonwealth Bureau of Meteorology 2010a, Climate statistics for Gascoyne Junction, viewed 15 June 2010, <http://www.bom.gov.au/climate/averages/tables/cw_006022.shtml>.

Commonwealth Bureau of Meteorology 2010b, Climate statistics for Mount Phillip, viewed 15 June 2010, <http://www.bom.gov.au/climate/averages/tables/cw_007058.shtml>.

Cooper, RW, Langford, RL and Pirajno, F 1998, Mineral occurrences and exploration potential of the Bangemall Basin: Geological Survey of Western Australia, Report 64, 42p.

Cornelius, M, Robertson, IDM, Cornelius, AJ and Morris, PA 2007, Laterite geochemical database for the western Yilgarn Craton, Western Australia: Geological Survey of Western Australia, Record 2007/9, 44p.

de Broekert, P and Sandiford, M 2005, Buried inset-valleys in the Eastern Yilgarn Craton, Western Australia: geomorphology, age, and allogenic control: Journal of Geology, v. 113, p. 471–493.

Denman, PD, Hocking, RM, Moore, PS, Williams, IR and Van De Graaff, WJE (compilers) 1985, Wooramel, Western Australia (2nd edition): Geological Survey of Western Australia, 1:250 000 Geological Series Explanatory Notes, 23p.

Department of Sustainability, Environment, Water, Population and Communities 2007, Australian natural resource atlas: Commonwealth of Australia, Canberra, Australian Capital Territory, viewed 7 July 2010, <http://www.anra.gov.au/topics/agriculture/pubs/summary_reports/ag_in_aust/_aa_07.html>.

Dodson, WD 2009, Groundwater recharge from the Gascoyne River, Western Australia: Western Australia Department of Water, Hydrogeological Record Series HG 32, 226p.

Dunkerley, DL and Brown, KJ 1995, Runoff and runon areas in a patterned chenopod shrubland, arid western New South Wales, Australia: characteristics and origin: Journal of Arid Environments, v. 30, p. 41–55.

Eggleton, RA (editor) 2001, The regolith glossary: surficial geology, soils and landscapes: CRC LEME, Canberra, Australian Capital Territory, 144p.

Elias, M and Williams, SJ (compilers) 1980, Robinson Range, Western Australia: Geological Survey of Western Australia, 1:250 000 Geological Series Explanatory Notes, 32p.

Frakes, LA and Kemp, EM 1972, Influence of continental positions on early Tertiary climates: Nature, v. 240, p. 97–100.

Glassford, DK and Semeniuk, V 1995, Desert-aeolian origin of late Cenozoic regolith in arid and semi-arid Southwestern Australia: Palaeogeography, Palaeoclimatology, Palaeoecology, v. 114, p. 131–166.

Gozzard, JR 2006, Regolith–landform mapping: a classical approach using new imagery, *in* GSWA 2006 extended abstracts: promoting the prospectivity of Western Australia: Geological Survey of Western Australia, Record 2006/3, p. 5–7.

Gozzard, JR 2007, Understanding the landscape, *in* Geological Survey of Western Australia Annual Review 2005–06: Geological Survey of Western Australia, Perth, Western Australia, p. 21–25.

Hasiotis, ST 2002, Continental trace fossils: SEPM (Society of Sedimentary Geology), Short Course Notes 51, 132p.

Hocking, RM, Langford, RL, Thorne, AM, Sanders, AJ, Morris, PA, Strong, CA, Gozzard, JR and Riganti, A 2007, A classification system for regolith in Western Australia (March 2007 update) (3rd edition): Geological Survey of Western Australia, Record 2007/8, 19p.

Hocking, RM, Moors, HT and Van De Graaff, WJE 1987, Geology of the Carnarvon Basin, Western Australia: Geological Survey of Western Australia, Bulletin 133, 289p.

Holden, E 1925, The Cause of Color in Smoky Quartz and Amethyst. American Mineralologist, v. 9, p. 203–252.

Johnson, SP, Sheppard, S, Krapf, CBE and Hocking, RM 2011, Lockier WA Sheet 2048: Geological Survey of Western Australia, 1:100 000 Geological Series.

Johnson, SP, Sheppard, S, Krapf, CBE and Thorne, AM 2010a, Pink Hills, WA Sheet 2248: Geological Survey of Western Australia, 1:100 000 Geological Series.

Johnson, SP, Sheppard, S, Rasmussen, B, Muhling, JR, Fletcher, IR, Wingate, MTD, Kirkland, CL and Pirajno, F 2009, Meso- to Neoproterozoic reworking in the Gascoyne Complex and what it means for mineral exploration, *in* GSWA 2009 extended abstracts: promoting the prospectivity of Western Australia: Geological Survey of Western Australia, Record 2009/2, p. 23–25.

Johnson, SP, Sheppard, S, Rasmussen, B, Wingate, MTD, Kirkland, CL, Muhling, JR, Fletcher, IR and Belousova, E 2010b, The Glenburgh Orogeny as a record of Paleoproterozoic continent–continent collision: Geological Survey of Western Australia, Record 2010/5, 54p.

Langford, RL 2007, Regolith–terrain mapping in the Tanami, *in* GSWA 2007 extended abstracts: promoting the prospectivity of Western Australia: Geological Survey of Western Australia, Record 2007/2, p. 3–4.

Macphail, M 2007, Australian palaeoclimates: Cretaceous to Tertiary — a review of palaeobotanical and related evidence to the year 2000: CRC LEME, Special Volume, Open File Report 151, 266p.

Magee, J 2009, Paleovalley groundwater resources in arid and semi-arid Australia — a literature review: Geoscience Australia, Record 2009/3, 224p.

Mann, AW and Howitz, RC 1979, Groundwater calcrete deposits in Australia — some observations from Western Australia: Geological Society of Australia Journal, v. 26, p. 293–303.

Marnham, J and Hall, G 2002, Karridale–Tooker, Sheet 1929-IV and part Sheet 1829-I: Geological Survey of Western Australia, 1:50 000 Regolith–Landform Resources Series.

Martin, DM, Sheppard, S and Thorne, AM 2005, Geology of the Maroonah, Ullawarra, Capricorn, Mangaroon, Edmund, and Elliott Creek 1:100 000 sheets: Geological Survey of Western Australia, 1:100 000 Geological Series Explanatory Notes, 65p.

Martin, DM, Sheppard, S, Thorne, AM, Farrell, TR and Groenewald, PB 2007, Proterozoic geology of the western Capricorn Orogen — a field guide: Geological Survey of Western Australia, Record 2006/18, 43p.

McGowran, B 1979, The Tertiary of Australia: foraminiferal overview: Marine Micropaleontology, v. 4, p. 235–264.

Morris, RC and Ramanaidou, ER 2007, Genesis of the channel iron deposits (CID) of the Pilbara region, Western Australia: Australian Journal of Earth Sciences, v. 54, no. 5, p. 733–756.

Muhling, PC, Brakel, AT and Davidson, WA (compilers) 1978, Mount Egerton, Western Australia: Geological Survey of Western Australia, 1:250 000 Geological Series Explanatory Notes, 28p.

Pain, CF and Ollier, CD 1992, Ferricrete in Cape York Peninsula, north Queensland: BMR Journal of Australian Geology and Geophysics, v. 13, no. 3, p. 207–212.

Pillans, B 1998, Regolith dating methods: a guide to numerical dating techniques: CRC LEME, Perth, Western Australia, 30p.

Pillans, B 2005, Geochronology of the Australian regolith, *in* Regolith landscape evolution across Australia *edited by* RR Anand and P de Broekert: CRC LEME, Perth, Western Australia, p. 41–61.

Rasmussen, B, Fletcher, IR, Muhling, JR, Thorne, AM, Cutten, HN, Pirajno, F and Hell, A 2010, In situ U–Pb monazite and xenotime geochronology of the Abra polymetallic deposit and associated sedimentary and volcanic rocks, Bangemall Supergroup, Western Australia: Geological Survey of Western Australia, Record 2010/12, 31p.

Sanders, AJ 2000, Regolith geochemistry in sand-dominated terrain: a case study on the Ajana 1:250 000 sheet, *in* GSWA 2000 extended abstracts: Geological data for WA explorers in the new millennium: Geological Survey of Western Australia, Record 2000/8, p. 17–19.

Sanders, AJ, Davy, R, Pirajno, F and Morris, PA 1999, Regolith geochemical mapping as an adjunct to geological mapping and mineral exploration, *in* Geological Survey of Western Australia Annual Review 1997–98: Geological Survey of Western Australia, Perth, Western Australia, p. 104–111.

Sanders, AJ, Morris, PA, Subramanya, AG and Faulkner, JA 1997a, Geochemical mapping of the Mount Phillips 1:250 000 sheet: Geological Survey of Western Australia, 1:250 000 Regolith Geochemistry Explanatory Notes, 51p.

Sanders, AJ, Morris, PA, Subramanya, AG and Faulkner, JA 1997b, Regolith materials — Mount Phillips, WA Sheet SG 50-2, *in* Geochemical mapping of the Mount Phillips 1:250 000 sheet *by* AJ Sanders, PA Morris, AG Subramanya and JA Faulkner: Geological Survey of Western Australia, 1:250 000 Regolith Geochemistry Series, Plate 1.

Sheppard, S, Johnson, SP, Groenewald, PB, Bodorkos, S, Rasmussen, B, Fletcher, IR, Muhling, JR and Selway, K 2008, Recent advances in our understanding of the Gascoyne Complex, *in* GSWA 2008 extended abstracts: promoting the prospectivity of Western Australia: Geological Survey of Western Australia, Record 2008/2, p. 1–3.

Sheppard, S, Johnson, SP, Wingate, MTD, Kirkland, CL and Pirajno, F 2010, Explanatory Notes for the Gascoyne Province: Geological Survey of Western Australia, Perth, Western Australia, 336p.

Skwarnecki, MS 2005, Regolith–landform mapping and hyperspectral data for the Kalgoorlie–Kanowna area: Geological Survey of Western Australia, Record 2005/7, 49p.

Summerfield, MA 1982, Distribution, nature and genesis of silcrete in arid and semi-arid southern Africa: Catena, Supplement, v. 1, p. 37–65.

Taylor, G 1994, Landscapes of Australia: their nature and evolution, *in* History of the Australian vegetation: Cretaceous to recent *edited by* RS Hill: Cambridge University Press, Cambridge, UK, p. 60–79.

Thorne, AM 2010, Western Capricorn Orogen, 2009 update: Geological Survey of Western Australia, 1:100 000 Geological Information Series.

Tucker, ME 2001, Sedimentary petrology (3rd Edition): Blackwell Science, Oxford, UK, 262p.

Van De Graaff, WJE, Crowe, RWA, Bunting, JA and Jackson, MJ 1977, Relict early Cainozoic drainages in arid Western Australia: Zeitschrift für Geomorphologie, v. 21, p. 379–400.

Vasconcelos, PM, Knesel, KM, Cohen, BE and Heim, JA 2008, Geochronology of the Australian Cenozoic: a history of tectonic and igneous activity, weathering, erosion, and sedimentation, Australian Journal of Earth Sciences, v. 55: 6, 865–914.

Wakelin-King, GA 1999, Banded mosaic ('tiger bush') and sheetflow plains: a regional mapping approach: Australian Journal of Earth Sciences, v. 46, p. 53–60.

Webb, JA and Golding, SD 1998, Geochemical mass-balance and oxygen-isotope constraints on silcrete formation and its paleoclimatic implications in southern Australia: Journal of Sedimentary Research, v. 68, no. 5, p. 981–993.

Williams, SJ, Williams, IR and Hocking, RM (compilers) 1983b, Glenburgh, Western Australia: Geological Survey of Western Australia, 1:250 000 Geological Series Explanatory Notes, 25p.

Williams, SJ, Williams, IR, Chin, RJ, Muhling, PC and Hocking, RM (compilers) 1983a, Mount Phillips, Western Australia: Geological Survey of Western Australia, 1:250 000 Geological Series Explanatory Notes, 29p.

Wright, VP and Tucker, ME (editors) 1991, Calcretes: Blackwell Scientific Publications, Oxford, UK, 352p.

Appendix 1

Gazetteer of localities

Place name	MGA coordinates (Zone 50J)	
	Eastings	Northings
Big Bend Bore locality (CEKGAS000070)*	478558	7243628
Chalba Well locality, Lockier Station (CEKGAS000023)	389677	7248808
Coondoondoo Creek headwaters locality (CEKGAS000063)	467375	7274609
Corner Well locality, Eudamullah Station (CEKGAS000021)	356461	7298898
Dallys Bore locality, Yinnetharra Station (CEKGAS000038)	434775	7253390
First Bore locality, Cobra Station	472454	7279812
Location 1 (CEKGAS000060)	479006	7281140
Location 2 (CEKGAS000059)	479489	7281598
Location 3 (CEKGAS000065)	479150	7282293
Location 4 (CEKGAS000058)	479739	7281748
Landor Homestead locality, Landor Station	490344	7220466
Location 1 (CEKGAS000080)	493981	7231946
Location 2 (CEKGAS000082)	493485	7216395
Lyons River Crossing locality, Eudamullah Station (CEKGAS000002)	349642	7300771
Marloo Bore	378269	7269613
No. 6 Bore locality, Eudamullah Station	383256	7286817
Location 1 (CEKGAS000011)	383507	7286675
Location 2 (CEKGAS000007)	383542	7286347
Location 3 (CEKGAS000005)	383476	7286222
Location 4 (CEKGAS000015)	385857	7289201
Rampaddock Well locality, Yinnetharra Station	419455	7273483
Location 1 (CEKGAS000044)	417896	7273081
Location 2 (CEKGAS0000045)	416632	7275057
Teddy Bore	387276	7293758
Victory Bore locality, Yinnetharra Station	412770	7278787
Location 1 (CEKGAS000030)	412515	7278937
Location 2 (CEKGAS000032)	412963	7278854

* Number prefixed by CEKGA refer to DMP internal WAROX database

Appendix 2

Gascoyne geochemistry 2009 results

Sample units	Location	Eastings	Northings	Sample medium	Au ppb	Pt ppb	Pd ppb	SiO_2 %	Al_2O_3 %	CaO %	Fe_2O_3 %	K_2O %	MgO %	Na_2O %
199503	CK005	383476	7286222	silcrete (silicified calcrete)	1	-1	-1	96.1	0.08	0.1	1.65	0.01	0.1	0.02
199505	CK007	383542	7286347	calcrete	1	-1	-1	2.45	0.49	52.9	0.26	0.06	0.74	-0.01
199508	CK011	383507	7286675	silicified calcrete	5	-1	-1	35	0.32	35	0.81	0.05	0.4	-0.01
199510	CK015-1A	385857	7289201	saprock	1	-1	-1	67.5	20	0.13	1.62	0.29	0.48	1.38
199511	CK015-1B	385857	7289201	saprolite	2	-1	-1	60	16.3	0.45	12.4	0.23	0.64	1.01
199512	CK015-2A	385857	7289201	ferruginous duricrust in situ	1	-1	-1	62.5	19.5	0.16	6.49	0.27	0.76	0.99
199513	CK015-2B	385857	7289201	ferruginous duricrust in situ	2	-1	1	47.2	18.4	0.13	24	0.11	0.38	0.3
199514	CK015-2C	385857	7289201	ferruginous duricrust in situ	2	-1	1	62.7	13.9	0.09	15.6	0.14	0.35	0.16
199515	CK015-3	385857	7289201	ferruginous duricrust in situ	1	1	1	34.5	7.79	0.12	48.4	0.32	0.22	0.1
199518	CK002-1	349642	7300771	calcrete	2	-1	-1	70	9.43	4.75	4.05	2	1.77	1.36
199519	CK002-2	349642	7300771	older alluvium	1	-1	-1	62	8.54	9.98	4.21	1.8	1.39	0.93
199520	CK002-3	349642	7300771	channel sand	-1	-1	-1	84.9	7.02	0.55	2.03	2.85	0.19	1.09
199521	CK023	389827	7248875	calcrete	3	-1	2	20.9	2.69	36.6	4.83	0.4	4.73	0.1
199526	CK030	412515	7278937	calcrete	2	-1	1	18.5	1.08	43	0.66	0.17	0.58	0.03
199527	CK031-1	412540	7278946	ferruginized duricrust transported	6	-1	-1	79.5	8.54	0.91	3.58	2.81	0.86	0.25
199528	CK031-2	412540	7278946	carbonate-cemented ferruginous duricrust transported	2	-1	-1	35.6	4.95	30.2	2.1	1.54	0.75	0.16
199529	CK031-3	412540	7278946	carbonate-cemented ferruginous duricrust transported	2	-1	1	31	4.73	32	2.35	1.22	1	0.1
199530	CK031-4	412540	7278946	carbonate-cemented ferruginous duricrust transported	1	-1	-1	7.56	1.34	47.3	0.76	0.26	2.16	0.02
199531	CK032-1	412963	7278854	silicified ferruginous caprock	2	-1	-1	79.4	0.93	9.5	1.05	0.09	0.24	0.02
199532	CK032-2	412963	7278854	calcrete	9	-1	2	32.7	1.16	33.5	0.6	0.19	2.04	0.04
199533	CK033	412934	7278874	weathered calcified sst	2	-1	1	78	8.69	1.26	3.01	3.46	1.31	0.32
199535	CK038	437775	7253390	silicified calcrete	4	-1	-1	30.7	0.18	31.2	0.34	0.04	6.08	-0.01
199536	CK039	437404	7254234	pisolithic duricrust	1	-1	-1	51.3	15.1	0.1	23.8	0.11	0.09	0.05
199537	CK040-1	437289	7254584	termite mound	-1	-1	-1	82.4	6.94	0.43	4.23	1.86	0.35	0.2
199538	CK040-2	437289	7254584	eolian sand	-1	-1	-1	86.4	5.88	0.13	3.1	1.8	0.17	0.21
199549	CK058	479739	7281748	ferruginous duricrust transported	2	-1	2	67.6	15.8	0.12	7.84	0.58	0.44	0.07
199550	CK059	479489	7281598	pisolithic ferruginous duricrust transported	1	-1	1	69.3	13.5	0.11	9.32	0.58	0.32	0.05
199551	CK060	479006	7281140	pisolithic ferruginous duricrust transported	1	-1	1	61.7	22.9	0.15	4.41	0.05	0.37	0.08
199556	CK070	478558	7243628	calcrete	1	-1	-1	2.77	0.53	31.7	0.17	0.03	19.2	0.16
199560	CK080-1	493981	7231946	calcrete	1	-1	-1	8.64	0.2	44.7	0.08	0.04	6.65	0.02

Appendix 2 (continued)

Sample units	Location	Eastings	Northings	Sample medium	P_2O_5 %	TiO_2 %	MnO %	LOI/1000 %	Cr ppm	Ni ppm	V ppm	Sc ppm	Zn ppm	Ag ppm
199503	CK005	383476	7286222	silcrete (silicified calcrete)	0.008	-0.01	0.02	1.34	20	36	5	-1	6	-0.5
199505	CK007	383542	7286347	calcrete	0.015	0.03	0.08	42.5	10	14	5	-1	8	-0.5
199508	CK011	383507	7286675	silicified calcrete	0.175	0.03	0.02	27.9	10	10	5	-1	10	-0.5
199510	CK015-1A	385857	7289201	saprock	0.006	0.21	0.01	8.48	20	46	10	6	10	-0.5
199511	CK015-1B	385857	7289201	saprolite	0.023	0.77	0.09	7.95	60	14	120	7	10	-0.5
199512	CK015-2A	385857	7289201	ferruginous duricrust in situ	0.006	0.48	0.02	8.54	40	20	55	8	14	-0.5
199513	CK015-2B	385857	7289201	ferruginous duricrust in situ	0.018	0.94	0.02	8.05	210	24	340	7	16	-0.5
199514	CK015-2C	385857	7289201	ferruginous duricrust in situ	0.014	0.78	0.01	6.04	80	18	175	8	12	-0.5
199515	CK015-3	385857	7289201	ferruginous duricrust in situ	0.034	2.8	0.08	5.43	280	16	600	18	12	-0.5
199518	CK002-1	349642	7300771	calcrete	0.051	0.51	0.07	5.69	40	18	70	8	32	-0.5
199519	CK002-2	349642	7300771	older alluvium	0.039	0.54	0.05	9.96	50	22	75	8	28	-0.5
199520	CK002-3	349642	7300771	channel sand	0.036	0.14	0.02	0.59	40	14	35	3	16	-0.5
199521	CK023	389827	7248875	calcrete	0.054	0.14	0.71	28.4	40	28	35	2	38	-0.5
199526	CK030	412515	7278937	calcrete	0.104	0.09	-0.01	35.2	20	8	10	1	10	-0.5
199527	CK031-1	412540	7278946	ferruginized duricrust transported	0.033	0.3	0.03	2.9	30	14	65	7	26	-0.5
199528	CK031-2	412540	7278946	carbonate-cemented ferruginous duricrust transported	0.04	0.27	0.01	23.9	30	20	40	5	16	-0.5
199529	CK031-3	412540	7278946	carbonate-cemented ferruginous duricrust transported	0.048	0.34	0.07	26.9	40	20	50	6	18	-0.5
199530	CK031-4	412540	7278946	carbonate-cemented ferruginous duricrust transported	0.086	0.15	0.09	39.8	10	12	25	2	10	-0.5
199531	CK032-1	412963	7278854	silicified ferruginous caprock	0.383	0.06	0.14	7.9	10	10	15	1	22	-0.5
199532	CK032-2	412963	7278854	calcrete	0.056	0.09	-0.01	29.1	20	10	20	1	8	-0.5
199533	CK033	412934	7278874	weathered calcified sst	0.028	0.37	0.03	2.93	30	12	40	6	18	-0.5
199535	CK038	437775	7253390	silicified calcrete	0.041	0.02	-0.01	30.8	20	6	10	-1	10	-0.5
199536	CK039	437404	7254234	pisolithic duricrust	0.087	1.06	-0.01	8	60	10	405	20	10	-0.5
199537	CK040-1	437289	7254584	termite mound	0.043	0.38	0.04	2.9	40	16	65	6	22	-0.5
199538	CK040-2	437289	7254584	eolian sand	0.032	0.35	0.03	1.4	40	12	45	4	14	-0.5
199549	CK058	479739	7281748	ferruginous duricrust transported	0.045	0.9	0.03	6.02	80	24	125	16	30	-0.5
199550	CK059	479489	7281598	pisolithic ferruginous duricrust transported	0.016	0.7	-0.01	5.8	60	18	165	15	10	-0.5
199551	CK060	479006	7281140	pisolithic ferruginous duricrust transported	0.009	1.16	-0.01	8.88	50	42	65	20	4	-0.5
199556	CK070	478558	7243628	calcrete	0.013	0.03	-0.01	45.2	10	4	5	-1	6	-0.5
199560	CK080-1	493981	7231946	calcrete	0.051	0.02	-0.01	39	20	4	5	-1	6	-0.5

Appendix 2 (continued)

Sample units	Location	Eastings	Northings	Sample medium	As ppm	Ba ppm	Be ppm	Bi ppm	Cd ppm	Ce ppm	Co ppm	Cs ppm	Cu ppm	Ga ppm
199503	CK005	383476	7286222	silcrete (silicified calcrete)	-1	745	-0.1	-0.1	-0.5	0.7	2	-0.1	23	0.4
199505	CK007	383542	7286347	calcrete	-1	474	-0.1	-0.1	-0.5	5	1	0.2	13	0.8
199508	CK011	383507	7286675	silicified calcrete	-1	118	-0.1	-0.1	-0.5	2.9	1	-0.1	9	0.4
199510	CK015-1A	385857	7289201	saprock	-1	26	0.2	-0.1	-0.5	3.6	1	0.5	15	10.6
199511	CK015-1B	385857	7289201	saprolite	-1	176	0.8	0.2	-0.5	96.5	6	0.5	16	18.8
199512	CK015-2A	385857	7289201	ferruginous duricrust in situ	-1	27	1	-0.1	-0.5	33.1	4	0.6	14	16.2
199513	CK015-2B	385857	7289201	ferruginous duricrust in situ	2	18	0.9	0.8	-0.5	3.3	4	0.4	14	35.8
199514	CK015-2C	385857	7289201	ferruginous duricrust in situ	3	35	0.6	0.3	-0.5	6.6	2	0.3	11	32.4
199515	CK015-3	385857	7289201	ferruginous duricrust in situ	2	51	0.9	1.1	-0.5	7.9	7	0.3	27	91.4
199518	CK002-1	349642	7300771	calcrete	2	449	1.2	0.2	-0.5	40.1	5	2.3	17	7.6
199519	CK002-2	349642	7300771	older alluvium	2	489	1.1	0.2	-0.5	57.4	6	2.1	18	9.6
199520	CK002-3	349642	7300771	channel sand	2	609	0.8	0.1	-0.5	19.3	2	1.2	6	6.4
199521	CK023	389827	7248875	calcrete	7	142	0.7	0.2	-0.5	29.1	13	0.7	46	4
199526	CK030	412515	7278937	calcrete	-1	139	0.1	-0.1	-0.5	12.8	5	0.4	12	1.6
199527	CK031-1	412540	7278946	ferruginized duricrust transported	4	591	0.7	0.2	-0.5	27.1	5	3	21	9.2
199528	CK031-2	412540	7278946	carbonate-cemented ferruginous duricrust transported	5	349	0.6	0.1	-0.5	29.5	3	2	23	5.6
199529	CK031-3	412540	7278946	carbonate-cemented ferruginous duricrust transported	4	350	0.6	0.1	-0.5	24.1	8	1.8	21	5.6
199530	CK031-4	412540	7278946	carbonate-cemented ferruginous duricrust transported	-1	209	0.2	-0.1	-0.5	11.7	8	0.6	10	2
199531	CK032-1	412963	7278854	silicified ferruginous caprock	1	223	0.2	-0.1	-0.5	26.1	11	0.3	12	1.4
199532	CK032-2	412963	7278854	calcrete	2	110	0.2	-0.1	-0.5	10.6	3	0.4	19	1.4
199533	CK033	412934	7278874	weathered calcified sst	2	655	1	0.3	-0.5	39.3	4	3	14	8.8
199535	CK038	437775	7253390	silicified calcrete	-1	458	-0.1	-0.1	-0.5	2.4	2	-0.1	13	0.6
199536	CK039	437404	7254234	pisolithic duricrust	4	1050	0.8	1	-0.5	84.6	3	0.6	7	44.6
199537	CK040-1	437289	7254584	termite mound	3	484	0.7	0.3	-0.5	53.8	5	1.7	15	8.8
199538	CK040-2	437289	7254584	eolian sand	3	453	0.6	0.2	-0.5	51.1	4	1.3	9	6.6
199549	CK058	479739	7281748	ferruginous duricrust transported	4	199	0.8	0.4	-0.5	35.7	6	3.1	27	20.2
199550	CK059	479489	7281598	pisolithic ferruginous duricrust transported	4	316	0.6	0.4	-0.5	16.4	5	2.7	19	16.2
199551	CK060	479006	7281140	pisolithic ferruginous duricrust transported	2	64	1.2	0.4	-0.5	14.6	8	0.5	4	21.8
199556	CK070	478558	7243628	calcrete	-1	92	0.2	-0.1	-0.5	21.2	2	0.4	6	1.2
199560	CK080-1	493981	7231946	calcrete	5	21	-0.1	-0.1	-0.5	0.8	-1	-0.1	7	0.4

Appendix 2 (continued)

Sample units	Location	Eastings	Northings	Sample medium	Hf ppm	La ppm	Li ppm	Lu ppm	Mo ppm	Nb ppm	Pb ppm	Rb ppm	Sb ppm	Sn ppm
199503	CK005	383476	7286222	silcrete (silicified calcrete)	-0.2	0.7	-0.5	-0.02	0.5	-0.5	-1	0.4	-0.2	-1
199505	CK007	383542	7286347	calcrete	-0.2	2.7	1.5	0.04	-0.5	-0.5	2	3.8	-0.2	-1
199508	CK011	383507	7286675	silicified calcrete	-0.2	1.4	2.5	-0.02	-0.5	-0.5	-1	2.2	-0.2	-1
199510	CK015-1A	385857	7289201	saprock	1.4	2.1	33	-0.02	-0.5	4	1	15.4	-0.2	2
199511	CK015-1B	385857	7289201	saprolite	1.6	36.2	29.5	0.06	1.5	7	9	12.2	-0.2	6
199512	CK015-2A	385857	7289201	ferruginous duricrust in situ	4	1.9	39	0.1	0.5	10	4	15.6	-0.2	4
199513	CK015-2B	385857	7289201	ferruginous duricrust in situ	2.4	3.8	44.5	0.02	1.5	12	10	6.6	-0.2	4
199514	CK015-2C	385857	7289201	ferruginous duricrust in situ	2.6	4.6	42	0.06	1	19.5	8	8	-0.2	4
199515	CK015-3	385857	7289201	ferruginous duricrust in situ	4.2	5.9	12.5	0.06	2	8.5	15	12.6	-0.2	4
199518	CK002-1	349642	7300771	calcrete	2	22.1	25	0.18	-0.5	4.5	15	75.2	2	1
199519	CK002-2	349642	7300771	older alluvium	2.4	30.3	14	0.2	0.5	6	16	69.6	0.2	2
199520	CK002-3	349642	7300771	channel sand	1	11	5.5	0.08	-0.5	3	17	82.8	-0.2	-1
199521	CK023	389827	7248875	calcrete	1	17.5	2	0.22	0.5	8	5	26.2	-0.2	1
199526	CK030	412515	7278937	calcrete	0.4	6.3	2.5	0.04	-0.5	1	2	8.4	-0.2	-1
199527	CK031-1	412540	7278946	ferruginized duricrust transported	1.2	13.2	19.5	0.12	1	5	25	98.4	-0.2	1
199528	CK031-2	412540	7278946	carbonate-cemented ferruginous duricrust transported	0.8	17.9	13	0.14	-0.5	5	14	60.2	-0.2	1
199529	CK031-3	412540	7278946	carbonate-cemented ferruginous duricrust transported	1	13.3	12.5	0.12	0.5	5	12	48.2	-0.2	-1
199530	CK031-4	412540	7278946	carbonate-cemented ferruginous duricrust transported	0.2	4.8	6	0.04	-0.5	1.5	4	13	-0.2	-1
199531	CK032-1	412963	7278854	silicified ferruginous caprock	0.2	5.7	3.5	0.04	-0.5	0.5	3	5.8	-0.2	-1
199532	CK032-2	412963	7278854	calcrete	0.2	5.7	1.5	0.04	-0.5	1	2	8.8	-0.2	-1
199533	CK033	412934	7278874	weathered calcified sst	1.2	16.6	18.5	0.14	-0.5	6	26	123	-0.2	1
199535	CK038	437775	7253390	silicified calcrete	-0.2	0.8	1	-0.02	-0.5	-0.5	-1	2.6	-0.2	-1
199536	CK039	437404	7254234	pisolithic duricrust	3.2	54.9	14	0.1	4.5	21	44	8.6	-0.2	5
199537	CK040-1	437289	7254584	termite mound	1.4	29.1	9	0.14	0.5	5.5	19	78.8	-0.2	1
199538	CK040-2	437289	7254584	eolian sand	1	27.2	7	0.1	-0.5	4	17	68.8	-0.2	-1
199549	CK058	479739	7281748	ferruginous duricrust transported	2.8	16	16.5	0.14	1.5	16.5	21	45	0.4	3
199550	CK059	479489	7281598	pisolithic ferruginous duricrust transported	2.8	8.3	9.5	0.1	1.5	8	24	45.8	-0.2	3
199551	CK060	479006	7281140	pisolithic ferruginous duricrust transported	3.2	6.5	28.5	0.12	1	13	13	3.4	-0.2	3
199556	CK070	478558	7243628	calcrete	-0.2	7.3	2.5	-0.02	-0.5	0.5	6	2.4	-0.2	-1
199560	CK080-1	493981	7231946	calcrete	-0.2	0.2	5.5	-0.02	-0.5	-0.5	-1	1.4	-0.2	-1

Appendix 2 (continued)

Sample units	Location	Eastings	Northings	Sample medium	Sr ppm	Ta ppm	Th ppm	Tl ppm	U ppm	W ppm	Y ppm	Zr ppm
199503	CK005	383476	7286222	silcrete (silicified calcrete)	27	-0.1	-0.1	-0.1	20.7	-0.5	0.6	7
199505	CK007	383542	7286347	calcrete	134	-0.1	0.5	-0.1	1	-0.5	4.6	2
199508	CK011	383507	7286675	silicified calcrete	75	-0.1	0.4	-0.1	11.5	-0.5	0.9	2
199510	CK015-1A	385857	7289201	saprock	10	0.2	1.5	-0.1	1.4	1.5	0.9	33
199511	CK015-1B	385857	7289201	saprolite	18	0.6	49.2	0.1	10.2	5	8.5	29
199512	CK015-2A	385857	7289201	ferruginous duricrust in situ	21	0.5	16.3	-0.1	5.4	0.5	4.6	141
199513	CK015-2B	385857	7289201	ferruginous duricrust in situ	18	1.2	22.1	-0.1	5.2	6	1.4	71
199514	CK015-2C	385857	7289201	ferruginous duricrust in situ	14	2.2	26.6	-0.1	3.2	1.5	3.7	61
199515	CK015-3	385857	7289201	ferruginous duricrust in situ	21	0.2	131	0.1	3.6	-0.5	3	140
199518	CK002-1	349642	7300771	calcrete	160	0.4	10.1	0.4	3.9	-0.5	12.2	63
199519	CK002-2	349642	7300771	older alluvium	190	0.4	13.9	0.3	5.6	-0.5	13.9	71
199520	CK002-3	349642	7300771	channel sand	77	0.1	4.6	0.4	1	-0.5	4.9	31
199521	CK023	389827	7248875	calcrete	119	0.6	5.7	0.1	2.9	0.5	24.3	30
199526	CK030	412515	7278937	calcrete	83	0.1	2.3	-0.1	5.1	-0.5	3.3	12
199527	CK031-1	412540	7278946	ferruginized duricrust transported	41	0.4	6.8	0.4	1.9	1	7.5	37
199528	CK031-2	412540	7278946	carbonate-cemented ferruginous duricrust transported	62	0.4	5.6	0.3	1.8	0.5	10.7	25
199529	CK031-3	412540	7278946	carbonate-cemented ferruginous duricrust transported	72	0.4	5	0.2	3.2	1	9.1	32
199530	CK031-4	412540	7278946	carbonate-cemented ferruginous duricrust transported	353	0.1	1.8	-0.1	8.7	1	2.7	10
199531	CK032-1	412963	7278854	silicified ferruginous caprock	27	-0.1	1.2	0.1	27.7	-0.5	3.6	3
199532	CK032-2	412963	7278854	calcrete	48	-0.1	1.5	-0.1	6.6	-0.5	2.6	9
199533	CK033	412934	7278874	weathered calcified sst	51	0.5	8.4	0.5	4.7	0.5	8.5	34
199535	CK038	437775	7253390	silicified calcrete	125	-0.1	0.4	-0.1	6.3	-0.5	0.6	4
199536	CK039	437404	7254234	pisolithic duricrust	50	1.6	162	-0.1	3.5	2	6.3	101
199537	CK040-1	437289	7254584	termite mound	59	0.4	22.6	0.4	1.8	1	8.9	60
199538	CK040-2	437289	7254584	eolian sand	50	0.2	17.3	0.3	1.3	-0.5	7.2	40
199549	CK058	479739	7281748	ferruginous duricrust transported	25	0.7	17.9	0.3	2.4	2	7.8	86
199550	CK059	479489	7281598	pisolithic ferruginous duricrust transported	18	1.1	20.5	0.3	3.4	1	5.8	117
199551	CK060	479006	7281140	pisolithic ferruginous duricrust transported	14	1.4	13.2	-0.1	4.2	2.5	5.3	98
199556	CK070	478558	7243628	calcrete	381	-0.1	1.3	-0.1	3.6	-0.5	1.1	5
199560	CK080-1	493981	7231946	calcrete	391	-0.1	0.2	-0.1	3	-0.5	0.2	2

RECORD 2011/22

NEW INSIGHTS INTO THE REGOLITH OF PARTS OF THE GASCOYNE REGION

Krapf

This Record is published in digital format (PDF) and is available as a free download from the DMP website at <http://www.dmp.wa.gov.au/GSWApublications>.

Further details of geological products produced by the Geological Survey of Western Australia can be obtained by contacting:

Information Centre
Department of Mines and Petroleum
100 Plain Street
EAST PERTH WESTERN AUSTRALIA 6004
Phone: (08) 9222 3459 Fax: (08) 9222 3444
http://www.dmp.wa.gov.au/GSWApublications